

This is to certify that the
dissertation entitled

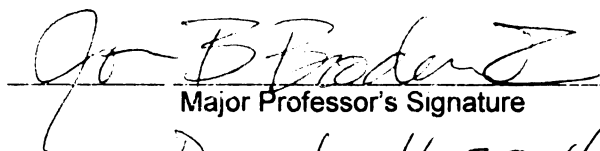
STUDIES OF THE ACTIVATION AND DEACTIVATION OF
PYRUVATE FORMATE-LYASE FROM ESCHERICHIA COLI

presented by

Mbako Ronald Nnyepi

has been accepted towards fulfillment
of the requirements for the

Ph.D. degree in Chemistry


Major Professor's Signature
December 16, 2004
Date

PLACE IN RETURN BOX to remove this checkout from your record.
TO AVOID FINES return on or before date due.
MAY BE RECALLED with earlier due date if requested.

DATE DUE	DATE DUE	DATE DUE

**STUDIES OF THE ACTIVATION AND DEACTIVATION OF PYRUVATE
FORMATE-LYASE FROM ESCHERICHIA COLI**

By

Mbako Ronald Nnyepi

A DISSERTATION

Submitted to
Michigan State University
In partial fulfillment of the requirements
for the degree of

DOCTOR OF PHILOSOPHY

Department of Chemistry

2004

ABSTRACT

STUDIES OF THE ACTIVATION AND DEACTIVATION OF PYRUVATE FORMATE-LYASE FROM ESCHERICHIA COLI

By

Mbako Ronald Nnyepi

This study set out to investigate the conditions necessary for deactivation of pyruvate formate-lyase from *Escherichia coli* by alcohol dehydrogenase (AdhE) from the same species. One of the objectives was to gain some insight into the mechanism by which AdhE achieves this reported deactivation of PFL, and particularly what role each of the putative cofactors implicated in this activity, plays in the mechanism.

To that end, the *adhE* gene was successfully engineered and cloned onto a commercial vector using standard molecular biological techniques. Recombinant plasmid DNA engineered as such was then transformed into a DNA amplification *Escherichia coli* strain, purified, fingerprinted, and subsequently introduced to a protein expression strain for overproduction of AdhE. AdhE was chromatographically purified to homogeneity and characterized by gel electrophoresis as well as by enzymatic assays with respect to its known activities. Pyruvate formate-lyase and pyruvate formate-lyase activating enzyme (PFL-AE) were purified according to procedures optimized in Dr. Joan Broderick's research laboratory.

A new method for activating PFL was developed whereby the activation mix was allowed to react at room temperature and ambient light. This was different from the method previously used in our lab in which the activation mix was intensely illuminated in ice. PFL activated by the new method was characterized both by electron paramagnetic resonance (EPR) and by a coupled enzymatic method.

Systematic deactivation studies of PFL using various combinations of AdhE and the putative cofactors CoA, Fe^{2+} and NAD^+ revealed that the presence of AdhE did not make a difference to the rate and extent of PFL deactivation. Our results, however, showed that both chemical and biological reductants, including Fe^{2+} and, to a lesser extent CoA, deactivate PFL in a significant and systematic manner. Investigation of thiols also revealed that their rate of PFL deactivation is generally inversely related to their size, thus suggesting diffusion-limited access to the buried radical of active PFL. It was significant to observe that after deactivation by thiols, PFL can be fully reactivated.

This study also revealed that NADH is a relatively potent deactivator of PFL and that the presence of AdhE stabilizes active PFL towards deactivation by this coenzyme. The presence of AdhE was also found to confer a greater degree of reactivatability to PFL, compared to PFL that is deactivated in the absence of AdhE. Our findings have thus revealed that AdhE, rather than deactivate PFL, actually provides some kind of protection for active PFL against deactivation. This role is consistent with the fact that PFL, which is activated under anaerobic conditions, is extremely sensitive to oxygen and would therefore need to be protected from oxygenolytic degradation under microaerophilic conditions during the transition from anaerobiosis to aerobiosis. Since it is expressed under similar conditions, AdhE would be a logical candidate for such a protective role.

I dedicate this work in part to my mother Lechedzani Saina Nyepi for her sacrifice and commitment to the education of all her children, inspite of enormously daunting economic circumstances. I also dedicate it to my wife Maria for her helping to keep us both sane in the middle of our bewildering responsibilities as parenting graduate students, and to our children Mbano, Titi and Bubuya for putting up with less than a fair share of their father's time.

ACKNOWLEDGEMENTS

I would like to express sincere and heartfelt appreciation to my advisor Dr. Joan Broderick. For the years that I have worked on this project, I have been privileged to receive from her unreserved academic guidance, personal and sometimes much needed financial support. It has been a truly special privilege to have such a renowned and capable scientist as my advisor. From Joan I have come to appreciate that it is possible to be both a highly successful scientist and still maintain one's humanity. Thank you for everything and my best wishes to you in all that you aspire for.

I also thank my guidance committee which comprised Dr. Milton Smith, III., Dr. James Geiger and Dr. Babak Borhan. It is my hope that I will have an opportunity to meet you again one day, maybe in Botswana!

I would like to thank Dr. Sheila Smith for showing me how to carry out enzymatic assays. Tim Henshaw was tremendously helpful with the molecular biological techniques of the project. My thanks also go to Dr. Jennifer Cheek for EPR measurements. I have also been very fortunate to have a great group of laboratory mates over the years, each of whom, in their own way, has made my stay at MSU (and particularly in the lab) an enriching experience. I thank Dan for his occasional assistance with ChemDraw and (not less significantly) for keeping the lab environment warm and friendly with his baking, and for recognizing the birthdays of each group member. Thanks to Jeff for the stimulating discussions of current events and for his friendship and to Cliff for interesting perspectives on research topics. It has been a pleasure to have you as a friend.

I appreciate Magdalena for always being ready to assist those who need help in the lab. I am grateful for her input during my preparation for my defence and her friendliness. I wish all the best to her. I thank and acknowledge Shujuan for sharing her PFL with me for the last set of experiments when I desperately needed it. Thanks for being a good friend. I could always count on Meng for her computer skills, whether it be for editing a figure or preparing for a presentation. I will remember you with much appreciation. I also acknowledge Sofia, Yi, Liton and Washington for their friendship. I will always remember you with a smile. My thanks also go to Egis and Thalia for sharing so much of yourselves with me. My interaction with you has left me culturally enriched and broadened. Thank you all for being such a great bunch collectively and special friends individually.

Lastly, I would like to thank all those who have contributed one way or another to the advancement of my educational career. I particularly thank Mr. Tafilani “Taf” Machacha at Botswana Geological Surveys for his encouragement and support when I joined the department straight from college. I also thank Sjaak Meulenberg for giving me the opportunity to switch from government work to academia.

TABLE OF CONTENTS

LIST OF TABLES	XI
LIST OF SCHEMES	XII
LIST OF FIGURES.....	VII
 CHAPTER I LITERATURE OF STUDIES ON PYRUVATE FORMATE- LYASE: DISCOVERY, ACTIVATION-CATALYTIC MECHANISMS AND DEACTIVATION	 1
I.1. INTRODUCTION	2
I.2. EARLY WORK ON PYRUVATE FORMATE-LYASE.....	3
I.2.1. Discovery	4
I.2.2. The Formate-Pyruvate Exchange System is Oxygen-Sensitive	5
I.2.3. Activation Studies.....	5
I.2.4. “Enzyme III” and “Fraction IV” are Essential For PFL Activity.....	6
I.2.5. Enzyme II Requires Fe (II) for Activity	7
I.2.6. The Identity of “Enzyme I” and “Enzyme II”	9
I.2.7. Comparison of Reducing Systems	10
I.3. STRUCTURE OF PFL	14
I.4.THE RADICAL COFACTOR OF PFL	18
I.5. ACTIVATION OF PFL REQUIRES THE PRESENCE OF PYRUVATE OR A STRUCTURAL ANALOGUE	19
I.6. THE MECHANISM OF PFL RADICAL GENERATION.....	21
I.7. INVESTIGATIONS OF THE CATALYTIC MECHANISMS OF PFL	24
I.8. THEORETICAL STUDIES	41
REFERENCES.....	44
 CHAPTER II PFL: PURIFICATION , ACTIVATION AND STABILITY	 51
ABSTRACT	52
II.1. INTRODUCTION.....	53

II.2. MATERIALS AND METHODS	56
II.2.1. Chemicals, bacterial cells and plasmids	56
II.2.2. Bacterial production of PFL	56
II.2.3. Bacterial synthesis of PFL-AE.....	58
II.2.4. Purification of PFL.....	59
II.2.5. Determination of PFL concentration	63
II.2.6. Activation of PFL.....	67
II.3. RESULTS	71
II.3.1. Expression	71
II.3.2. Purification of PFL.....	71
II.3.3. Activation and stability of PFL	72
II.4. CONCLUSIONS	73
REFERENCES.....	74

CHAPTER III STUDIES OF ALCOHOL DEHYDROGENASE FROM *ESCHERICHIA COLI* 75

ABSTRACT	76
III.1. INTRODUCTION AND BACKGROUND	77
III.2. MATERIALS AND METHODS.....	84
III.2.1. Cloning of His₆-tagged AdhE	84
III.2.2. Extraction and analysis of PET-21⁺ (+)-adhE.....	85
III.2.3. Transformation of BL21(DE3)pLysS with PET-21a(+)-adhE	87
III.2.4. Streaking of the glycerol stocks to obtain colonies.....	88
III.2.5. Growth, Harvesting and Lysis	90
III.2.6. Purification of His₆- AdhE	91
III.2.6.1. Purification Principle	91
III.2.6.2. Purification and Analysis of His₆-tagged AdhE.....	92
III.2.7. Cloning, Growth and Purification of untagged AdhE.....	96
III.2.7.1. PCR and ligation.....	96
III.2.7.2. Transformation, plating, DNA extraction and fingerprinting	100
III.2.7.3. Growth of Cell Cultures and Purification	104
III.2.7.4. Characterization of untagged AdhE.....	110
III.2.7.5. Characterization of the His₆-tagged AdhE.....	111

III.3. RESULTS.....	115
III.3.1. Over-expression and Characterization of Untagged AdhE	115
III.3.1.1. Overexpression of untagged AdhE	115
III.3.1.2. Characterization of AdhE.....	116
III.3.2. Over-expression and Purification of His₆- AdhE	117
III.3.2.1. Test growths	117
III.3.2.2. Purification.....	118
III.3.2.3. Alcohol Dehydrogenase Activities.....	119
III.3.2.4. Iron Content of AdhE.....	123
III.3.2.5. Comparison of “as isolated” and iron-stripped AdhE activities.....	124
III.3.2.6. Effect of Fe²⁺ on the alcohol dehydrogenase activity of AdhE	126
III.3.2.7. Investigation of PFL deactivation	128
III.4. DISCUSSION.....	139
III.5. CONCLUSIONS.....	142
REFERENCES.....	143
 CHAPTER IV DEACTIVATION OF PFL BY SMALL MOLECULES.....	 144
ABSTRACT	145
IV.1. INTRODUCTION	146
IV.2. MATERIALS AND METHODS.....	147
IV.2.1. Materials	147
IV.2.2. The PFL deactivation experiment	148
IV.3. RESULTS.....	150
IV.3.1.Deactivation by DTT and β-ME.....	150
IV.3.2. Effects of Illumination on the deactivation of PFL	152
IV.3.3.Deactivation of PFL by other thiols and small molecules.....	156
IV.3.4. Investigation of PFL deactivation by other small molecules.....	157
IV.3.5. Comparison of methionine and cysteine	160
IV.3.6. Other non-thiol reducing agents	161
IV.3.7. Deactivation of PFL by β-ME is reversible.....	162
IV.3.8. Effect of the NADH/NAD⁺ Ratio on PFL Deactivation by ADHE	166
IV.4. DISCUSSION AND CONCLUSIONS.....	176
REFERENCES.....	179

CHAPTER V: MOTIVATION FOR THIS STUDY, SUMMARY OF FINDINGS AND FURTHER INVESTIGATIONS	180
V.1. MOTIVATION FOR THIS STUDY	181
V.2. ACTIVATION AND STABILITY OF PFL	183
V.2.1. Some Philosophical and Practical Considerations on Activation.....	183
V.2.2. Activation Without Intense Illumination is Advantageous.....	184
V.2.3. In vivo PFL Activation Employs A light-independent Reductant	184
V.3. STUDIES OF THE DEACTIVATION OF PFL BY ADHE.....	186
V.4. CONTEXT, RELEVANCE AND OTHER STUDIES.....	189
V.5. DEACTIVATION BY THIOLS AND OTHER REDUCTANTS.....	196
V.6. SUGGESTED EXPERIMENTS FOR FURTHER STUDIES.....	199
V.6.1. Mechanistic Studies	199
V.6.2. In vivo studies.....	199

List of Tables

Table I.1. Minimum required conditions for PFL activation.....	8
Table I.2. Catalytic Efficiency of PFL-activase in Various Reducing Systems	11
Table I.3. Minimum required conditions for PFL activation	19
Table II.1. Mixes for the Bradford assay	64
Table II.2. Typical series of standards used for calibration.....	65
Table II.3. The typical protein concentration caculated from the calibration curve.....	66
Table III.1. PCR Reaction Components	98
Table III.2. Mixes for experimental and control PETBlue-adhE fingerprinting.	102
Table III.3. Activities of crude extracts from Tuner(DE3)pLacI-adhE	106
Table III.4. Typical composition of mixes used for ADH activity of AdhE.....	110
Table III.5. Typical composition of mixes for alcohol dehydrogenase activity assay ..	112
Table III.6. Typical composition of mixes used for acetaldehyde assay.....	113
Table III.7. The components of the mix used to investigate PFL deactivation.....	130
Table III.8. Reaction mixes to investigate deactivation under anaerobic conditions....	133
Table III.9. Isolating the species responsible for PFL deactivation.	1354
Table III.10. Effect of Fe(II) on Extent of PFL Activation	137
Table IV.1. Residual PFL activities of PFL with small molecules.....	159
Table IV.2. Mixes to study effect of NADH/ NAD ⁺ on PFL deactivase of AdhE.	168
Table IV.3. Mixes for investigation of NADH and AdhE effect on PFL deactivation .	174

List of Schemes

Scheme I.1. The first committed step in pyruvate catabolism following glycolysis	3
Scheme I.2. The two steps of the anaerobic pyruvate “dissimilation	4
Scheme I.3. The Structural Formulae of Pyruvate and Oxamate.....	19
Scheme I.4. The overall reaction catalyzed by PFL.....	25
Scheme I.5. The Ping-Pong Mechanism proposed by Knappe and co-workers	26
Scheme I.6. The mechanism of PFL action as proposed by Kozarich and co-workers...	28
Scheme I.7. Formation of the acety-PFL radical intermediate	30
Scheme I.8. Hypophosphite and acetyl-PFL; acetylphosphinate and active PFL	33
Scheme I.9. The salt bridge between oxamate and Arg 435 in the active site of PFL.....	35
Scheme I.10. Chemical structures of pyruvate and alpha-oxobutyrate.....	36
Scheme I.11. Comparison of residues found at the active sites of TdcE and PFL.....	37
Scheme I.12. Proposed mechanism of transfer of the radical and acetyl group of PFL ...	38
Scheme I.13. The mechanism proposed by Knappe and co-workers.	39
Scheme I.14. Mechanism Proposed by Himo and Siegahn.....	43
Scheme II.1. A structural depiction of the activation of PFL	53
Scheme III.1. A Schematic of glycolysis.....	78
Scheme III.2. TCA: acetyl-CoA oxidation, production of the NADH and FADH ₂	79
Scheme III.3. Reduction of pyruvate to ethanol during alcoholic fermentation.....	81
Scheme III.4. Two reactions catalyzed by AdhE.	82
Scheme III.5. The reaction catalyzed by PFL.....	82
Scheme III.6. The proposed role of AdhE as a PFL deactivase	83
Scheme III.7. The ADH/acetaldehyde reductase reaction catalyzed by AdhE	112

Scheme III.8. The coupled enzymatic assay for the PFL activity.....129

Scheme IV.1. Enzymatic activity assay used to monitor residual activity of PFL 149

List of Figures

(Images in this dissertation are presented in color)

Figure I.1. Plot of redox potentials necessary for PFL activation.....	10
Figure I.2. Time course of the activation of PFL with variously treated PFL-activase ...	12
Figure I.3. Anaerobic gel filtration chromatograph of activation mixture.	13
Figure I.4. Cartoons of the partial crystal structure of PFL	16
Figure II.1. A Chromatogram of PFL purification by ion exchange.	60
Figure II.2. SDS-PAGE of PFL fractions obtained from the first.	61
Figure II.3. A chromatogram from the second purification of PFL	62
Figure II.4. Calibration curve used to calculate the concentration of PFL.....	66
Figure II.5. The EPR spectrum of the glycy radical on activated PFL	68
Figure II.6. A time course activation of PFL under ambient light and 23°C.....	69
Figure III.1. The primers used to amplify the AdhE gene of <i>E. coli</i> by PCR..	84
Figure III.2. Fingerprints of DNA digested with Xho 1 and <i>BamH</i> -1..	86
Figure III.3. Streaking a glycerol stock onto an agar plate for overnight incubation.	89
Figure III.4. Typical appearance of colonies after overnight incubation..	89
Figure III.5. Ni is coordinated to a nitrilotriacetic acid (NTA) support.	91
Figure III.6. Interactions between NTA-bound nickel and histidines from the His ₆	92
Figure III.7. Effect of protein load on purification quality.	94
Figure III.8. The oligonucleotide primers used to amplify untagged AdhE.	97
Figure III.9. The <i>adhE</i> PCR product for the untagged AdhE.....	99
Figure III.10. Agarose gel of PETBlue- <i>adhE</i> plasmid digested with Sca1.....	103
Figure III.11. DNA finger-prints of plasmids extracted from colonies 2, 3 and 4.....	104
Figure III.12. Overexpression of untagged AdhE by colonies 1 and 2.....	105

Figure III.13. Whole cell SDS-PAGE of Tuner (DE3) pLacI cells	115
Figure III.14. AdhE lacking a His ₆ tag was also partially purified by gel filtration.. ...	116
Figure III.15. SDS-PAGE of BL21(DE3) cells transformed with PET21a ⁽⁺⁾ -adhE.	117
Figure III.16. The level of purity achieved for His ₆ -tagged AdhE using a Ni-NTA	119
Figure III.17. Acetaldehyde reductase/alcohol dehydrogenase activities of by AdhE..	121
Figure III.18. Activity was measured by monitoring ΔA_{340} of NADH	122
Figure III.19. Correlation between the amount of AdhE and Fe.....	123
Figure III.20. Comparison of specific activity of apo-AdhE and holo-AdhE	125
Figure III.21. Effect of Fe ²⁺ on the activity of holo- and apo-AdhE.....	126
Figure III.22. Time course of PFL deactivation by AdhE, NAD ⁺ , Fe ²⁺ and CoA... 13129	
Figure III.23. Time course of PFL deactivation by AdhE, NAD ⁺ , Fe ²⁺ and CoA.... 1321	
Figure III.24. PFL deactivation using various combinations of cofactors and AdhE.. 1332	
Figure III.25. Isolation the component responsible for PFL deactivation.....	1353
Figure III.26. Effect of Fe (II) in the reactivation of PFL.....	135
Figure III.27. Effect of Fe (II) on the reactivation of PFL.....	137
Figure IV.1. Small molecules used in deactivation studies.....	147
Figure IV.2. The effect of DTT and β -ME on the activity of PFL	151
Figure IV.3. The effect of DTT on the activity of PFL over extended period of time... 152	
Figure IV.4. Effect of DTT and β -ME on the activity of PFL under ambient light.	153
Figure IV.5. Deactivation of previously reactivated PFL	155
Figure IV.6. PFL deactivation properties of ethanethiol, DTT, and β -ME..	156
Figure IV.7. Comparison of deactivation rates of various thiols and small molecules.. 158	
Figure IV.8. Comparison of methionine and cysteine as PFL deactivators.	160

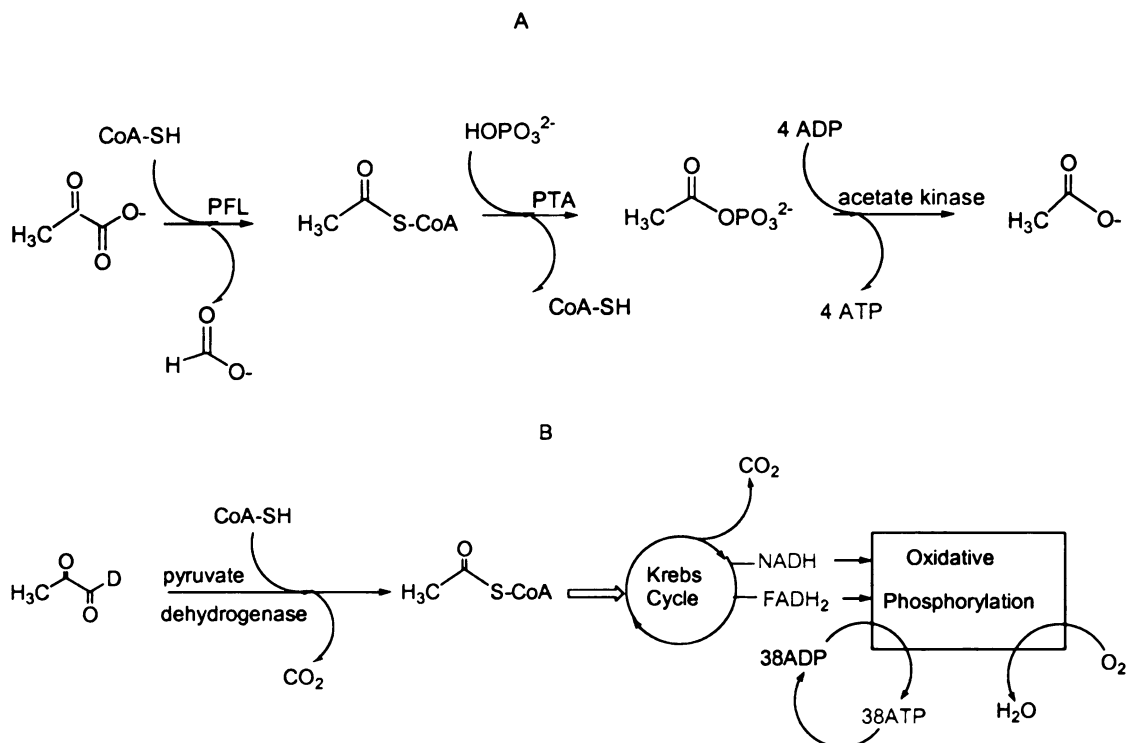
Figure IV.9. Effect of non-thiolic reductants on the activity of PFL.....	162
Figure IV.10. PFL deactivation by β -ME.	164
Figure IV.11. Effect of different NADH/NAD ⁺ ratios and AdhE on PFL activity	169
Figure IV.12. The residual PFL activities after 9 hours of incubation..	171
Figure IV.13. PFL activation-deactivation cycles in the reaction mixes.....	172
Figure IV.14. The effect of NADH and AdhE on the activity of PFL.	175

CHAPTER I

LITERATURE OF STUDIES ON PYRUVATE FORMATE-LYASE: DISCOVERY, ACTIVATION-CATALYTIC MECHANISMS AND DEACTIVATION

I.1. INTRODUCTION

As a facultative anaerobe, *Escherichia coli* (*E.coli*) is capable of growing under both aerobic and anaerobic conditions. In the presence of oxygen, this organism metabolizes glucose via a pathway that employs pyruvate dehydrogenase to convert pyruvate to acetyl-CoA. The next step in this pathway is the consumption of acetyl-CoA in the Krebs's cycle, wherefrom oxidative phosphorylation leads to the production of 38 molecules of ATP per glucose molecule. However when conditions are anaerobic, an alternative metabolic route is followed, whereby pyruvate formate-lyase (PFL) catalyses the reversible and non-oxidative cleavage of pyruvate to acetyl-CoA and formate.¹ The acetyl-CoA is then fed into an alternative metabolic pathway that generates only 4 molecules of ATP per molecule of glucose. Thus, pyruvate dehydrogenase and pyruvate formate-lyase catalyze the first committed aerobic and anaerobic metabolic steps, respectively, in the catabolism of the pyruvate generated by glycolysis. The two reactions are summarized in Scheme I.1, where **A** represents the anaerobic reaction and **B** represents the reaction under aerobic conditions. Though adaptable to both aerobic and anaerobic conditions, *Escherichia coli* (*E.coli*) grows more efficiently under aerobic conditions, as more ATP is produced per molecule of glucose, reverting to the anaerobic catabolic route only when necessary.

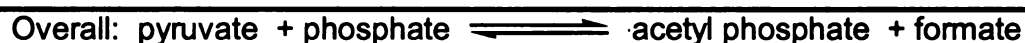
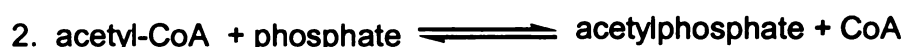
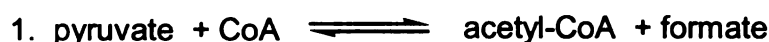


Scheme I.1. The first committed step in pyruvate catabolism following glycolysis under aerobic conditions (A) and anaerobic conditions (B). PFL, Pyruvate formate-lyase; PTA, phosphotransacetylase.

I.2. EARLY WORK ON PYRUVATE FORMATE-LYASE

I.2.1. Discovery

The anaerobic “dissimilation” of pyruvate was first discovered in 1943 by Kalnitsky and Werkman.² Lipmann and Tuttle later found that cell extracts of *E.coli* required prolonged incubation under assay conditions in order to induce the dissimilation activity.³ From the work of Chantrenne and Lipmann and that of Stadtman the “dissimilation” reaction was recognized as proceeding in two steps as shown in Scheme I.2.^{4,5}



Scheme I.2. The anaerobic pyruvate “dissimilation” reaction was found to occur in two steps

Other characteristics of the PFL dissimilation activity from various species were investigated by several other workers including Asnis and co-workers, who observed that the dissimilation activity in *E. coli* was stimulated by addition of boiled extracts of yeast, whereas for both *E. coli* and *Micrococcus lactilyticus*, stimulation could be achieved by adding extracts of the respective organisms heated to 65°C.^{6,7,8} These observations suggest the involvement of non-protein co-factors in the reactions. The intriguing cleavage of the C-C bond of pyruvate in the first step of pyruvate dissimilation, catalyzed by the enzyme now known as pyruvate formate-lyase (PFL), led several workers to

investigate the mechanism by which this cleavage occurs, and this reaction has continued to attract the interest of researchers from a broad spectrum of specializations.

1.2.2. The Formate-Pyruvate Exchange System is Oxygen-Sensitive

During some of their early work on the activity of PFL, Knappe and co-workers observed that during the dissimilation reaction there was a time lag of several minutes before formate was produced, after which it was produced at a constant rate. They attributed this to poisoning of at least one of the essential reaction components by residual oxygen. In order to test this hypothesis, they added several oxygen-removing reagents to the substrate mixture of the assay system. Since the enzyme mix was already supplemented with Fe(II), it was assumed to be already oxygen-free and was therefore not treated with any of these oxygen-removing reagents. Interestingly, the previously observed time lag was abolished by addition of these reagents, thus supporting the hypothesis that the delay in pyruvate production had been due to poisoning of the PFL activity by oxygen. It is now known that PFL must be post-translationally activated, with the activation requiring strictly anaerobic conditions due to the PFL activating enzyme (PFL-AE), and that the activated PFL is also very oxygen sensitive.^{9,10} Essentially all reactions of PFL are therefore carried out under strictly anaerobic conditions.

1.2.3. Activation Studies

In 1965 Knappe and co-workers demonstrated that the pyruvate dissimilation activity required the presence of two (then unidentified) protein factors and S-adenosyl-L-methionine (SAM).¹¹ Wood had previously used isotopic labeling to show that the

exchange reaction between formate and the C-2 carbon of pyruvate proceeds at a physiologically significant rate, and therefore Chase and Rabinowitz were able to use this exchange reaction to measure catalytic activity by mixing ^{14}C -labeled formate with unlabelled pyruvate in the presence of PFL.^{12,13} Since both reactions shown in Scheme I.2 are reversible, incorporation of ^{14}C was used as evidence that reaction (1) had taken place and therefore that the pyruvate “dissimilation” activity was present. They referred to the activity as pyruvate formate-lyase and to the enzyme responsible for this exchange simply as “the formate-pyruvate exchange system”.¹³ From this study, these workers were able to establish that the pyruvate formate-lyase activity was stimulated by the presence of both pyruvate and SAM and that the effect of the two components was additive.¹³ The work of Knappe and co-workers using sedimentation and anaerobic sucrose gradient techniques revealed for the first time that there were at least four components involved in the pyruvate formate-lyase reaction, which they referred to simply as enzymes I, II, III and fraction IV.¹⁴ Based on subsequent investigations using primarily ultraviolet-visible spectroscopy and gradient centrifugation techniques, this team was able to identify enzyme III as a flavoprotein containing 1 molecule of flavin mononucleotide (FMN). Fraction IV was not identified, but it was recognized to be a protein.¹⁵

I.2.4. “Enzyme III” and “Fraction IV” are Essential For PFL Activity

Further investigation showed that exclusion of either one of “enzyme III” or “fraction IV” abolished PFL activity, whereas substitution of Co(II) / thiol for both afforded PFL activity.¹⁴ Consequently, these investigators suggested that “enzyme III”

and “fraction IV” only play an auxiliary role in the PFL reaction.¹⁴ Based on the fact that Co^{2+} and thiols form strongly reducing complexes, these researchers suggested that the role of enzyme III and fraction IV in the PFL reaction is to provide an appropriate redox potential via pyruvate as an electron donor.¹⁶ For the first time this group demonstrated that, in the presence of either one of the auxiliary systems (Co(II)/thiol or enzyme III/enzyme IV), the only other condition necessary for pyruvate formate-lyase activity was the interaction of enzyme I, enzyme II and SAM.¹⁶ The fact that these two pairs of components were essential but interchangeable suggested that they played a vital role in the activity of the system but did not interact with the “pyruvate-formate exchange system” in a specific manner.

1.2.5. Enzyme II Requires Fe (II) for Activity

Contrary to the previously held view that the primary role of iron was to scavenge for oxygen, subsequent studies had shown that cobalt (II) competitively interfered with Fe (II) to inhibit pyruvate dissimilation in the “pyruvate-formate exchange system”, thus leading Knappe and co-workers to conclude that iron actually binds to enzyme II as a prosthetic group.^{14,15} Furthermore, incubation of Fe-reconstituted enzyme II with a chelating agent afforded retention of a significant amount of activity, thus suggesting that Fe was indeed tightly and specifically bound by the enzyme.¹⁴ Having shown that Fe (II) was essential for the “pyruvate-formate exchange reaction”, it became necessary to identify the exact component of the system whose activity required Fe (II). In pursuit of this, a series of reactions were performed in which various components of the exchange reaction system were pre-incubated with Fe (II) before the reaction was initiated. The

extent of reaction was then determined by measuring the total amount of formate produced when the components were mixed.

The various pre-incubations investigated are listed in Table I.1, in which the amounts of formate produced upon mixing the components together (right column) were used as an indicator of the activity of the system. The results demonstrated unequivocally that pre-incubation with Fe (II) was essential for the activity of “enzyme II” but had no effect on “enzyme I”. Dithiothreitol (DTT) was also proved necessary for significant activity of the “exchange system”. However, based on this data it was not possible to determine which of “enzyme I” or “enzyme II” required DTT.

Table I.1. Initial Turnover Results Identifying Minimal Required Conditions for PFL activity¹⁴

Components preincubated with Fe(II) and DTT	μmoles of formate formed
Enzyme I plus enzyme II	1.70
Enzyme I	0
Enzyme II	1.71
Enzyme I plus enzyme II without Fe ²⁺	0
Enzyme I plus enzyme II without dithiothreitol	0.1

The data in Table I.1 clearly identified enzyme II to be the one specifically activated by pre-incubation with Fe (II), while Co (II) was not able to activate enzyme II, and was indeed found to be inhibitory to activation.¹⁴ The findings from this work led to the first suggestion that the pyruvate formate-lyase reaction is catalyzed by the interaction of “enzyme I” and “enzyme II”. The kinetics of the PFL reaction suggested that the nature of the interaction of “enzyme II” with enzyme I during the PFL reaction was catalytic, since the amount of formate produced was found to be dependent only on the

amount of “enzyme I”.¹⁴ These kinetics were observed when Fe (II) was used alone, or when it was present in excess over Co (II). However, when Co (II) was present in excess, the rate of formate production depended on both the concentration of both “enzyme I” and “enzyme II”, indicating that enzyme II was activated by binding Fe (II), and that Co (II) competed with Fe (II) for the binding site on the enzyme but was itself not a viable co-factor.¹⁴

1.2.6. The Identity of “Enzyme I” and “Enzyme II”

The work of Knappe and co-workers shed some more light into the identity of the components required for pyruvate formate-lyase activation and also corroborated a previous investigation in which it was established that “enzyme I”, now known as pyruvate formate-lyase (PFL), was a polypeptide of molecular weight of about 140 kD, which could be converted from an inactive to an active form upon interaction with “enzyme II”, now known as the pyruvate formate-lyase activating enzyme (PFL-AE).^{14,15} PFL-AE was confirmed to have a molecular weight of about 30 kD as previously reported and was shown to require pre-incubation with iron and a thiol in order to convert PFL to the catalytically active form.¹⁵ The essential role of S-Adenosyl-L-methionine (SAM) was again recognized but was at this point believed to be only allosteric. It was of interest, however, that in addition to the requirement for the absence of oxygen in the reaction mix, PFL activation was found to be more efficient under highly reducing conditions.¹⁵

At potentials above -390 mV (more oxidizing), no activation was detected, whereas optimum activation was achieved at -440 mV (Figure I.1). Once activated and bound to its substrate (pyruvate), however, PFL was observed to become dramatically

more stable, converting to its inactive form only when conditions were more oxidizing than -170 mV (Figure I.1 B).¹⁶ This turned out to be of practical advantage as it suggested a means to trap activated PFL by adding pyruvate, as demonstrated by Chase and Rabinowitz.¹³

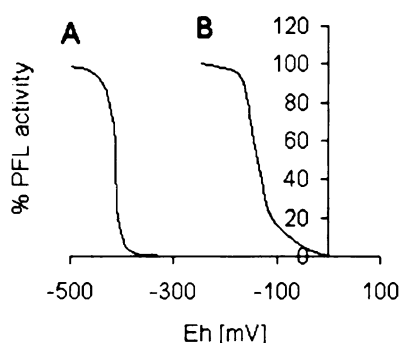


Figure I.1. Plot of redox potentials necessary for PFL activation (A) and stability of the PFL-pyruvate complex. In the presence of the substrate (pyruvate) active PFL was shown to withstand relatively highly oxidizing conditions, only breaking down when conditions became more oxidizing than about -170 mV (B).¹⁶

I.2.7. Comparison of Reducing Systems

A number of reducing systems were investigated in an effort to identify one with the most suitable potential for the activation reaction.¹⁶ Although all of the experiments were carried out in vitro, they shed some light on the broader aspects regarding the nature of the reductant components involved in the activation of PFL.¹⁶ At least four reducing systems, including 3 mM Fe^{2+} / 12 mM 2,3-dimercaptopropanol and 4 mM Co^{2+} /12 mM

DTT, were shown to be suitable for achieving the potential required for PFL activation.¹⁶ However, using photo-reduced flavodoxin, it was observed that the PFL-activase had a higher catalytic efficiency as shown in Table I.2.¹⁶ This reducing system was therefore employed for the subsequent studies of PFL activation.

♦**Table I.2.** Catalytic Efficiency of PFL-activase in Various Reducing Systems

Reducing System	PFL _{inactive} (μg)	PFL-activase (μg)	PFL _{active} (units)
Co ²⁺ -DTT	16	50	1.8
Fe ²⁺ -dimercaptopropanol	16	50	1.2
Photoreduced Flavodoxin	16	50	8.6
	800	50	395

1 unit corresponds to 1 μmole of formate formed per hour at 28°C. ♦ Adapted from reference; Metabolic Interconversion of Enzymes, Springer, Berlin Heidelberg New York, pp319-329, Ed.: Wieland, O; Helmreich, E; Holzer, H.

Further support for the suggestion that ferrous iron actually binds to PFL-AE came from two important experiments. In the first experiment, the activation reaction was carried out using PFL-AE that had been previously incubated with ferrous iron and DTT, leading to successful activation of PFL.¹⁶ The other experiment was done similarly, except that PFL-activase was incubated in 10 mM Trion (a strong iron-chelating agent) for 10 minutes.¹⁶ The activation of PFL with activase from this incubation was significantly reduced (Figure I.2).¹⁶ The third data set shows that in the absence of adenosylmethionine, essentially no activity is observed, therefore indicating that it is likely an essential component in the reaction rather than an allosteric effector as previously postulated.

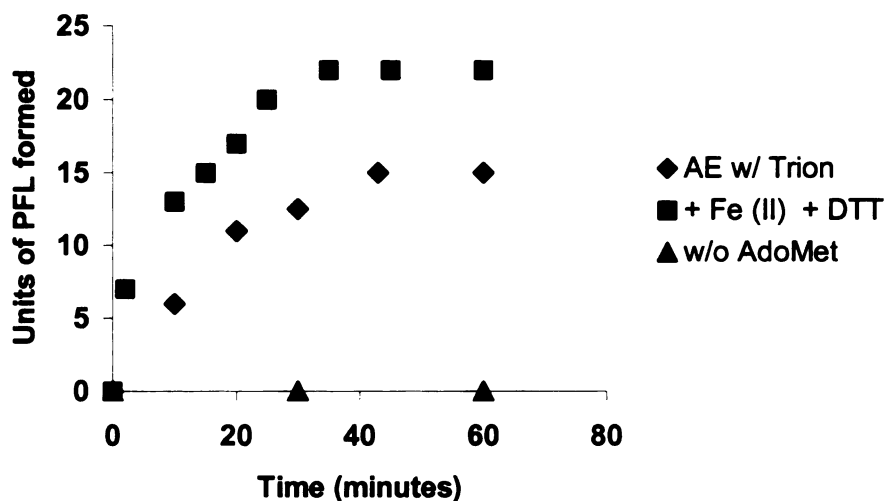


Figure I.2. Time course of the activation of PFL (32 μ g) with variously treated PFL-activase (217 μ g). The reducing agent used was Co^{2+} /DTT.¹⁶

Kinetic studies showed that the rate of PFL activation is a function of both inactive PFL and PFL-activase, thus indicating that the activation process involves direct interaction between the two proteins.¹⁵ Chromatographic studies (Figure I.3), however, showed that activated PFL elutes out of a gel filtration column at the same buffer volume as inactive PFL. In addition, no PFL-activase was detected in the peak of active PFL. Previously, sedimentation studies by Knappe and co-workers had shown that the molecular dimensions of PFL do not change upon activation.¹⁴ Taken together, these findings strongly suggested that though both proteins interact with each other during the activation reaction, they do not bind to each other to form a complex.

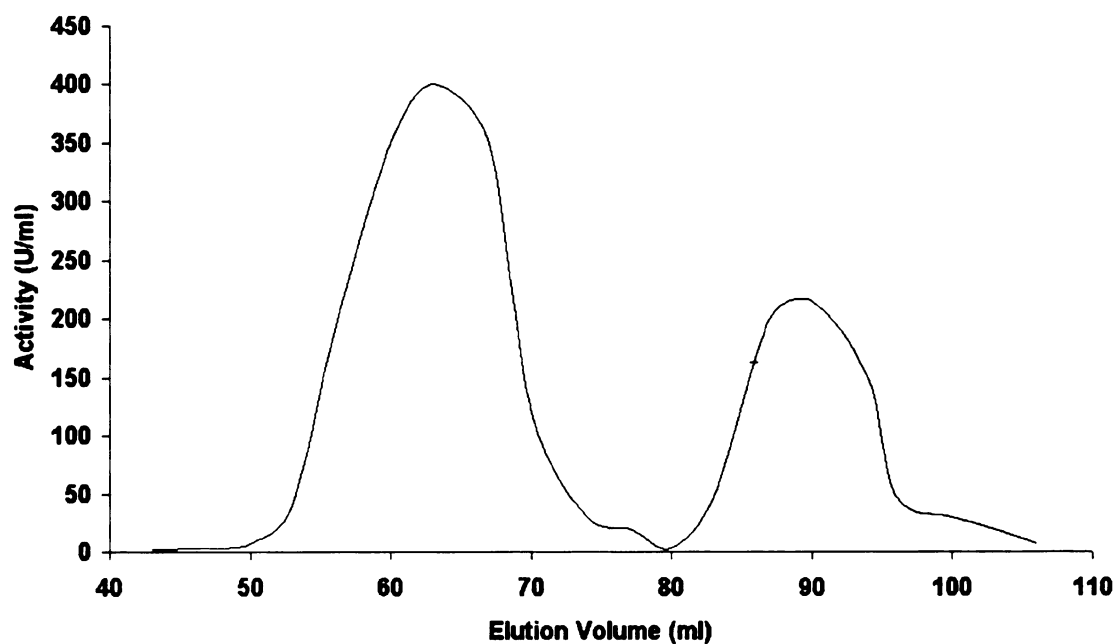


Figure I.3. Anaerobic gel filtration chromatograph of a PFL activation mixture on Sephadex G-100. The peaks at 63 ml and 90 ml correspond to active PFL and PFL-activase respectively.¹⁶

I.3. STRUCTURE OF PFL

PFL is a homodimeric enzyme consisting of 85,000 dalton monomeric subunits, thus making PFL a 170,000-dalton enzyme. Goldman and co-workers, following on earlier work by Knappe and others, reported the first well resolved crystal structure of a PFL fragment.^{17,18} The crystal structure solved by Knappe and co-workers³¹ earlier had been poorly resolved because of the difficulties encountered obtaining isomorphous heavy metal derivatives, “due to the pair of the adjacent cysteines (C418 and C419).”³⁰ Goldman and co-workers circumvented this challenge by using a combination of both multiple isomorphous replacement with anomalous scattering (MIRAS) and multiple wavelength anomalous diffraction (MAD). They were able to obtain a well-resolved electron density map of residues 4-614 (Figure I.4.). The first three and last ten residues were found to be disordered and were therefore excluded from the structure analysis. The structure was fine-tuned by truncating to alanine those surface loops and residues that showed weak density. The refined crystal structure was resolved to 2.8 Å with an R factor and R_{free} of 22.8 and 25.2 respectively.

Structurally, the protein was found to comprise two domains consisting of parallel barrels with large excursions (Figure I.4). The overall structure was found to resemble a right hand with fingers slightly curved in and the thumb folded from the right across the palm. Significantly, the catalytically essential C418 and C419 are located on the thumb. Viewed from the top of the barrels, the structure resembles the capital letter G written backward, with the thumb located on the inside and a β -finger on the outside curvature of the letter (Figure I.4 B). These workers thus referred to the barrel as the “G-barrel”.¹⁷

The excursions wrap around the G-barrel and create the finger domain. Goldman and co-workers established that there are a total of five “up” and three “down” strands all forming part of the α/β barrel. C419 and C418 reside on a unique β -finger that links the two sets of β -sheets. One of the significant findings from this work is that PFL has structural homology to anaerobic ribonucleotide reductase III (RNR-III), an enzyme that, in its active form, also harbors a glycine-centered radical.²⁰ Both PFL and RNR-III also require SAM and an activating enzyme for the generation of the glycy radical co-factor.^{48,20} These two enzymes have also been shown by several workers to have extensive structural and mechanistic similarities.^{49,8,10} Subsequently, it was discovered that the activating enzymes for both belong to the same superfamily of SAM-dependant radical enzymes referred to as the “Radical SAM Superfamily.”⁵¹

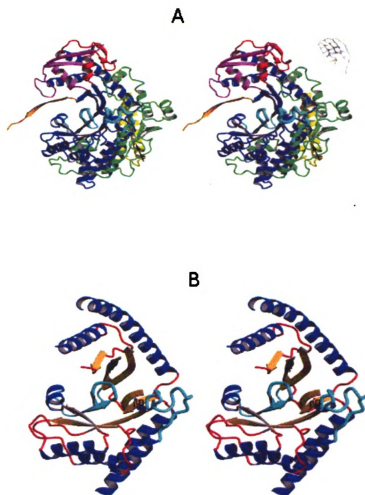


Figure I.4. MOLSCRIPT and Raster3D Cartoons of the partial crystal structure of PFL as solved by Goldman and co-workers (adapted from reference 17). Helices are shown as spirals and strands as ribbons. **(A)** The overall fold of PFL in stereo, shown from the front to emphasize the right-hand nature of the structure. A right hand is drawn to the side for comparison. The three large *excursions* are labeled E1, E2 and E3. **(B)** The left-handed G-barrel of PFL in stereo, viewed from the ‘top’ where substrate enters. The secondary structure elements are labeled.¹⁷

In a later study, Becker et al. reported the crystal structure of full length but inactive PFL co-crystallized with oxamate, as well as the crystal structure of the double mutant C418A, C419A.⁵⁰ Whereas the previous workers had concluded that there were three “down” strands,²⁰ these workers described the structure as comprising a “10-

stranded α/β barrel assembled in an anti-parallel manner from two parallel five-stranded β -sheets.”⁵⁰ However, the Becker structure also confirmed the earlier observation by Goldman and co-workers that PFL bears homology to RNR-III.¹⁷

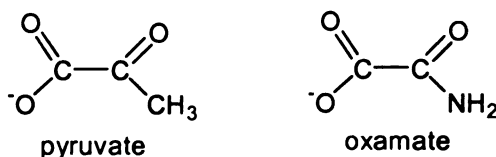
It is noteworthy that due to the difficulty of obtaining isomorphous heavy-metal derivatives for PFL, Becker et al. capitalized on the fact that the reflection intensities of the double mutant (C418A/C419A) crystals have very good correlation to those of the data of wild type PFL co-crystallized with oxamate. They therefore used a difference Fourier technique to elucidate the wild-type structure and its complex with oxamate.⁵⁰ From this work it was established that G734 and C419 are located at the tips of two opposing loops, again showing consistency with the findings of Goldman and co-workers.¹⁷ Furthermore, this work revealed that the two residues meet at the center of the barrel structure. The catalytically essential C418 was also confirmed to be in juxtaposition with C419, and oxamate was found to be lodged in a tight cleft with C2 symmetry at a distance of only 3.3Å from the sulfur of C418. The sulfur atoms of C418 and C419 were found to be 3.7Å apart.

I.4. THE RADICAL COFACTOR OF PFL

Active PFL exists as a radical.²⁰ Knappe and co-workers, through C-13 and N-15 isotopic labeling techniques and EPR spectroscopy first identified the exact location of the radical.²² The splitting of the EPR signal observed as a result of coupling between the spins of the glycy radical and the isotopically labeled atoms was used as the main analytical tool in this investigation. This study also revealed that the activation process involves the abstraction of the pro-S hydrogen of the Gly-734 residue by a 5'-deoxyadenosyl radical, as proven by incorporation of the hydrogen isotopic label into 5'-deoxyadenosine.²² In addition, when active PFL was exposed to oxygen, it underwent rapid oxidative cleavage leading to the formation of two fragments of 82 and 3 kDa respectively. N-terminal block on the 3 kDa fragment and analysis by mass spectrometry identified the small fragment as an oxylyl residue derived from G734, thus assigning the position of the glycy radical to G734. Following this assignment, the vast majority of work done on PFL was centered on the questions 1) what is the mechanism by which the glycy radical of activated PFL is generated? and, 2) how does active PFL proceed to mediate homolysis of the C-C bond during catalytic pyruvate turnover. The first of these questions involves the participation of another enzyme, namely, pyruvate formate-lyase activating enzyme (PFL-AE). Both of these questions have continued to receive a great deal of attention from several researchers.^{9, 33, 45}

I.5. ACTIVATION OF PFL REQUIRES THE PRESENCE OF PYRUVATE OR A STRUCTURAL ANALOGUE

The observation that PFL activation required the presence of the substrate, pyruvate, raised the question as to whether the activation of PFL and its subsequent catalysis of pyruvate homolysis were intimately related, or whether the two processes were separate and distinct from one another. To address this question, PFL was activated in the presence of pyruvate and its structural analogue oxamate, which does not act as a substrate, in separate reactions (Scheme I.3). As a negative control, another activation reaction was carried out in the absence of both pyruvate and oxamate and a fourth was done in the absence of SAM. The level of PFL activity was measured and the results are shown in Table I.3. Oxamate was found to have the same effect on the activation of PFL as pyruvate both qualitatively and quantitatively. There was no detectable difference in the extent of PFL activation when using oxamate instead of pyruvate as indicated by the data on Table I.3.



Scheme I.3. The Structural Formulae of Pyruvate and Oxamate.

Table I. 3. Minimum required conditions for PFL activation¹⁶

Activation reaction	Active PFL units
Complete including pyruvate	6.2
Without pyruvate	0.1
Pyruvate replaced by oxamate	6.5
Without S-Adenosyl-L-adenosyl methionine	0

It was significant that oxamate proved to be non-competitive to pyruvate for activated PFL in the dissimilation reaction, in spite of its facility to replace pyruvate in the activation reaction.¹⁶ This observation led to the suggestion that oxamate (and therefore pyruvate) probably has a regulatory role, whereby it binds to the activating enzyme, as was also suggested for SAM.¹³ More recently, however, Knappe and co-workers solved the crystal structure of the double mutant of PFL (C418S, C419S) co-crystallized with both pyruvate and oxamate, from which they were able to show that both these molecules do bind to PFL.²⁶ Interestingly, and perhaps uniquely, pyruvate and oxamate are not just allosteric effectors; they actually bind to the active site of PFL. The binding of pyruvate to PFL, therefore, presumably results in an essential conformational change on the enzyme, which in turn, affords the subsequent steps leading to activation.

I.6. THE MECHANISM OF PFL RADICAL GENERATION

The work of Conradt et al. revealed that PFL is translated in an inactive form (PFL_i) and is subsequently converted to the active form (PFL_a) by a sophisticated post-translational mechanism involving an activating enzyme (PFL-activase) and a number of co-factors.¹⁹ Owing to the work of Knappe and co-workers, it is now well accepted that the active form of PFL comprises a glycy radical that is produced by abstraction of a hydrogen atom at Gly-734.²⁰

Based on EPR spectroscopy and isotopic labeling techniques, active PFL has been shown to consist of a free radical co-factor located on the protein backbone.^{19,20} Knappe and co-workers further probed the mechanism by which the radical at G734 is generated.²² They activated PFL by illuminating a mix containing PFL, PFL-AE, riboflavin as a photoreductant, oxamate as an allosteric effector, 5'-deoxyadenosyl-L-methionine, and DTT, all in MOPS buffer, pH 7.2. By using deuterium labeling at G734 and nuclear magnetic resonance (NMR) and mass spectrometric (MS) analyses, they observed that ²H was stoichiometrically incorporated at the methyl group of 5'-deoxyadenosine, a byproduct of the activation reaction.²² In the same study, this team used synthetic short chain peptides to model the region containing G734. The objective was to gain insight into the features of the active site that are responsible for recognition between PFL and PFL-AE. The approach entailed identification of peptides that are able to produce ¹⁴C-labeled 5'-deoxyadenosine from ¹⁴C-labeled SAM under activation conditions. Significantly, and as predicted, the models that showed activity in this respect also proved to be competitive inhibitors to PFL during activation, that is, to the generation of the G734 radical.²² A small peptide of sequence Arg-Aal-Ser-Gly-Tyr-Ala-

Val, corresponding to the sequence of residues 731-737 of PFL, was used as the model to investigate the interaction between PFL and PFL-AE. The results of this investigation showed that substitution of glycine for L-alanine preserved the affinity of the peptide for PFL-AE, whereas replacement with D-alanine abolished the affinity, thus proving that interaction between PFL and its activating enzyme is stereospecific with respect to Gly734. Taken together with the observed incorporation of ^2H into 5'-deoxyadenosine at the methyl carbon (as determined by isotopic labeling and mass spectrometry), two conclusions were reached:

- 1) The abstraction of the hydrogen at C-2 of G734 is stereospecifically pro-S
and
- 2) The abstracting chemical species is a 5'-deoxyadenosyl radical.

At this point, however, the involvement of the 5'-deoxyadenosyl radical was only based on strong circumstantial evidence, rather than direct observation, and the PFL radical was surmised to reside on a β -turn segment of PFL.²² At this point, the nature of and the mechanism operational at the active site of PFL were not well understood.

Based on work done previously by various other workers, the solvent exchangeability of the G734 hydrogen had been unequivocally established through isotopic labeling and EPR techniques. It was now known, for instance, that activation of PFL in D_2O resulted in a singlet EPR signal as opposed to the doublet (due to spin-coupling to the α -hydrogen) observed when the activation was carried out in H_2O .²³ It was also known at this point, primarily due to the work of Gautney and Miyagawa²⁴, that the glycyl radical undergoes hydrogen exchange both intra- and inter-molecularly, with the former being too rapid to be observed by EPR.²³ Indeed it was on the basis of these

findings that Knappe and co-workers suggested that the α -hydrogen of G734 must have an uncharacteristically low pK_a .²⁰

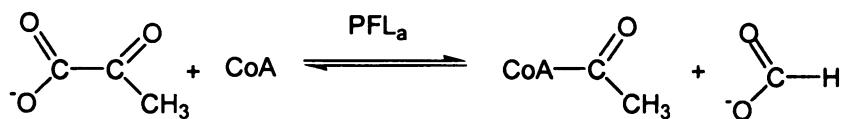
In order to push the frontiers of understanding of the mechanistic features of the exchange reaction further, Kozarich and co-workers carried out site-directed mutagenesis and mechanism-based inactivation studies on PFL.²³ They discovered that when wild type PFL, or the mutants C418S and C419S were activated in H_2O , EPR recorded doublet signal. The doublet arose from magnetic coupling between the radical on Gly734 and hydrogen on the α -hydrogen. When activated wild type PFL is incubated in D_2O , an exchange takes place between the α -H and D. This exchange between the magnetically active α -hydrogen with deuterium from D_2O results in the EPR doublet collapsing into a singlet. When Kozarich and co-workers activated wild type PFL and the mutants C418S and C419S in H_2O , followed by equilibration with excess D_2O , the glycy radical EPR signal of the C418S mutant and wild type PFL collapsed from the characteristic doublet to a singlet, whereas the signal remained a doublet in the case of C419S. This finding provided evidence that the α -hydrogen in the C418S mutant exchanges with deuterium from the solvent and that this exchange does not involve C418. On the other hand, the fact that the glycy radical EPR signal of C419S remained as a doublet, even after incubating with D_2O over a relatively extended period of time, proved that C419 is directly involved in the mechanism of α -hydrogen exchange between G734 and solvent. This finding would prove to be one of the fundamental considerations in subsequent proposals of the mechanism by which PFL accomplishes the homolytic cleavage of pyruvate during catalytic turnover.

I.7. INVESTIGATIONS OF THE CATALYTIC MECHANISMS OF PFL

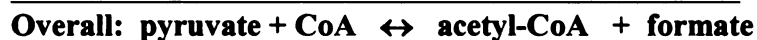
One of the significant findings in the investigation of the catalytic mechanism of PFL was the discovery that active PFL can be acetylated with preservation of the radical cofactor. The acetyl-PFL intermediate was generated by incubating active PFL with pyruvate in the absence of CoA and formate.²³ Exclusion of CoA eliminated the conditions necessary for turnover, as this coenzyme is the co-substrate for PFL. Formate was excluded from the reaction in order to ensure that the position of the equilibrium was favorable for the production of detectable amounts of acetylated PFL, as formate is one of the products of the acetylation reaction. The effect of PFL acetylation on hydrogen exchange was helpful in shedding some light on the catalytic mechanism of PFL.²³ Consistent with the findings of Unkrig and co-workers²⁵, the EPR signal of acetylated PFL was found to be a doublet identical to that of free PFL. When acetylated PFL was incubated in D₂O, the doublet collapsed into a singlet, once again indicating that the α -hydrogen is still solvent exchangeable. This observation, taken together with the observation that mutation of C419 abolishes hydrogen exchange between G734 and solvent²³, provided indirect evidence that acetylation of active PFL takes place at C418.

After the aforementioned studies and the data obtained therefrom, the conditions required for activation of PFL were reasonably well established. Another intriguing question that needed to be addressed, however, involved the mechanistic details by which activated PFL mediates the non-redox homolytic cleavage of the C-C bond of pyruvate to transfer the acetyl group to CoA and produce formate in the process. Knappe and co-workers probed this mechanism by using elegant inhibition kinetics experiments.¹⁵ When they added formate to the PFL reaction mix and measured the rate of CoA consumption,

they observed competitive inhibition. Given that the overall PFL-catalyzed reaction can be represented as in Scheme I.4, competitive inhibition of the CoA-pyruvate reaction by formate suggested that the reaction had to involve a second step in the mechanism. However, when the experiment was repeated by varying pyruvate instead, inhibition was found to be non-competitive, suggesting that formate and pyruvate do not compete for a common reactant.¹⁵ These observations led these workers to propose the “ping-pong” mechanism depicted in Scheme I.5.¹⁵ According to this proposed mechanism, the acetyl group from pyruvate is transiently transferred to the active PFL to form the acetylated active PFL intermediate. Since reaction in the first step (a) is reversible, addition of formate shifts this reaction to the left, thereby decreasing the amount of PFL-acetyl available to react with CoA to yield



Scheme I.4. The overall reaction catalyzed by PFL



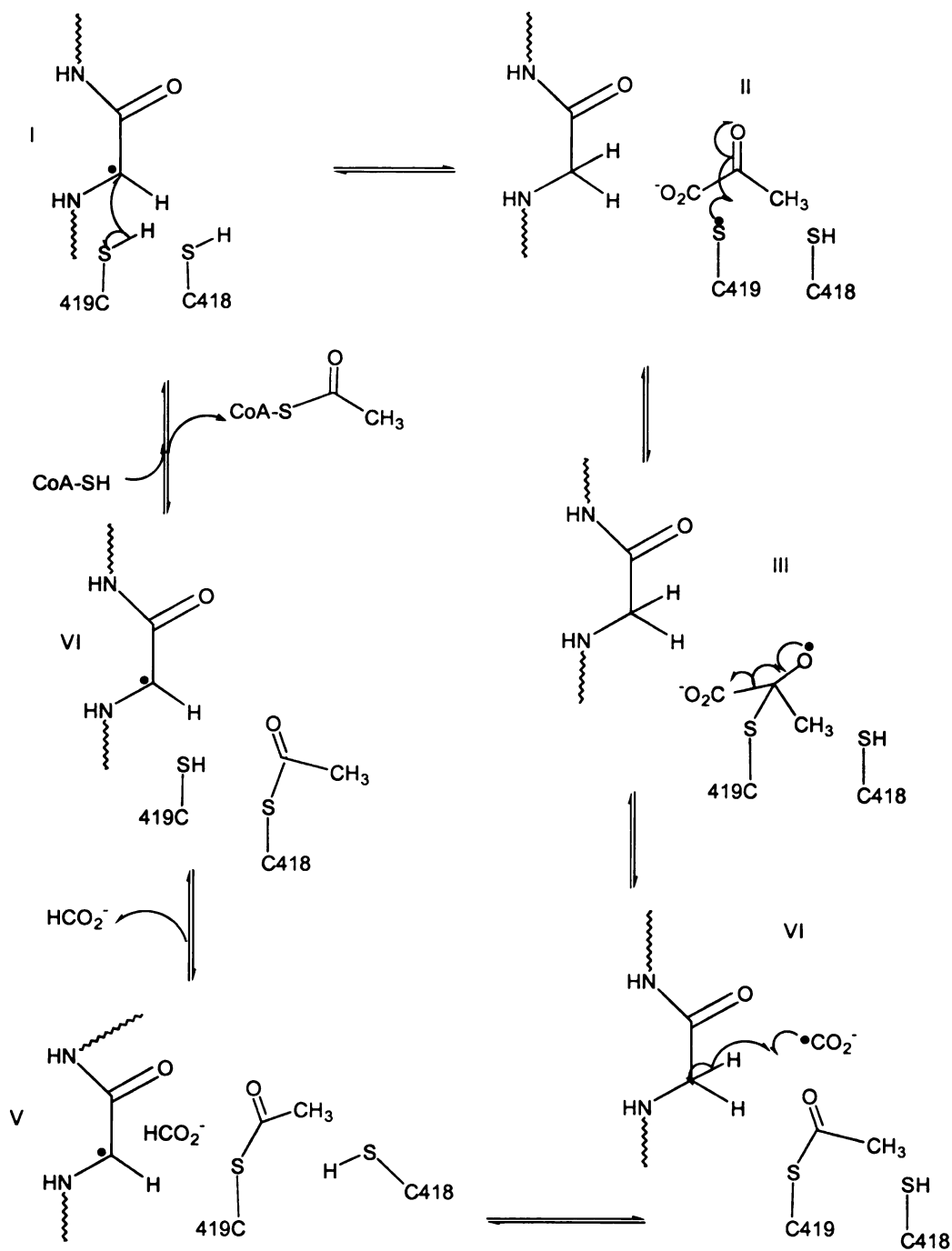
Scheme I.5. The Ping-Pong Mechanism proposed by Knappe and co-workers

acetyl-CoA. Consistent with the observed kinetics, CoA and formate do not interact with each other directly, nor do they have a common reactant.

At this point the available evidence to prove that the intermediate species was indeed acetylated PFL was largely circumstantial. Direct and definitive proof was provided by radioactive labeling experiments in which pyruvate was labeled at C-2 with ^{14}C and then reacted with active PFL in the absence of CoA.¹⁵ If the mechanism proposed in Scheme I.5 was correct, then 1) the acetylated PFL would be produced and would be trapped since the co-substrate (CoA) was not available to participate in the next step leading to a turnover, and 2) the radioactive label attached to active PFL would be detectable. The results showed that indeed radioactivity was incorporated into the protein only when the radiolabel was at C-2 of pyruvate but not at C-1. In addition, only activated PFL was able to incorporate the radioactivity at C-2 of pyruvate, whereas inactive PFL and all the other enzymes involved in the activation process were not. These observations provided positive proof that during homolysis of pyruvate, mediated by PFL, the acetyl group of pyruvate is transiently attached to PFL before being transferred to CoA to form the acetyl-CoA.¹⁵

Though considerable progress has been made toward understanding of the mechanism of the PFL reaction, so far there is no consensus on one mechanism for the

processing of pyruvate by PFL. Based on the sum total of the findings of various workers as discussed above, a number of mechanisms have been proposed, all of which involve the participation of the catalytic triad comprising G734, C418 and C419.^{15,23,30} Based on previous work by several workers and their own extensive studies on PFL, Kozarich and co-workers proposed the mechanism shown in Scheme I.6.²³



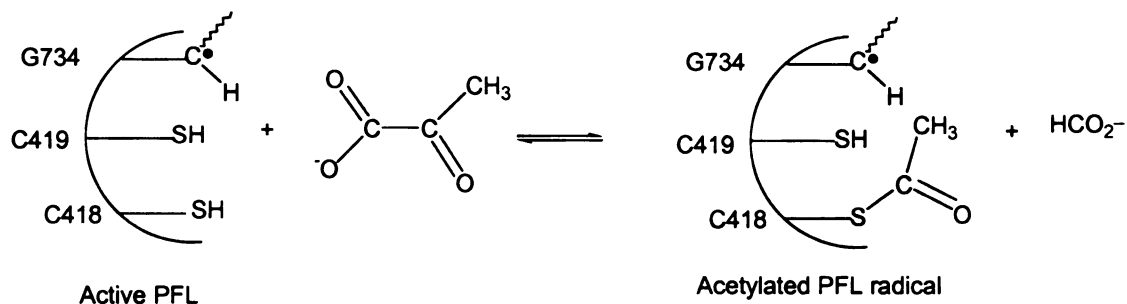
Scheme I.6. The mechanism of PFL action as proposed by Kozarich and co-workers.²³

In this mechanism, it is proposed that the radical at G734 on activated PFL is transferred to C419. The thiyl radical at C419 then attacks the C-2 carbonyl group of pyruvate, whereupon a tetrahedral intermediate is formed in which the radical resides on the C-2 oxygen of the pyruvate moiety. This intermediate then collapses to a more stable thioester with concomitant elimination of a formate radical anion. The radical anion then abstracts a hydrogen atom from G734 and is then released as formate. Simultaneously, the acetyl group at C419 is transferred to C418. In the last step the acetyl group is postulated to transfer from C418 to CoA by a transesterification process, thereby completing the catalytic cycle.

It is intriguing to note that this proposed mechanism involves an acetyl group transfer from C419 to C418 immediately prior to transesterification of CoA. The above mechanism was proposed based on data from several experiments including studies by Knappe's groups in which they demonstrated that the glycyl radical EPR signal (centered at $g = 2.0037$) is a doublet with a splitting of 15 G resulting from hyperfine coupling with the α -hydrogen of G734.^{20,25} The studies of the Knappe laboratory had also shown that the α -hydrogen of G734 rapidly exchanges with solvent, as demonstrated by the collapse of the doublet EPR spectrum into a singlet when active PFL is incubated in D₂O, leading them to suggest that the rapid exchangeability of the α -hydrogen with solvent was due to an unusually low K_a .²⁵ However, Mulliez et al. later demonstrated that though structurally very similar to the PFL glycyl radical, the glycyl radical of RNR-III of *E. coli* does not exchange with solvent.²⁶ Because the active site of PFL differs from that of RNR-III in having the two residues C418 and C419, Kozarich and coworkers used site-directed mutagenesis to investigate the role that these residues play in the H-exchange process.²³

Their results showed that whereas the exchange reaction in the C418S mutant is identical to that of the wild type enzyme, such exchange is totally abolished in the C419S mutant. Contrary to the conclusions of Wagner and co-workers, these findings proved that hydrogen exchange is not a spontaneous process inherent in the properties of the G734 α -hydrogen but that it requires the participation of C419.²⁰

Further implication of C419 in the exchange mechanism arose from investigation of the α -hydrogen exchange in acetylated PFL.²³ Knappe and co-workers had earlier shown that in the absence of CoA and formate, stable acetylated PFL could be isolated with the G734 radical intact.¹⁵ Thus, the reaction can be stopped after the first half reaction when one of the reactants needed for the second reaction (CoA) is not available. The exclusion of formate minimizes the shift of equilibrium back to the reactants. Scheme I.7 represents the reaction involved.



Scheme I.7. The formation of the acety-PFL radical intermediate by reaction of activated PFL with pyruvate in the absence of CoA and formate. Only the reactants and products are shown.

Following upon the work of Unkrig et al.²⁵, Kozarich's group acetylated active PFL by reacting it with pyruvate in the absence of CoA and formate.²³ Knappe and co-workers had previously reported the equilibrium constant for PFL acetylation to be 50, and based on this equilibrium constant the concentration of acetylated PFL was calculated to be

10,000-fold that of free PFL.¹⁸ In all practicality, therefore, active PFL was completely converted to the acetylated PFL radical intermediate. The EPR spectrum of the acetylated PFL was indistinguishable from that of activated wild type PFL, showing the doublet centered at $g = 2.0037$.²³ Upon incubation in D₂O, however, the doublet EPR signal collapsed to a singlet identical to that observed in the deuterated C418S mutant and wild type PFL, indicating that acetylated active PFL is capable of α -hydrogen exchange with solvent and therefore, on the basis of the mutagenesis experiments, provided evidence that C419 is free to facilitate the exchange.²³ These findings suggested very strongly that C418 is favored overwhelmingly over C419 as the site of acetylation during pyruvate turnover by PFL. Based on the foregoing discussion, two conclusions followed.

1. The α -hydrogen of the glycyl radical in activated PFL undergoes rapid exchange with solvent by a mechanism involving active and necessary participation of C419.
2. Acetylation of active PFL during the homolytic cleavage of pyruvate in the first of the two-step “ping pong” mechanism of pyruvate catabolism in *E. coli* takes place with overwhelming preference for C418 over C419.

The results obtained from PFL inactivation by hypophosphate, however, introduced an additional complication to the mechanism by which reaction at the active site of PFL proceeds during pyruvate turnover, particularly the role that each of the cysteines plays in the transfer of the acetyl group to its position on PFL following homolytic lysis of pyruvate.²³ Knappe and co-workers and Brush had previously demonstrated that hypophosphite (H₂PO₂⁻) is a mechanism-based inactivator of acetyl-PFL.^{21,27} Unkrig et al. then later demonstrated that when either pyruvate or acetyl-CoA is

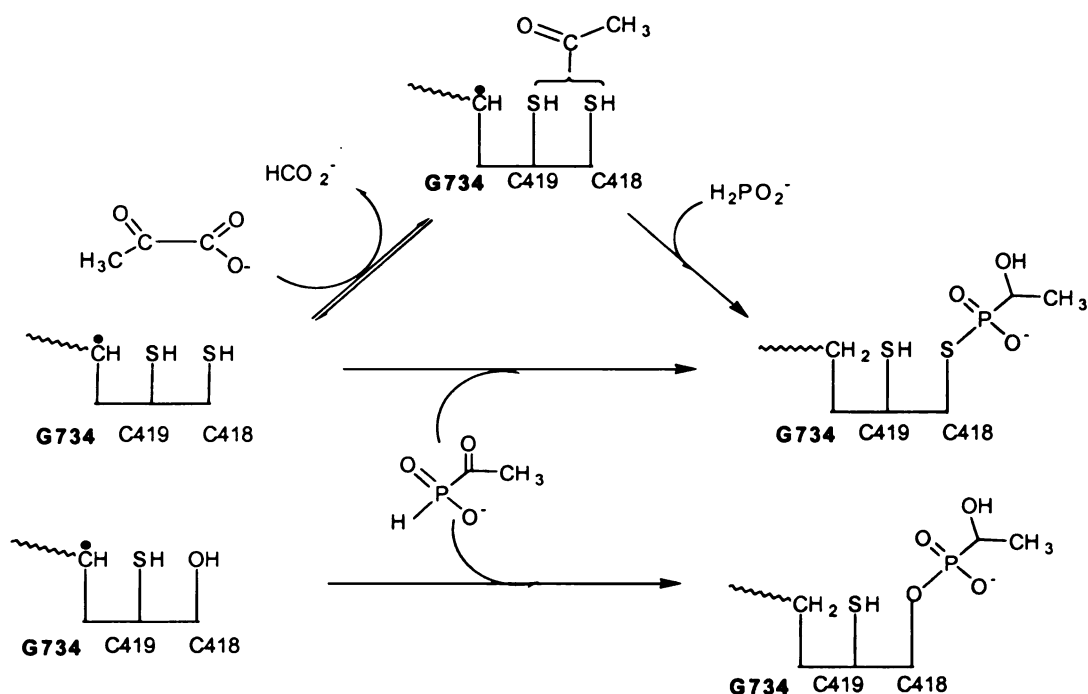
present, hypophosphite reacts with active PFL to produce a new and stable radical characterized by a distinct and highly split EPR signal.²⁵ These workers concluded that the radical on this intermediate was localized at C418, based on the observations that:

1. Perdeuteration of the acetyl group of pyruvate leads to perturbation of the EPR spectrum of this radical, and
2. A peptide modified by attachment of a (hydroxyethyl) phosphonate moiety at C418 was isolated.

An additional perspective was provided by the work of Ulissi-Demario et al.²⁸ who discovered that acetylphosphinate also inactivates PFL and generates a radical species with identical features to that generated by the reaction of hypophosphite with acetyl-PFL. With the benefit of this knowledge, Kozarich and co-workers carried out experiments aimed at establishing which of C418 and C419 is responsible for the transfer of the radical to the inactivator, as this might shed light on the extent to which each is involved in the acetyl group transfer during pyruvate turnover.²³ To address this question, acetylphosphinate was added to the glycyl radical in the PFL mutants C418S and C419S. The experiment was done under anaerobic conditions to avoid destruction of the radical by oxygen. For the C419S mutant, no radical intermediate was observed. Instead, the glycyl radical was found to persist unchanged for up to 15 minutes in the presence of acetylphosphinate. The C418S mutant, however, reacted in less than 30 seconds to generate a radical intermediate stable enough to be detected by EPR.²³ It was observed that the splitting pattern and splitting constants for the C418S radical intermediate were slightly different from those of the radical formed with wild type PFL. These differences

were interpreted to be a result of the change from a sulfur-phosphorus bond in the wild type to an oxygen-phosphorus bond in C418S.²³ Theoretical calculations are also consistent with these findings.²⁹

The foregoing findings led to the proposal by Ulissi-Demario et al., and later corroborated by Knappe and co-workers, that inactivation of acetyl-PFL by hypophosphite and inactivation of PFL by acetylphosphinate mechanistically converge to a common radical intermediate as summarized by the Scheme I.8.^{28,22}



Scheme I.8. Reactions of hypophosphite with acetyl-PFL and acetylphosphinate with active PFL lead to the same product.

At this point, data obtained from site-directed mutagenesis experiments had led to the following conclusions;

- C418 is exclusively acetylated when activated PFL is reacted with pyruvate in the absence of CoA and formate;

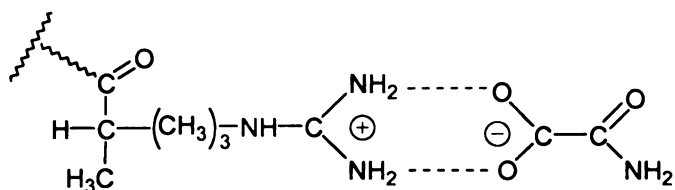
- b) C419, but not C418, is absolutely required for α -hydrogen exchange with solvent;
- c) trapping of the G734 radical by acetylphosphinate requires C419; and
- d) following acetylphosphination of both wild type and the C418S mutant, the (hydroxyethyl)phosphonate moiety, covalently attaches to residue 418.

The observation that C418 is necessary for thioester transfer during the CoA-acetyl-CoA exchange reaction, proved that it is necessary in the initial homolytic cleavage of the C₁-C₂ bond in pyruvate.²³ The reaction of PFL with acetylphosphinate, on the other hand, suggested that C418 is not necessary for the transfer of the radical to acetylphosphinate.²³ Instead, this transfer was found to require C419.²³ This apparently divergent findings introduced an unwelcome complication to the mechanistic investigations of the PFL-pyruvate reaction. To reconcile these findings, Kozarich and coworkers proposed that C419 is the “direct mediator of the glycyl radical action” while C418 mediates the transfer of the acetyl moiety to CoA after homolysis of the pyruvate C₁-C₂ bond.²³ It was on this basis that they modified the mechanism of Brush et al. by proposing a step involving transesterification of the acetyl group between both residues.^{23,27} Thus, it is proposed that upon cleavage of the pyruvate C₁-C₂ bond, the acetyl group is first transferred to C419 and subsequently to C418 from where it is transferred to CoA in the second step of the reaction.²³

Knappe and co-workers proposed an alternative mechanism based on the crystal structure of wild type PFL, both in its free state and as a complex with oxamate.³⁰ In the same study, they solved the crystal structure of the C418S, C419S double mutant at 2.6Å resolution and found that oxamate and pyruvate bind specifically and uniquely at the

active site without affecting the overall structure of the protein. An interesting, and perhaps unique, finding was that pyruvate and oxamate are not simply allosteric effectors, but that they bind to the active site of PFL.³⁰ Since PFL activation is known to require the presence of either one of the two¹⁵, it can be inferred that the positioning of either one of these two at the active site facilitates H-abstraction from G734. The nature of this facilitation is not yet understood and is therefore a subject for on-going investigation.

The mechanism that Knappe and coworkers proposed was based primarily on structural information obtained from crystal crystallographic studies, with the PFL-oxamate co-crystal providing significant insight into the special relation between the PFL active site residues and the substrate pyruvate.³⁰ The structure revealed both electrostatic and hydrophobic interactions between PFL and oxamate, in which the carboxylate oxygen atoms form a salt bridge with the guanidino group of Arg 435 as illustrated in Scheme I.9. The delocalized negative charge on the carboxylate oxygen atoms leads to the formation of a salt bridge with the delocalized positive charge on the N ϵ of Arg.

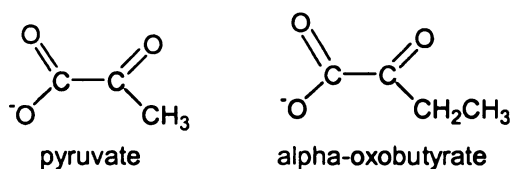


Scheme I.9. The salt bridge formed between oxamate and Arg 435 in the active site of PFL

The flat moiety is also sandwiched between two aromatic and hydrophobic sided chains, Phe 432 and Trp 333, the catalytically essential C418 being situated with its S atom at a distance of 3.3Å from the C1 and C2 of oxamate, and inserted between the planes of Trp

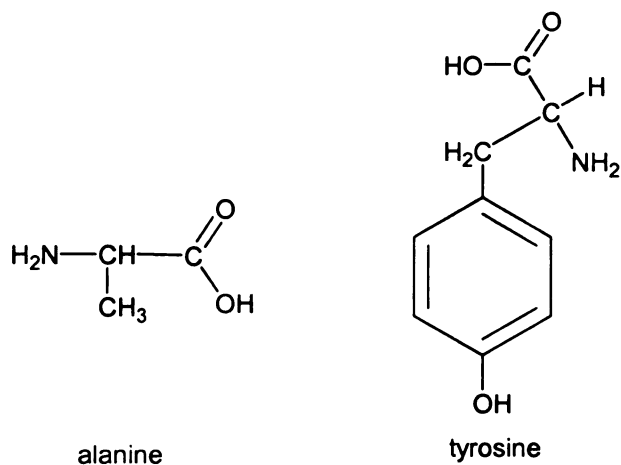
333 and oxamate. Of particular interest was the observation that the O-C-S angle at C2 is $\sim 103^\circ$, which is very close to the optimal angle of 109° optimally required for nucleophilic attack at an sp^2 carbon of the carbonyl group.

Using the crystallographic distances observed in the PFL-oxamate complex, Knappe and coworkers deduced that if pyruvate, which is structurally homologous to oxamate (CH_3 in pyruvate instead of NH_2 in oxamate), were to be substituted for oxamate in this structure, its methyl group would be within 3.4\AA of the CH_3 group of Ala 272. Ala 272, in turn, is hydrogen-bonded to the OH group of Tyr 323. This inferred binding mode for pyruvate at the active site of PFL was corroborated by the situation in α -oxobutyrate formate-lyase (TdcE).⁴⁶ This enzyme is homologous and bears 82% sequence identity to PFL.⁴⁶ It carries out an analogous reaction to PFL but acts on α -oxobutyrate (Scheme I.10) as substrate.

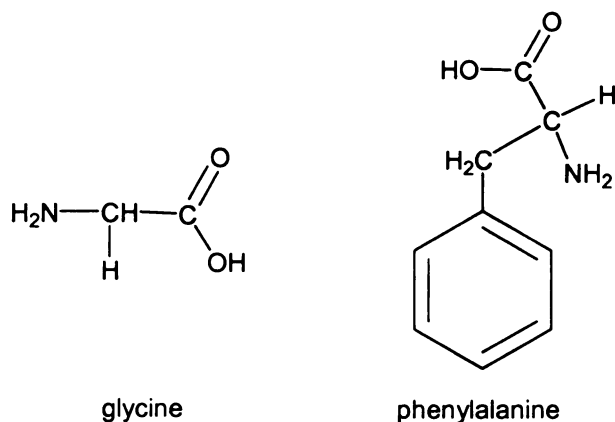


Scheme I.10. Chemical structures of pyruvate and alpha-oxobutyrate

At analogous positions to Ala 272 and Tyr 323 in PFL, TdcE has glycine and phenylalanine. These are both smaller residue residues than the corresponding alanine and tyrosine in PFL (Scheme I.11) and therefore affording more room for the larger substrate α -oxobutyrate.



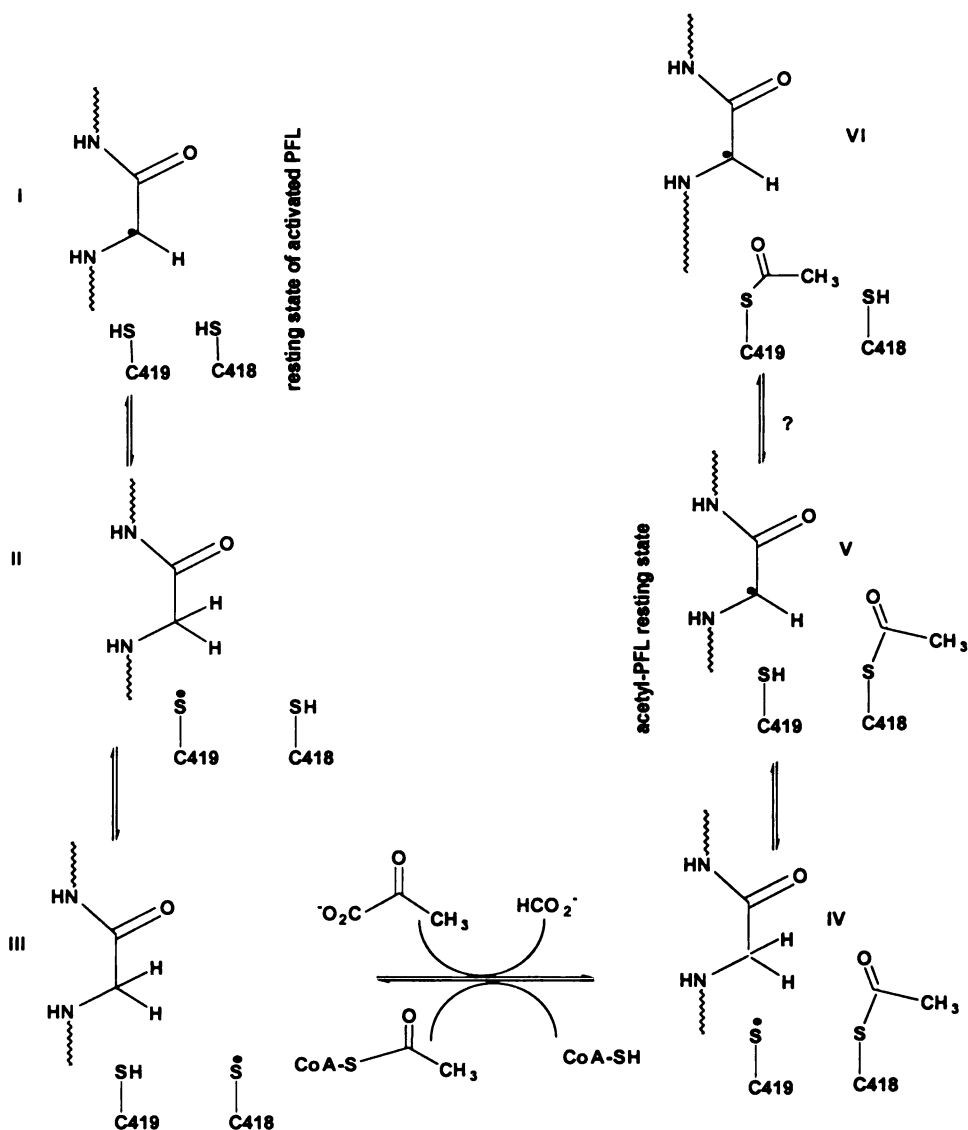
A



B

Scheme I.11. Comparison of residues found at the active sites of TdcE (A) and PFL (B)

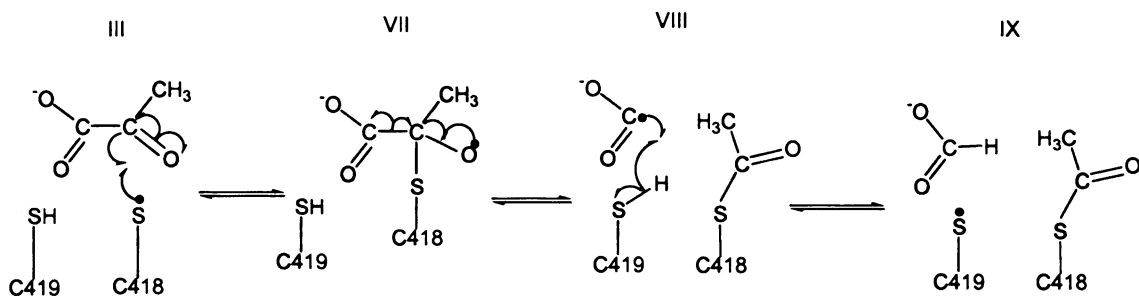
Relying, in part, upon previous biochemical studies, which showed that C419 is situated within 3.7Å of the G734 α-C and C418 and the data obtained in this work, Knappe's group proposed the catalytic mechanism shown in Scheme I.11, involving the cooperation of the catalytic triad during the acetylation of PFL in the first step of the “ping pong” mechanism.³⁰



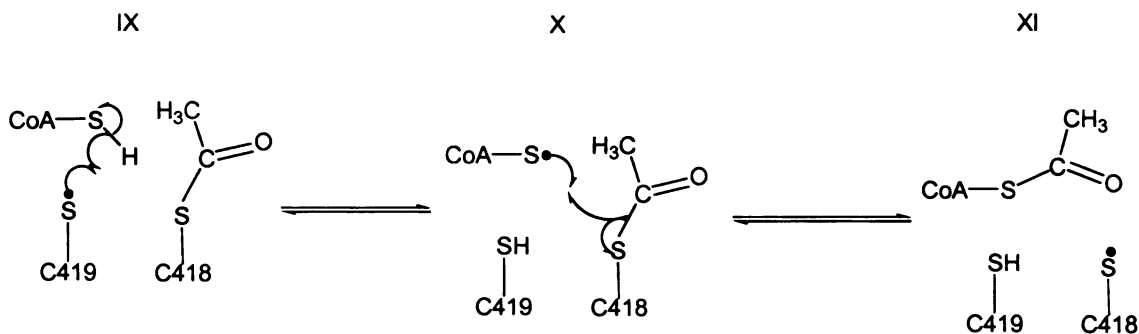
Scheme I.12. Proposed mechanism for the transfer of the radical and acetyl group within the amino acid triad at the active site of PFL. Adapted from ref. 30.

The conversion of **I** to **II** and **III** constitutes the initiation step. The formation of the acetyl-PFL intermediate involves the reaction of **III** with either pyruvate or acetyl-CoA, with concomitant production of formate or CoA respectively. The processing of pyruvate by PFL is proposed to begin with PFL **III** above and proceed as illustrated by Scheme I.13.

Step 1: "ping"



Step 2: "pong"



Scheme I.13. The mechanism proposed by Knappe and co-workers.³⁰

The proposals put forward by Knappe and co-workers are fundamentally similar to those of Kozarich, both starting with the transfer of the radical from G734 to C419.³⁰ However, whereas Kozarich and co-workers propose that the thiyl radical at C419 directly attacks the C2 carbon of pyruvate to form the tetrahedral hemiketal intermediate²³, Knappe's group suggested that the thiyl radical is first transferred to C418 and that the tetrahedral intermediate forms at this residue.³⁰ Since it is now known that the acetyl group in acetyl-PFL is located at C418, the mechanism of Kozarich and others

includes the transfer of the acetyl group from C419 to C418 immediately prior to the acetyl group transfer to CoA to form the thioester linkage in acetyl-CoA. Kozarich's group used as part of their rationale for the transesterification step between C418 and C419, the fact that mutagenesis experiments showed that radical trapping by acetylphosphinate takes place only when C419 is in place, whereas C418 is not required for this process.²³ However, C418 was shown to be essential for the transfer of the acetyl group to CoA.³⁰

In their latest proposal, on the other hand, Knappe and co-workers preclude the involvement of C419 in acetyl group transfer to C418 and instead suggest that acetylation takes place directly at C418. Notably, in Kozarich's proposal, the G734 radical is recovered after every turnover as would be expected in a catalytic cycle, while Knappe's proposal involves multiple turnovers "without regeneration of the glycy radical."³⁰ Clearly, the mechanism by which PFL processes pyruvate remains a controversial and on-going area of investigation.

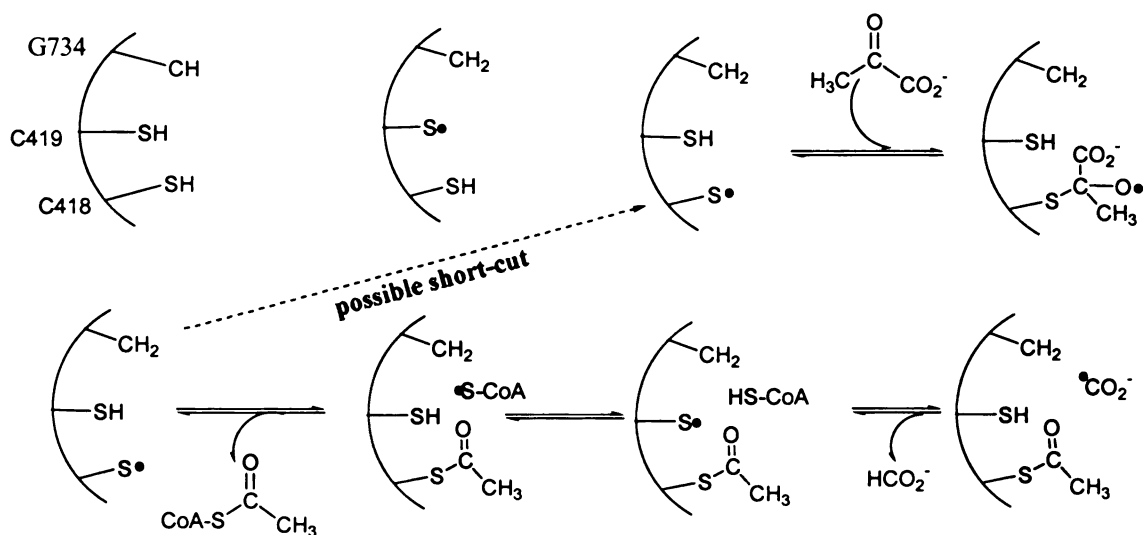
I.8. THEORETICAL STUDIES

Owing to the lack of consensus regarding the mechanisms by which pyruvate is processed by PFL, a number of workers have carried out theoretical studies aimed at testing the feasibility of some of the steps proposed in the various mechanisms.^{32,33} The stability of the glycyl radical has been proposed to be due to the captodative effect, a chemical phenomenon whereby an electron-withdrawing group and electron-donating group cooperate to enhance the resonance stability of a radical located between them.³⁴⁻³⁷ The glycyl radical in PFL is located between an electron donating amino group and an electron withdrawing amide carbonyl group and was therefore hypothesized to benefit from stabilization by the captodative effect.⁵²

The other phenomenon that affects the stability of amino acid radicals is the non-bonding interaction between the side chain and the carbonyl group. It is known that this interaction has the effect of destabilizing a radical at the alpha carbon. Since the glycyl radical is located on a planar (sp^2 -hybridized) carbon, this interaction is absent, thereby rendering the radical more stable than other corresponding $C\alpha$ -amino acid radicals. This phenomenon has been studied extensively by a several workers.³⁸⁻⁴⁴ The stability of the glycyl radical was confirmed by calculating the bond dissociation energies (BDE) of the $C\alpha$ -H bond in a series of models wherein it was discovered that whereas the substitution of $-NH_2$ and $-CHO$ in methane lower the $C\alpha$ -H bond energy by 13.1 kcal/mol and 10.7 kcal/mol, respectively; the combined effect of the two groups in NH_2-CH_2-CHO decreases the BDE by 33.5 kcal/mol.³⁹ When the chain length was increased with additional peptide bonds to both the $-CHO$ and the $-NH_2$ groups, it was found that there was a smaller decrease in BDE. This was consistent with the expected lowering of the

electron-donating and withdrawing effects of the -NH_2 and the -CHO groups respectively, and suggested that the captodative effect on glycy radical situated along the backbone of a polypeptide will be lower than was observed in $\text{NH}_2\text{-CH}_2\text{-CHO}$. Calculations have also shown that the $\text{C}\alpha\text{-H}$ and S-H BDEs are within 2 kcal/mol of each other, thereby affording reversibility in the transfer of the radical between G734 and either one of C418 and C419.

The mechanism proposed by Kozarich and co-workers was further subjected to analysis by DFT calculations, which proved that all of the steps subsequent to the transfer of the radical from G734 to the C419 are energetically plausible.⁴⁰ Although the regeneration of the glycy radical by abstraction of a hydrogen atom by the formyl radical was also found to be energetically plausible, Himo and Eriksson proposed that the hydrogen is abstracted from C419.⁴⁰ This subsequently facilitates the transfer of the acetyl group to CoA. Taking into consideration the proposed mechanisms of both the groups of Kozarich and the Knappe, Himo and Siegbahn used the results of the calculations to propose the presently accepted and slightly different mechanism depicted in Scheme I.14.⁴⁵



Scheme I.14 Mechanism Proposed by Himo and Sieghahn. Adapted from ref. 45.

However, Ramos and co-workers recently published results from a theoretical study in which they modeled pyruvate as an anionic species, since, given its pK_a of 2.5, it is expected to be deprotonated at physiological pH. Based on the interpretation of their DFT data, these workers conclude that thiol addition to pyruvate occurs via a quasi-planar structure and not a tetrahedral transition state as hitherto proposed by several workers. These workers also contend that rather than the C-C bond cleavage, it is the H transfer between G734 and C419 that is the rate limiting step. They therefore propose yet another mechanism for the processing of pyruvate by PFL. Clearly, much work remains to be done before consensus on the PFL mechanism is reached.

I.9. THE ROLE OF ALCOHOL DEHYDROGENASE (AdhE)

I.9.1. Reported role of AdhE as a PFL deactivase

The discovery of pyruvate formate-lyase activating enzyme (PFL-AE)^{14, 15} led researchers working on the PFL-AE system to think of the possibility of a second activity that would play an opposite role to the activating enzyme, namely to enzymatically converting PFL from its active radical form to its inactive form. From the standpoint of metabolic economy the existence of such an activity seemed rational since it would ensure that PFL was deactivated conservatively, thus leaving it intact and well poised for reactivation when conditions required its deployment.

In 1992 Kessler and Knappe⁵³ reported that they had discovered the PFL deactivase activity to reside in the multifunctional alcohol dehydrogenase (AdhE). This report therefore provided the activity that achieved the reverse reaction to PFL-AE, thereby completing the interconversion cycle between active and inactive states in response to the growth conditions of *Escherichia coli*. It is with respect to this reported activity that this study was conducted, with the aim of elucidating the nature and mechanistic role of the purported cofactors, namely Fe^{2+} , co-enzyme A and NAD^+ .

I.9.2. Other physiological characteristics of AdhE

In addition to its latest reported role as a PFL deactivase, AdhE is known to play a major role in the anaerobic metabolism of *Escherichia coli*. It catalyzes the reduction of acetyl-CoA by NADH to ethanol via a two-step mechanism involving acetaldehyde as an intermediate.⁵⁴ In this physiological role, AdhE is very similar to the alcohol

dehydrogenase from the obligate anaerobe and pathogenic protozoan *Entamoeba histolytica* to which it also bears striking structural resemblance.⁵⁵ Both enzymes are also NAD⁺ and Fe²⁺-dependent form helical assemblies of protomers called spirozomes. Clark and co-workers⁵⁶ exploited these structural and functional similarities and successfully cloned the *E. histolytica* alcohol dehydrogenase (AhADH2) into *E. coli* and proceeded to use the *E. coli*/EhADH2 clones to screen various compounds for their ability to inhibit anaerobic growth of the clone by interfering with EhADH2. This provided a rapid assay for identifying possible pharmaceuticals against *E. histolytica*, with the aim of finding efficacious drugs for amebic dysentery.

I.9.3. Regulation of AdhE

In addition to being anaerobically induced Clark discovered what appeared to be a positive correlation between induction of the *adhE* gene and the levels of NADH in the growth medium.⁵⁷ In order to determine the role of this co-enzyme in the induction of the *adhE* gene, Clark and co-workers carried out a systematic study in which they grew *E. coli* on various carbon sources whose metabolism is known to produce various relative amounts of NADH. They also used treatments that are known to change the NAD⁺ : NADH ratio or alter the NAD⁺ and NADH pool. Some of the treatments included the use of chemical inhibitors and mutations to block the electron transport chain and thus artificially induce the *adhE* gene under aerobic conditions. These workers also introduced mutational blocks into the biosynthetic pathway for nicotinic acid in order to limit the synthesis of NAD⁺, while in some experiments they introduced exogenous NAD⁺ and nicotinic acid. The results obtained from these studies led to the conclusion

that “the enzymatic activity of of the AdhE protein modulates the level of NADH under anaerobic conditions, and thus indirectly regulating its own expression”. In another study⁵⁸, it was also found that the expression of the adhE gene is transcriptionally regulated by Cra and post-transcriptionally by RNase G. Thus, the physiological roles of AdhE are complex and very interesting, while its regulation under different conditions remains intriguing. In this study we hope to gain some insight into the role that this enzyme plays in the deactivation of the anaerobically indispensable pyruvate formate-lyase of *Escherichia coli*.

REFERENCES

1. Knappe, J and Sawers, G. **1990**, *FEMS Microbiol. Rev.* 75, 383-398
2. Kalnitsky, G.; Werkman, C.H. **1943**, *Arc. Biochem.* 2, 113-124.
3. Lipmann, F.; Tuttle, L.C. **1945**, *J. Biol. Chem.* 158,505-519
4. Chantrenne, H.; Lipmann, F. **1950**, *J. Biol. Chem.* 187, 757
5. Stadtman, E.R. **1951**, *Biol. Chem.* 191 365
6. G.D. Novelli, et al. **1954**, *Bacteriol. Proc.* p.97;
7. Novelli, G.D. **1955**, *Biophys. Acta* 18, 594-596.
8. McCormick, N. et. al. **1962**, *J. Bacteriol.* 83: 899-906.
9. Broderick, J.B.; Dederstardt, R.E.; Fernandez, D.C.; Wojtuszewski, K.; Henshaw, T.F.; Johnson, M.K.J. *J. Am. Chem. Soc.* **1997**, 119, 7396-7397.
10. Knappe, J.; Sawers, G. **1990**, *FEMS Microbiol. Rev.* 75, 383-398
11. Knappe, J.; Bohnet, E.; Brummer, W. **1965**, *Biochim. Biophys. Acta.* 107, 603-605.
12. Wood, N.P. *Methods in Enzymology*, **1966**, 69, 718.
13. Chase, T.Jr.; Rabinowitz, J. *J.Bacteriol.* **1968**, 1065-1078.
14. Knappe, J.; Schacht, J.; Mockel, W.; Hopner, Th.; Vetter, H. Jr.; Edenharder, R. *Eur. J. Biochem.* **1969**, 11, 316-327.
15. Knappe, J.; Blaschkowski, H.P.; Schmitt, T. *Eur. J. Biochem.* **1974**, 50, 253-263.
16. Knappe, J.; Blaschkowski, H-P.; Edenharder, R. *Metabolic Interconversion of Enzymes*, Springer, **1972**, 319-329.
17. Leppänen, V. M.; Merckel, M. C.; Ollis, D. L.; Wong, K. K.; Kozarich, J. W.; Goldman, A. **1999**. *Structure*, 7, 733-744.
18. Knappe, J.; Wagner, A.F.V. **1995**, *Methods Enzymol* 258, 343-362.

19. Conradt, H.; Hohmann-Berger, M.; Hohmann, H.P.; Blaschkowski, H.P.; Knappe, J. **1984**, *Arch. Biochem. Biophys.* 228, 133-142.
20. Wagner, A.F.V., Frey, M., Neugebauer, F.A., Schafer, W., and Knappe, J. **1992**, *Proc. Natl. Acad. Sci. U.S.A* 89, 996-1000.
21. Knappe, J.; Neugebauer, F.A.; Blaschkowski, H.P.; Ganzler, M. **1984**, *Proc. Natl. Acad. Sci. USA*, 81, 1332-1335.
22. Frey, M.; Rothe, M.; Wagner, A.F.V.; Knappe, J. **1994**, *J. Biol. Chem.* 269, 17, 12432-12437.
23. Parast, C.V.; Wong, K.K.; Lewisch, S.A.; Kozarich, J.W.; Peisach, J.; Magliozzo, R.S. **1995**, *Biochem.* 34 (8), 2394-2399.
24. Gautney, L.; Miyagawa, I. **1975**, *Radiat. Res.* 62, 12-17.
25. Unkrig, V., Neugebauer, F.A., Knappe, J. (1989) *Eur. J. Biochem.* 184, 723-728.
26. Mulliez, E.; Fontecave, M.; Gaillaid, J.; Riechard, P. **1993**, *J. Biol. Chem.*, 268, 2296-2299.
27. Brush, E.J., Lipsett, K.A., Kozarich, J.W. (**1988**) *Biochemistry*, 27, 2217-2220.
28. Ulissi-Demario, L.; Brush, E. J.; Kozarich, J.W. **1991**, *J. Am. Chem. Soc.* 113, 4341-4342.
29. Reed, A.E.; Schleyer, P. **1990**, *J. Am. Chem. Soc.* 112, 1434.
30. Becker, A.; Fritz-Wolf, K.; Kabsch, W.; Knappe, J.; Schultz, S.; Wagner, A.F.V. **1999**, *Nature: Struct. Biol.* 6 (10), 969-975.
31. Knappe, J.; Albert, S.; Frey, M.; Wagner, A.F.V. **1993**, *Biochem. Soc. Trans.* 21, 731-734.
32. Himo, F.; Eriksson, L.A. *J. Am. Chem. Soc.* **1998**, 120, 11449.
33. Gault, J.W.; Eriksson, L. A. **2000**, *J. Am. Chem. Soc.*, 122, 2035.
34. Wong, K. K.; Kozarich, J. W. In *Metal Ions in Biological Systems, Metalloenzymes Involving Amino Acid-Residue and Related Radicals*, Eds. Sigel, H.; Sigel A.; Marcel Dekker: New York, **1994**; Vol. 30, p 279.

35. Vieche, H. G.; Merenyi, R.; Stella, L.; Zanousek, Z. **1979**, *Angew. Chem., Int. Ed. Engl.* **18**, 917.
36. Vieche, H. G.; Zanousek, Z.; Merenyi, R.; Stella, L. **1985**, *Acc. Chem. Res.*, **18**, 148.
37. Stella, L.; Harvey, J. N. In *Radicals in Organic Synthesis, Volume 1: Basic Principles*, pp 360-380, Renaud, P., Sibi, M. P., Eds.; Wiley-VCH: New York, **2001**.
38. Armstrong, D. A.; Yu, D.; Rauk, A. **1996**, *Can. J. Chem.* **74**, 1192.
39. Rauk, A.; Yu, D.; Taylor, J.; Shustov, G. V.; Block, D. A.; Armstrong, D. A. **1999**, *Biochem.* **38**, 9089.
40. Himo, F. **2000**, *Chem. Phys. Lett.* **328**, 270.
41. Himo, F.; Eriksson, L. A. **1998**, *J. Chem. Soc., Perkin Trans. 2*, **2**, 305.
42. Barone, V.; Adamo, C.; Grand, A.; Brunel, Y.; Subra, R. **1995**, *J. Am. Chem. Soc.* **117**, 1083.
43. Barone, V.; Adamo, C.; Grand, A.; Subra, R. **1995**, *Chem. Phys. Lett.* **242**, 351.
44. Barone, V.; Adamo, C.; Grand, A.; Jolibois, F.; Brunel, Y.; Subra, R. **1995**, *J. Am. Chem. Soc.* **117**, 12618.
45. Himo, F.; Siegbahn, P.E.M. **2003**, *Chem. Rev.* **103**, 2421-2456.
46. Heßlinger, C.; Fairhurst, S.A.; Sawers, G. **1998**, *Mol. Microbiol.* **27**, 477-492.
47. Reichard, P., and Ehrenberg, A. **1983**, *Science* **221**, 514-519.
48. Sun, X.; Ollagnier, S.; Schmidt, P. P.; Atta, M.; Mulliez, E.; Lepape, L.; Eliasson, R.; Graslund, A.; Fontecave, M.; Reichard, P.; Sjöberg, B. M. **1996**, *J. Biol. Chem.* **271**, 6827-6831.
49. Logan, D. T.; Andersson, J.; Sjöberg, B.-M.; Nordlund, P. **1999**, *Science* **283**, 1499-1504.
50. Becker, A.; Kabsch, W. **2002**, *J. Biol. Chem.* **277**, **42**, 40036-40042.
51. Sofia, H.J.; Chen, G.; Hetzler, B.G.; Reyes-Spindola, J. F.; Miller, N. **2001**, *Nucleic Acids Research*, **29**, **5**, 1097-1106.

52. Sustman, R., Korth, H-G. **1990**. *Adv. Phys. Org. Chem.* 26:131-78.
53. Kessler, D and Knappe, J. **1992**. *J. Biol. Chem.* 267, 25, 18073-18079.
54. Goodlove, P.E. **1989**. *Gene*. 85, 209-214.
55. Espinosa, A.; Yan, L.; Zhang, Z.; Foster. L.; Clark, D.; Li, E.; Stanley, S.L., Jr.
2001. *J. Biol. Chem.* 276, 20136-20143.
56. Yong, T.; Li, E.; Clark, D.P.; Stanley, S.L., Jr.
57. Clark, D.P. **1989**. *FEMS Microbiol. Rev.* 63, 223-234.
58. Leonardo, M.R.; Dailly, Y.; Clark, D.P. *J. Bacteriol.* **1996**. 178, 6013-6018.

CHAPTER II

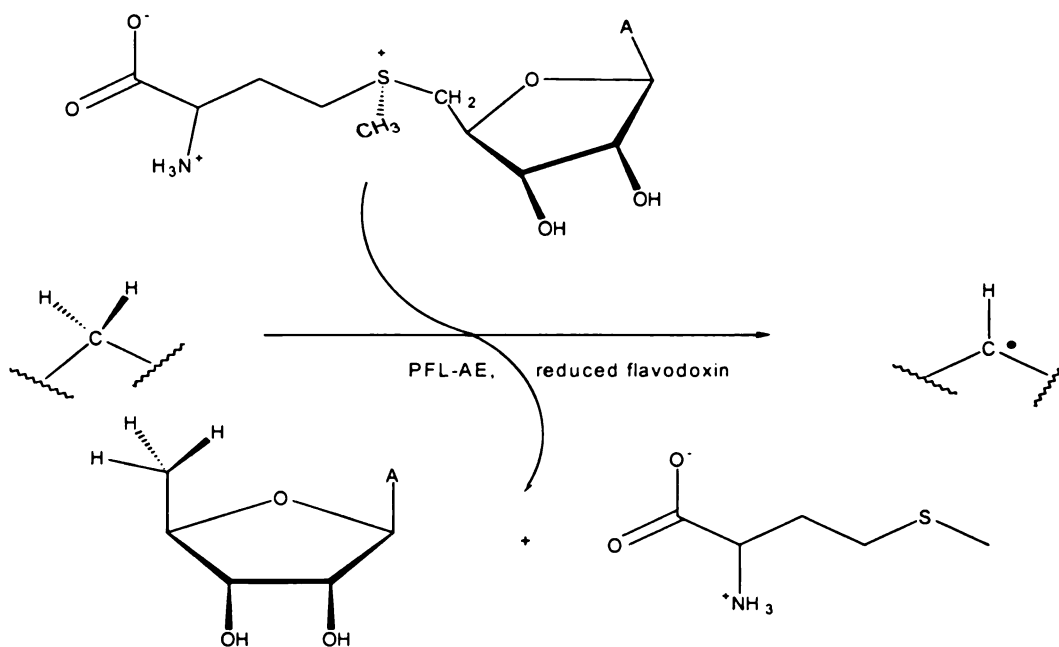
PFL: PURIFICATION, ACTIVATION AND STABILITY

ABSTRACT

PFL was overexpressed in BL21(DE3)pLysS cells that were previously transformed with the recombinant vector pKK-pfl. The recombinant vector was engineered by ligating the *pfl* gene (obtained from the polymerase chain reaction) onto the commercial vector pKK. Purified pyruvate formate-lyase (PFL) was then purified and activated according to the standard protocol in which all the activation components, including co-substrate S-adenosylmethionine (SAM), the photoreductant deazariboflavin and pyruvate formate-lyase activating enzyme (PFL-AE) were mixed and then subjected to an intense halogen lamp for 45 minutes. PFL thus activated was used to carry out deactivation studies using AdhE and various small molecules (Chapters III and IV). In the process of these deactivation studies, which were carried out under ambient light, we observed that the control reactions containing only PFL and buffer, or those containing components that proved unreactive to the glycyl radical of PFL, always showed a steady increase of PFL activity over time. This led us to the hypothesis that PFL can be activated under ambient light, if all of the essential components of the activation mix are available, thereby circumventing the use of a high intensity halogen lamp. This hypothesis was confirmed. By activating PFL under ambient light, we were able to achieve PFL activity that was comparable to the highest levels we have obtained using the illumination method. The maximum activity was achieved within a period of two hours. This discovery enabled us to carry out all subsequent PFL activations at ambient light and temperature, thus simplifying the procedure significantly. In addition, the glycyl radical in activated PFL proved to be extremely stable, being detectable for well over 24 hours at room temperature.

II.1. INTRODUCTION

Pyruvate formate-lyase (PFL), the enzyme which, in the presence of co-enzyme A (CoA) and under anaerobic conditions, converts pyruvate to acetyl-CoA and formate, is translated in an inactive form inside the cell. When conditions become anaerobic, it is converted to its active form by pyruvate formate-lyase activating enzyme (PFL-AE), which generates a radical on a glycine residue located at position 734 of the PFL polypeptide chain.¹ In vitro, this activation involves the participation of several cofactors and co-substrates and requires strictly anaerobic conditions.² The activation reaction is summarized as shown by Scheme II.1.



Scheme II.1. A structural depiction of the activation of PFL showing the essential participants in the activation process. Following reductive cleavage of SAM into methionine and a 5'-deoxyadenosyl radical, the transient 5'-deoxyadenosyl radical generates a glycyl radical on the PFL backbone by abstracting the pro-S hydrogen atom at Gly 734. PFL thus activated proceeds to catalyze homolysis of the C₂-C₃ bond of pyruvate followed by transacetylation of CoA and formation of formate.

The scheme shows only glycine 734 before and after hydrogen atom abstraction, representing the inactive and active states of the enzyme, respectively. The role of the photoreductant deazariboflavin is to reduce an iron-sulfur cluster on the PFL-AE to the catalytically active $[4\text{Fe-4S}]^+$ form. The reduced activating enzyme facilitates the abstraction of the hydrogen atom at glycine 734 via a process that requires the participation of S-adenosylmethionine (SAM) as described in Chapter I. In the process of the PFL activation reaction, S-adenosylmethionine is reductively cleaved to methionine and 5'-deoxyadenosine.³

Studies of the activation system have shown that the hydrogen atom abstracted from glycine 734 of PFL ends up at the 5'-carbon of 5'-deoxyadenosine, suggesting that the radical generated at glycine 734 is transferred to that position from the 5'-carbon of 5'-deoxyadenosine.⁴ That, in turn, led to the conclusion that the interaction between PFL-AE and SAM results in the generation of a 5'-deoxyadenosyl radical. The nature of this interaction is a subject of continuing investigation in our laboratory.

Activation of PFL *in vitro* is usually performed by mixing the activation components under anaerobic conditions, followed by illumination with a high intensity lamp.⁵ Maximum activity is generally achieved within 30 to 45 minutes. Because of the large amount of heat generated by the lamp, it is necessary to keep the activation mix cool by carrying out the process in an ice-water bath. This introduces technical difficulties in sample handling and conceivably introduces a further deviation from the natural activation conditions within the cell. We have now discovered that under conditions of ambient light and room temperature ($\sim 23^\circ\text{C}$), PFL can be activated to levels comparable to, and sometimes higher than, those previously achieved by illumination in

an ice-water bath as described above. We have also discovered that active PFL, as determined by the enzymatic activity assay, is extremely stable under the same conditions. These findings are significant because they afford simpler practical manipulations both in the preparation for activation as well as after the activation of PFL. Additionally, the activation conditions are a closer approximation of the situation in vivo.

II.2. MATERIALS AND METHODS

II.2.1. Chemicals, bacterial cells and plasmids

The plasmid pKK-PFL used to transform BL21(DE3)pLysS was from a stock solution obtained by amplification of pKK-PFL previously used in our laboratory.⁶ Plasmid pCAL-n-AE was also amplified from a stock solution previously engineered in our laboratory⁶ using pCAL-n-EK expression vector obtained from Stratagen™ and the pMG-AE plasmid generously donated by Dr. John Kozarich (Merck). 5-Deazariboflavin was synthesized by Megan Kibbey and Dr. W. Broderick following published procedures.⁷⁻⁹

II.2.2. Bacterial production of PFL

Escherichia coli (*E. coli*) BL21(DE3) pLysS was transformed with pKK-PFL according to the supplier's protocol. Single transformant colonies were inoculated into 50 mL LB media containing a total of 50 µg ampicillin per mL of LB liquid medium. The cultures so prepared were allowed to incubate for approximately 16 hours to reach maximum cell density. In order to check overexpression in each of the flasks, small pellets were routinely prepared from each growth and denatured in sodium dodecyl sulfate (SDS) denaturing buffer containing 3.5% 2-mercaptoethanol. Sodium dodecyl sulfate polyacrylamide gel electrophoresis (SDS-PAGE) was then carried out using a 12% Tris-HCl commercial gel from BioRad™ to check overexpression of the protein. A sample that showed good overexpression (in BL21(DE3)pLysS, PFL overexpresses even without induction) was used to inoculate 5 mL into each of 2.8 L Fernbach flasks containing 1 L of liquid LB medium impregnated with ampicillin to a final concentration of 50 µg/mL. Alternatively 50 mL of the saturated growth was inoculated into a bench

top fermentor (New Brunswick) containing 10 L of LB medium containing 50 μ g ampicillin per mL of medium. When Fernbach flasks were used, shaking the flasks vigorously at 250/min ensured good aeration. In the fermentor, the growing cells were aerated by continuously bubbling a stream of filtered air into the medium while simultaneously agitating vigorously with an electric stirrer. In either case, the cells were grown at a temperature of 37°C. When the optical density of the cell suspension reached ~0.7, PFL overexpression was induced by adding a sterile-filtered solution of isopropyl- β -D-thiogalactopyranoside (IPTG) to a final concentration of 1mM. Although the cells overexpressed even without induction, overexpression improved somewhat when IPTG was added. The cells were incubated for ~2 hours after IPTG induction, and then were harvested by centrifugation at 800 rpm using a Sorvall GS3 rotor. The supernatant was discarded and the cell pellet was weighed and then either lysed immediately or flash-frozen with liquid nitrogen and stored at -80°C to be used later.

II.2.3. Bacterial synthesis of PFL-AE

PCAL-n-AE, engineered in our lab according to published procedures⁶, was used to transform *E. coli* BL21(DE3) pLysS. Cell suspensions were prepared by inoculating half of a colony into each of a number of flasks containing 50 mL of autoclaved LB/Amp media. When the optical density of the cell suspension reached approximately 0.5 enough sterile-filtered IPTG was added to give a final concentration of 1 mM. The cells were grown for two hours post-induction and cell pellets were prepared for SDS-PAGE analysis. When overexpressing colonies were identified, the remaining half of the colony was used to grow a cell suspension that was then used to prepare glycerol stock cells. Glycerol stocks were prepared by mixing, in 1.5mL micro-tubes, equal volumes of autoclaved glycerol with a cell suspension grown to saturation overnight. These were flash-frozen and stored at -80°C to be used whenever needed.

A typical growth of PFL-AE began with the plating of the glycerol stock cells on LB-agar media containing ~50 µg ampicillin per mL of LB-agar and incubating overnight at 37°C. To prepare an overnight cell suspension for a growth, a single colony was inoculated in LB/Amp medium and incubated overnight. The overnight suspension was used to inoculate 10 L of LB/Amp using a bench-top fermentor (New Brunswick) equipped with a continuous airflow inlet and an agitator. 50 mL of the overnight culture was inoculated into 10 L of LB/Amp and grown at 37°C. At an optical density (OD₆₀₀) of 0.6, IPTG was added to a final concentration of 1mM.

II.2.4. Purification of PFL

Using a cell pellet from freshly harvested cells or one from a -80°C freezer, enough lysis buffer was added to make a suspension of approximately 2 mL of lysis buffer per gram of cells. The lysis buffer comprised 20 mM HEPES containing 1 mM DTT and adjusted to pH 7.2, 1% Triton X-100, 5%w/v glycerol, 10 mM MgCl₂, 8 mg lysozyme, 1 mM phenylmethylsulfonylsulfate (PMSF) and trace quantities (~0.1 mg) of each of RNase and DNase. The cell suspension was thoroughly mixed and then homogenized continuously with a magnetic stirrer at 4°C for 2 hours. The lysed cells were centrifuged at 15,000 rpm using a Sorvall SS34 rotor for 30 minutes at 4°C. In the first step 50 mL of the crude lysate was injected onto AP-5 Superdex ion-exchange column using a low ionic strength buffer (Buffer A) consisting of 20 mM HEPES - pH 7.2, 1 mM DTT. Purification was performed automatically using the BioLogic™ program from BioRad™. The program was written based on optimization carried out under the same conditions used for the experiment.

Immediately following sample injection, the column was flushed with the low ionic strength buffer (buffer A) for 60 minutes at a rate of 3 ml/min in order to wash out the proteins that were not bound specifically by the column. Following the initial wash, the column was eluted with a steadily increasing ionic strength starting from 100% buffer A to 100% buffer B but with a total combined flow rate of 3 ml/min. Buffer B was of identical composition to buffer A except that it also contained 500 mM NaCl. When the eluent composition reached 100% buffer B, it was kept isocratic for 60 minutes before dropping down to 100% buffer A. Under these conditions, PFL started to elute out of the column at approximately 375mM NaCl and was collected in 10mL fractions. The

fractions were analyzed using SDS-PAGE in order to determine which ones contained PFL and the relative amounts of it in each. Based on the SDS-PAGE results, fractions containing $\geq 75\%$ PFL were pooled together and, whenever necessary, concentrated down to ~ 50 mL. The pooled fractions were then dialyzed for 2 hours in enough buffer A to dilute the salt 40-fold (e.g. 50 mL dialyzed in 2L of buffer A). After 2 hours, the protein was dialyzed in fresh buffer overnight. When dialysis was complete, the protein was again concentrated down to less than 10 mL using an Amicon™ concentrator. Figure II.1 shows a typical chromatogram obtained from the first purification using ion exchange and an SDS-PAGE gel electrophoresis for fourteen fractions spanning the PFL peak is shown in Figure II.2.

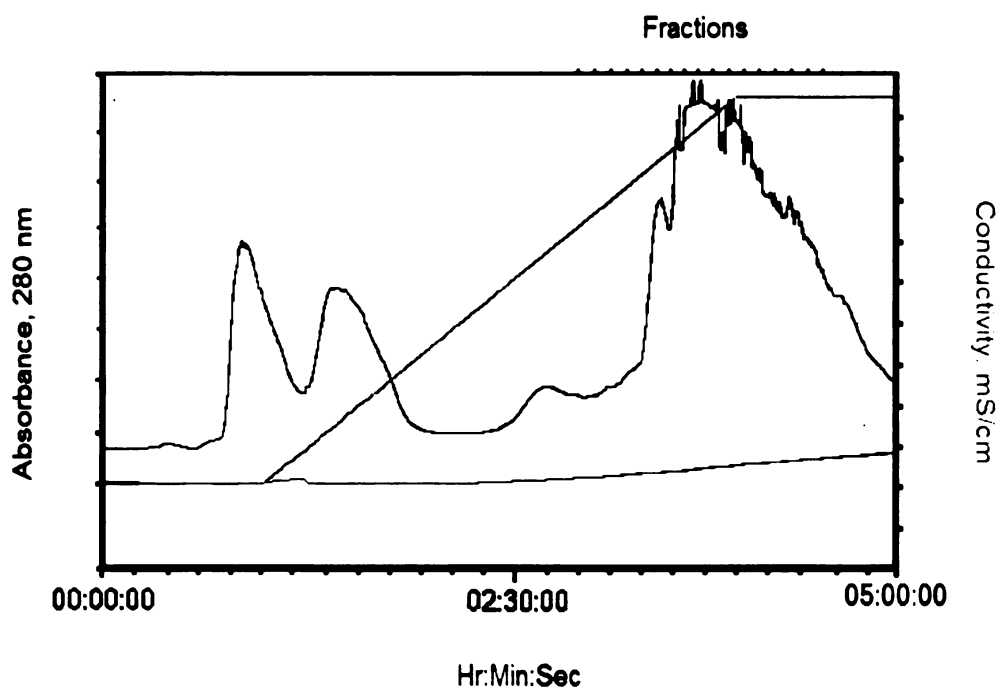


Figure II.1 A Chromatogram of PFL purification by ion exchange. PFL is in the peak eluting from approximately 3.5–4.5 hours.

In order to identify the fractions containing PFL and the relative concentration of PFL in each, SDS-PAGE was performed on the fractions spanning the PFL peak. Figure II.2. shows a typical SDS-PAGE gel of fractions from the ion-exchange column.

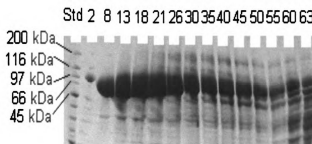


Figure II.2. SDS-PAGE of PFL fractions obtained from the first run on the Superdex ion exchange column. The fraction numbers are indicated at the top of the gel.

The fractions with $\geq 90\%$ purity, as judged by the relative intensity of the band at 85 kDa, were pooled together, and dialyzed into 20 mM HEPES (pH 7.2) containing 1 mM DTT. The fractions of lesser purity were also pooled together and stored to be run together with the next crude lysate to be purified.

After dialysis, the pooled fractions from the ion exchange column were concentrated down to $\leq 5\text{mL}$, dialyzed against 40mM HEPES (pH 7.2) containing 1mM DTT and 1M ammonium sulfate. The dialyzed protein sample was then loaded onto a Hi-Load phenylsepharose (Pharmacia) hydrophobic interaction column (1.6 cm x 10 cm) that had previously been equilibrated with a high ionic strength (high salt) buffer. The sample was injected using the high ionic strength buffer (buffer B) consisting of 40 mM HEPES at pH 7.2, containing 1 mM DTT and 1M ammonium sulfate. The purification

protocol was programmed to begin with a pre-wash, using the high ionic strength buffer in order to remove all the non-specifically associated species from the column. This was followed by elution with buffer of progressively decreasing ionic strength from 100% buffer B to 100% buffer A. The overall flow rate was set at 0.3 mL/min. Buffer A was compositionally similar to buffer B, except that it contained no ammonium sulfate. Fractions were collected in volumes of 2 mL each and analyzed using SDS-PAGE. Only fractions containing $\geq 95\%$ pure PFL were pooled and concentrated. After removing about 10 μ L for analysis, the concentrated protein was routinely flash frozen in O-ring-sealed micro-tubes and stored at -80°C . A typical chromatogram for this step of the purification is shown in Figure II.3.

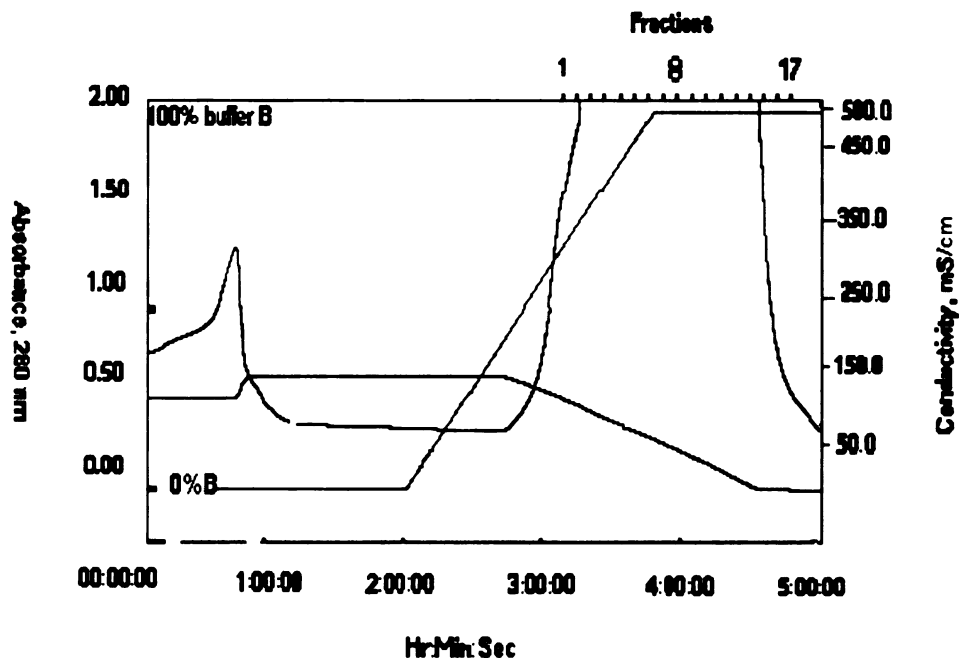


Figure II.3. A chromatogram from the second step in purification PFL using a phenylsepharose hydrophobic interaction column.

Typically, because a smaller volume of protein was used for the phenyl sepharose column, all protein eluted out of the column within a smaller buffer volume. The narrow bandwidth of the sample also proved that there was good interaction between the column and the sample. The fractions from this column therefore tended to be more concentrated as is attested to by the peak being off scale.

II.2.5. Determination of PFL concentration

The concentration of PFL was determined by using the method of Bradford⁵ with bovine serum albumin (BSA) as a standard. BSA was obtained from Sigma as a powder and the standard was prepared by preparing stock solutions of 1.19 mg/mL BSA. The working BSA solution was prepared by diluting the stock 10x. The procedure involved preparation of a protein-dye-water mixture to a final volume of 1000 μ l, of which 200 μ l was dye and the remaining 800 μ l was divided between water and protein. A standard curve was prepared by pipetting different volumes of the standard into 1.5mL micro tubes, incubating for 30 minutes to allow the blue color of the protein-dye complex to reach maximum intensity. The absorbance of the standards was measured at 595 nm and used to plot a calibration curve. The sample was prepared similarly using appropriately diluted sample as illustrated with Table II.1

Table II. 1. An example of the mixes used for the standard curve and sample during the determination of PFL concentration using the Bradford assay

Sample/Std #	Dye	Protein	H ₂ O
	volume transferred (μl)		
1	200	0	800
2	200	10	790
3	200	20	780
4	200	30	770

A typical analysis is illustrated by the data presented in Table II.2, Table II.3 and Figure II.4. The concentration of the standard was 0.119 mg/mL and the PFL was diluted 200-500 x before preparing sample for analysis. The concentration of the original concentrated PFL was calculated from the equation of the standard curve, taking into account the dilution factor. In determining the concentration of protein, samples were routinely prepared in duplicate or triplicate per given volume, and various volumes were used. This was done in order to test for both random error arising from the analyst, and any systematic error that might arise as a function of the amount of protein used. Analytically, only the absorbance values lying within the range of the standard curve can be used to calculate the unknown PFL concentration. In the example given in Table II.3, the sample containing 50 μl of diluted PFL could not be included in the calculation of PFL concentration because its absorbance was above the highest absorbance (0.885) measured for 7.14 μg of standard protein. The example used here also shows illustrate another tendency that was typically observed in the analysis of PFL, namely, that the higher the amount of PFL in the sample, the lower the estimate of the concentration of PFL in the original concentrated sample. Further investigation of this phenomenon

revealed that whenever the concentration of PFL in the sample was higher than the maximum possible for a linear response, the Bradford analysis tended to underestimate the concentration of the original protein solution, even if the sample absorbance may be within the linear range of the calibration curve. Thus it is important to ensure not only that the concentrations of the standard used fall within a linear response range, according to the Beer-Lambert law, but also that the amounts of PFL used in the samples also fall within linear response range for PFL. For all subsequent PFL concentration measurements using this method several PFL samples were measured and plotted to check for response linearity before subjecting them to analysis based on the BSA standard curve.

Table II.2 Typical series of standards used for calibration

0.119 mg/mL BSA standard		
Volume (μ l)	μ g Protein	Absorbance
0	0	0.475
5	0.595	0.502
10	1.19	0.551
15	1.785	0.592
20	2.38	0.633
40	4.76	0.762
60	7.14	0.885

Table II.3. The typical raw data and calculated protein concentration calculated from the calibration curve.

1/500x diluted PFL				
Volume (μl)	Absorbance	μg Protein	Original conc.(mg/ml)	Avg. conc.(mg/ml)
20	0.673	3.37	84.36	88.1
20	0.690	3.67	91.77	
40	0.851	6.48	80.95	
40	0.840	6.28	78.55	
40	0.843	6.34	79.20	79.6
50	0.913	7.56	75.56	75.8
50	0.898	7.29	72.94	
50	0.933	7.90	79.04	

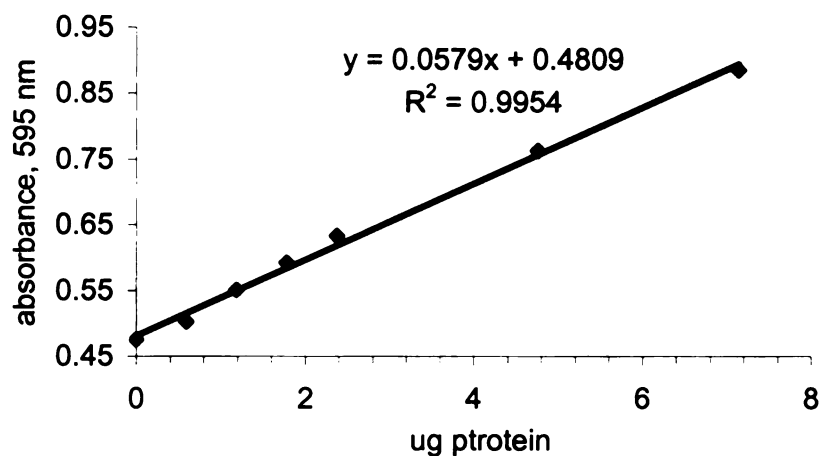


Figure II.4. An example of a calibration curve used to calculate the concentration of protein analyzed by the Bradford assay.

II.2.5. Activation of PFL

The standard protocol followed in our lab to activate PFL entailed mixing all the species involved in a specific order.⁶ A typical PFL activation mix consisted of 100-150 mM Tris-Cl buffer (pH 7.6), 0.1 M KCl, 10 mM oxamate, 8 mM DTT, 0.03 μ M PFL-AE, 2 μ M PFL, 0.2 mM AdoMet and 50 μ M 5-deazariboflavin, all added to the reaction vessel in the given order with the final concentration of each sample being as indicated. After mixing in all the reagents inside an anaerobic chamber, the mix was then illuminated with a high intensity (300W) halogen lamp. The temperature was maintained between 16 and 23°C using an ice bath. Illumination was carried out for 30 to 45 minutes at a time and the PFL activity was measured by using a coupled enzymatic assay containing 100-150 mM Tris-Cl (pH 8.5), 3 mM NAD⁺, 55 μ M CoA, 0.1 mg BSA, 10 mM pyruvate, 10 mM malate, 6 units of citrate synthase and 14 units of malic dehydrogenase. All reagents used for PFL activation and for the assay mix were pre-weighed into a Falcon tube and then pumped into an MBRAUN™ glove box. Tris-Cl and water were made anaerobic in advance using a Schlenk line, and then stored inside the anaerobic chamber. To 698 μ L of the assay mix was added 2 μ L of the mix containing active PFL. To prevent reaction, the active PFL mix was placed on the inside cuvette wall well above the surface of the assay mix. Because of the small volume of the active PFL delivered to the cuvette wall, surface tension was strong enough to keep it from flowing down into the assay mix, thus keeping the two separate until the desired moment. After sealing it with an air-tight screw-on rubber stopper, the cuvette was carefully placed upright inside the mini-chamber of the anaerobic box. Meanwhile, the computer-controlled spectrophotometer was pre-set to measure the rate of NADH production

indirectly through the rate of increase of absorbance at 340 nm, using a coupled enzymatic assay whereby the rate of production of NADH is directly related to the concentration of active PFL (Figure III.8.). The cuvette was brought out of the box and the active PFL and the assay mix were brought into contact with two rapid shakes. The cuvette was then placed in the instrument to measure the rate of NADH production in units of nmoles per minute. The activity of PFL was periodically confirmed by using EPR to directly detect and quantify the glycy radical on PFL. The characteristic signal for the glycy radical is shown in Figure II.5.

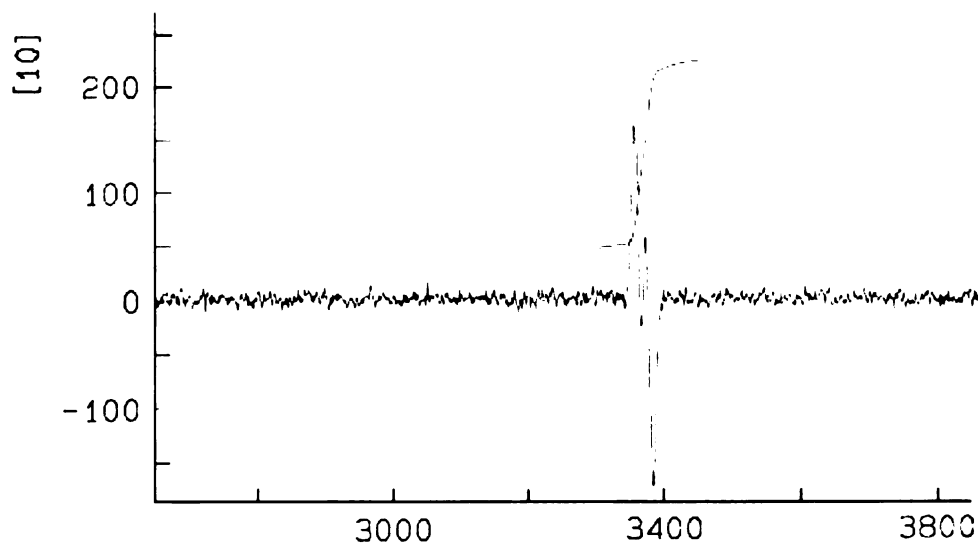


Figure II.5. The EPR spectrum of the glycy radical on activated PFL

During the studies of activated PFL, we discovered that previously activated PFL, upon prolonged exposure to ambient light, increased in activity, as measured by the rate of NADH production during the enzymatic assay. This led us to explore the possibility that PFL could be activated without need for high intensity illumination, but simply by

exposing the activation mix to ambient light. To investigate this, the reaction mix was prepared as usual and incubated inside the anaerobic chamber under ambient light and temperature of $\sim 23^{\circ}\text{C}$. PFL activity was monitored over time by periodically removing 2 μl of the activation mix and adding it to 698 μl of the assay mix. The change in PFL activity over time is shown in Figure II.6. The activity showed a dramatic increase from 0 to 116 nmolNADH/min in just less than 2 hours, reaching a maximum after approximately seven hours.

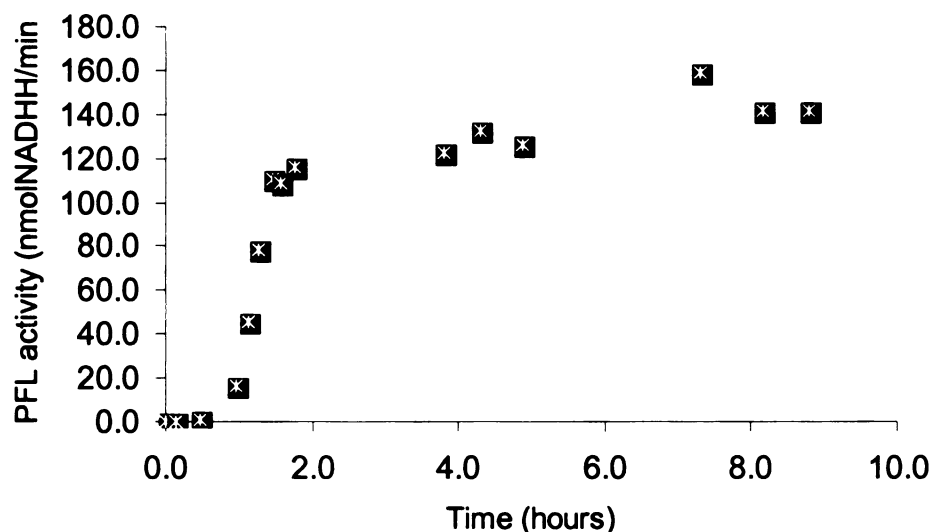


Figure II.6. A time course activation of PFL under ambient light and 23°C . The level of activation was found comparable to that achieved by high intensity illumination. As predicted, PFL activated by this method, once it reached a threshold activity, did not show any sign of reactivation during subsequent experiments. This was in contrast to PFL that had been previously activated by illumination, which showed evidence of additional activation upon exposure to ambient light.

These findings have led us to propose that high intensity illumination of PFL is not necessary for activation. Indeed, it may be detrimental as cooling with ice water

leads to rather sharp changes in temperature. We periodically observed some precipitation of PFL during activation by intense illumination. However, in that case, the temperature of the activation mix was always maintained below 23°C by using ice. We hereby suggest that such precipitation, though relatively uncommon during activation, presented a problem when it occurred because it effectively reduced the total PFL concentration in the activation mix. Consequently, the maximum achievable PFL activation would be decreased. It is also possible that activated PFL is less stable to denaturation than unactivated PFL, thereby aggravating the problem. That precipitation has been observed even at temperatures less than 23°C may be due to the rapid temperature changes resulting from local effects within the bulk solution, particularly when ice is added to cool the activation mix. This suggestion is also supported by the observation that PFL activated without illumination was found to be exceedingly stable, showing activities of over 50% of the original even after standing for 2 days at 23°C inside the chamber. It is also significant that when activation is done without need for introduction of ice into the anaerobic chamber, it is easier to maintain the oxygen level within the box at less than 1 ppm. It may also be argued that the latter activation conditions approximate more closely those that probably prevail inside a living organism. More quantitative studies are needed in order to determine the extent of activation during each set of conditions. Our preliminary findings strongly suggest that illumination offers no advantage over “dark” activation.

II.3. RESULTS

II.3.1. Expression

BL21(DE3)plysS *E. coli* strain transformed with the plasmid pKK-pfl, expressed PFL well. It was of interest to note that even though the plasmid used to clone the *pfl* gene has an IPTG-inducible promoter, the transformed cells were able to overexpress PFL extremely well, even without induction. There was only a marginal difference in the PFL yield between the induced and uninduced cells. Sometimes the cells were only grown to the stationary phase and harvested without induction.

II.3.2. Purification of PFL

We routinely purified PFL using ion-exchange chromatography. The fractions from this column generally contained PFL with at least 90% purity but still contained a significant amount of impurities. The main chromatographic peak corresponding to PFL in this purification appeared as essentially a single peak, thereby indicating that the impurities found in this purification had similar PIs as PFL. Some of the impurities were probably trapped in the PFL structure, just because of the high concentration of PFL relative to the other proteins. As a routine protocol in our lab, all fractions containing ~90% or more were pooled together, concentrated and run through a hydrophobic interaction column to improve purity. Based on SDS-PAGE analysis of the fractions, only those containing ~95% PFL were pooled together and concentrated and used for the investigations.

II.3.3. Activation and stability of PFL

Initially, activation was done by using high intensity illumination as described in the Materials and Methods section. However, our discovery that PFL could be activated under ambient light afforded us a way to routinely activate this enzyme by merely exposing it to regular fluorescence light in the presence of all the activation components. To our surprise, PFL could be activated to the same extent using this method. This method was preferred because it was practically far less cumbersome than activation by high intensity illumination. Ambient light also approximated more closely the natural conditions under which PFL would have to be activated.

During the course of experimental manipulations of PFL we also discovered that this enzyme is extremely stable both in its active and inactive forms. PFL left at room temperature to up to 10 days was found to be still activatable, for example. Notably, and quite amazingly, there was also no sign of precipitation. Presumably, some of the protein had denatured, but this was not immediately observable. That the enzyme could still be activatable after such prolonged exposure at room temperature was quite remarkable. Prompted in part by this observation, and during the course of other studies of PFL, we also observed that activated PFL also preserved its activity for well over 24 hours under anaerobic conditions, even at temperatures as high as 23°C. We therefore believe that in addition to the inherent stability enjoyed by the glycyl radical due to the captodative effect, the overall stability of the PFL protein plays some role in the unusual stability observed for the PFL radical.

II.4. Conclusion

PFL was successfully overproduced in an *E. coli* protein expression strain (BL21(DE3)plysS) that had been transformed with a plasmid carrying an IPTG-inducible promoter. Interestingly, this strain overexpressed PFL even without induction by IPTG. This property of the bacteria proved advantageous, as the cells could be grown to the stationary phase and harvested without need for induction. PFL was purified to homogeneity using ion-exchange chromatography followed by hydrophobic interaction. During the course of our experiments, we discovered that PFL can be activated by using ambient light, as opposed to the high intensity light that we previously used to illuminate it, consistent with published procedures. This proved advantageous because 1) it simplified the experimental manipulations significantly and 2) although the general conditions of activation remained artificial, they more closely approximated the natural conditions under which PFL activation takes place.

PFL is remarkably stable, both in its active and inactive forms. Unactivated PFL can be activated even after sitting at room temperature for over a week. Activated PFL was found to be capable of retaining essentially all its activity for 24 hours at 23°C. We suggest that this unusually high stability of activated PFL may be due to the inherent stability of the PFL protein itself as well as the local inductive effects that stabilize the radical captodatively. We expect that the discovery of this remarkable stability of PFL will prove useful in any future studies conducted on this enzyme.

REFERENCES

- 1 Wagner, A.F.V.; Frey, M.; Neugebauer, F.A.; Schafer, W.; Knappe, J. **1992**, *Proc. Natl. Acad. Sci.U.S.A* 89, 996-1000.
- 2 Knappe, J.; Sawers, G. **1990**, *FEMS Microbiol. Rev.* 75, 383-398
- 3 Knappe, J.; Elbert, S.; Frey, M.; Wagner, A.F. **1993**. *Biochem. Soc. Trans.* 21, 731-734.
- 4 Conradt, H.; Hohmann-Berger, M.; Hohmann, H.P.; Blaschkowski, H.P.; Knappe, J. **1984**, *Arch. Biochem. Biophys.* 228, 133-142.
- 5 Knappe, J.; Blaschkowski, H.P.; Schmitt, T. *Eur. J. Biochem.* **1974**, 50, 253-263.
- 6 Broderick, J.B.; Henshaw, T.F.; Cheek, J.; Wojtuszewski, K.; Smith, S.R.; Trojan, M.R.; McGhan, R.M.; Kopf, A.; Kibbey, M.; and Broderick, W.E. **2000**. *Biochem. Biophys. Res. Commun.* 269: 451-456
- 7 Janda, M.; and Hemmerich, P. **1976**, *Angew. Chem. Int. Ed. Engl.* 15,7
- 8 Ashton. W.T., Brown, R. D. and Tolman, R. L. **1978**, *J. Heterolytic Chem.* 15, 489-491.
- 9 Smit, P. **1986**, *Recl. Trav. Chim. Pays-Bays.* 105, 538-544.

CHAPTER III

STUDIES OF ALCOHOL DEHYDROGENASE FROM *ESCHERICHIA COLI*

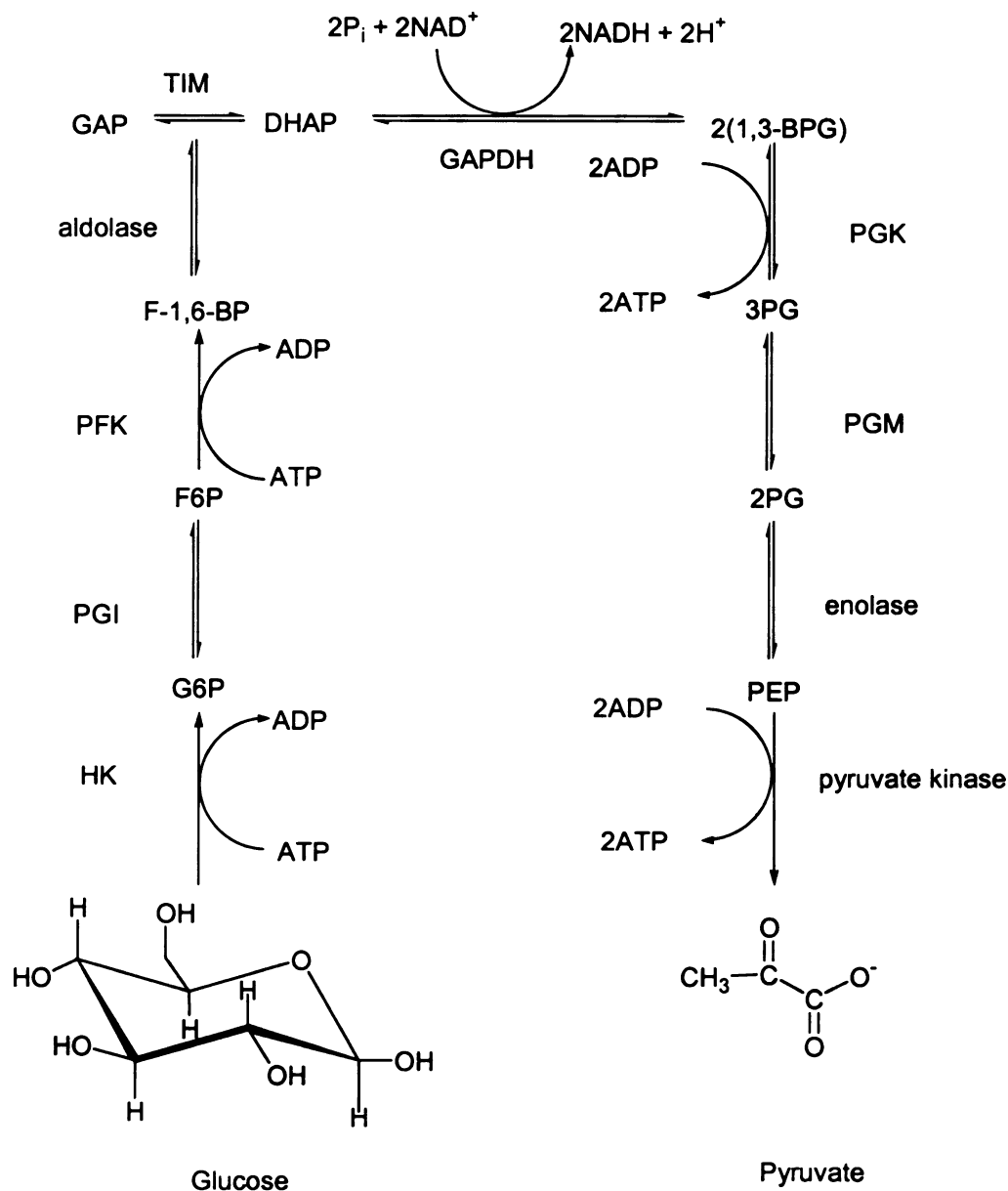
ABSTRACT

Alcohol dehydrogenase from *E. coli* (AdhE) is known to harbor both the alcohol dehydrogenase and acetaldehyde reductase activities. Both of these activities utilize the NAD^+/NADH redox pair during processing of substrate. In the last decade this enzyme has also been implicated as a pyruvate formate-lyase (PFL) deactivase, facilitating the conversion of PFL from the active radical state to the inactive non-radical state by quenching the radical that is characteristic of the active form of PFL. We were unable to confirm this activity for AdhE. We did, however, observe clear deactivation of PFL by other assay components in the assay mix. Significantly, some of these components were also included in the deactivation studies from which AdhE was implicated as a PFL deactivase. In this chapter we report the cloning, over-production and purification of AdhE and its characterization with respect to both the alcohol dehydrogenase and acetaldehyde reductase activities. Enzymatic assays were used to investigate further the purported role of this multienzyme as a PFL deactivase. Our findings suggest that this enzyme does not deactivate PFL. We propose that the deactivation observed in previous reports was due to other components in the assay mix rather than AdhE. This proposal is supported by the observation that several thiols that we investigated have proven to be effective deactivators of PFL under conditions similar to those reported in the literature (Chapter IV).

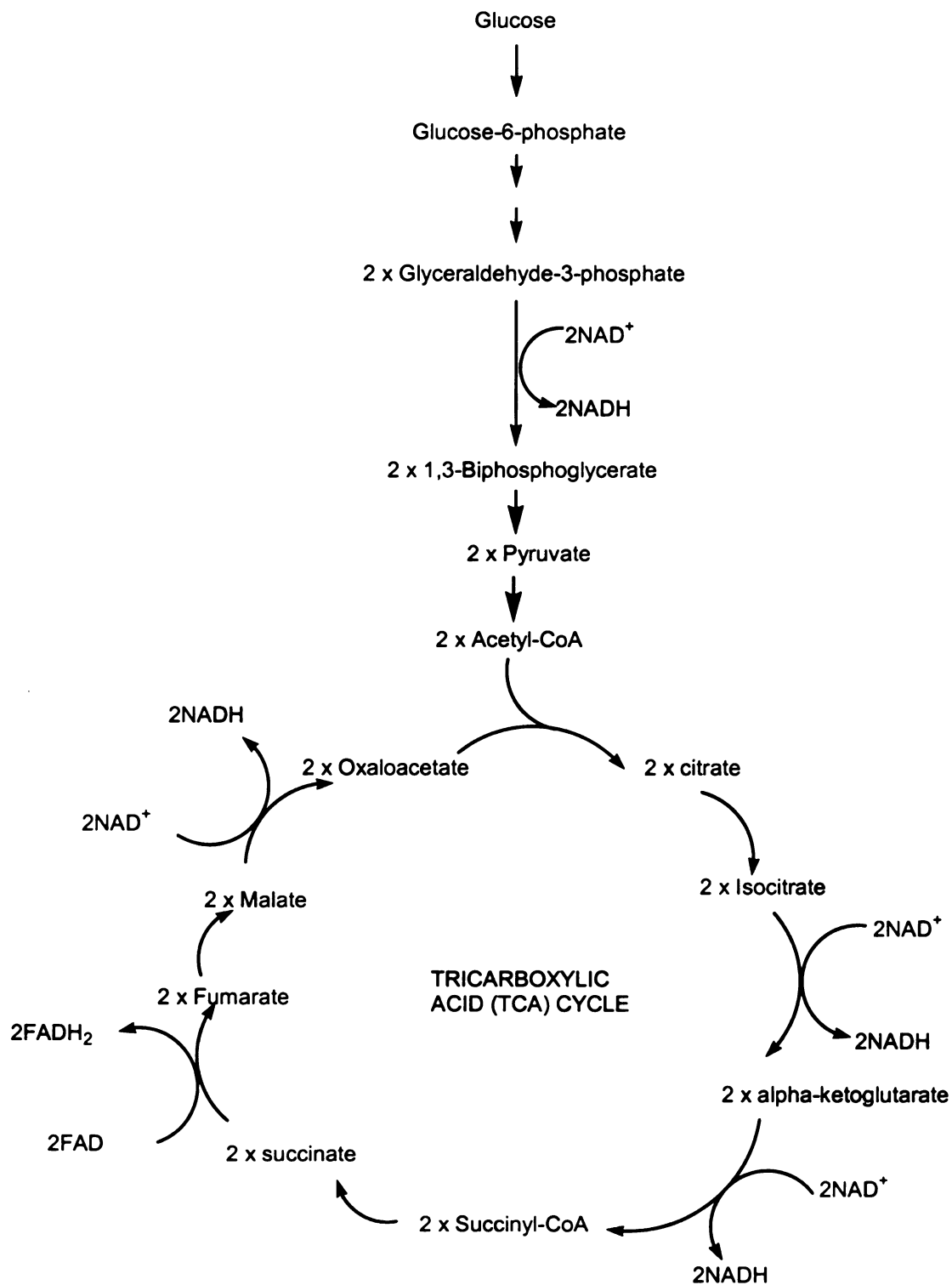
III.1 INTRODUCTION AND BACKGROUND

Metabolic breakdown of glucose in *Escherichia coli* (*E.coli*) takes place via glycolysis, a series of chemically coupled phosphorylation reactions involving multiple enzymes that ultimately lead to the production of pyruvate as the final product. Glycolysis occurs under both aerobic and anaerobic growth, and results in a net reduction of two NAD^+ molecules to two NADH molecules (Scheme III.1). During glycolysis, a net of 2 molecules of ATP are produced by substrate-level phosphorylation, supplying sufficient energy to enable *E. coli* to survive during anaerobiosis. During aerobic growth, pyruvate produced from glycolysis is oxidized to acetyl-CoA by NAD^+ under the mediation of the pyruvate dehydrogenase enzyme complex (PDHc), with concomitant production of NADH and CO_2 , whereas in the absence of oxygen the conversion of pyruvate to acetyl-CoA is catalyzed by pyruvate formate-lyase (PFL), a homodimeric enzyme whose active form harbors a radical co-factor. The PFL-catalyzed conversion of pyruvate to acetyl-CoA also produces formate as a by-product.

Subsequent processing of acetyl-CoA in *E. coli* leads to two possible fates. If catabolism occurs under aerobic conditions, acetyl-CoA enters the tricarboxylic acid (TCA) cycle wherein the acetyl group is oxidized to two CO_2 molecules (Scheme III.2). A molecule of ATP is also produced for every complete TCA cycle, that is, two molecules of ATP are generated for every molecule of glucose catabolized. The free energy released from this oxidation is stored in the reduced co-enzymes NADH and FADH_2 and is passed along the electron transport chain and ultimately used to reduce oxygen to water. Concomitant with the recovery of the oxidized co-enzymes during the electron transport, ATP is generated from ADP and phosphate in a process referred to as



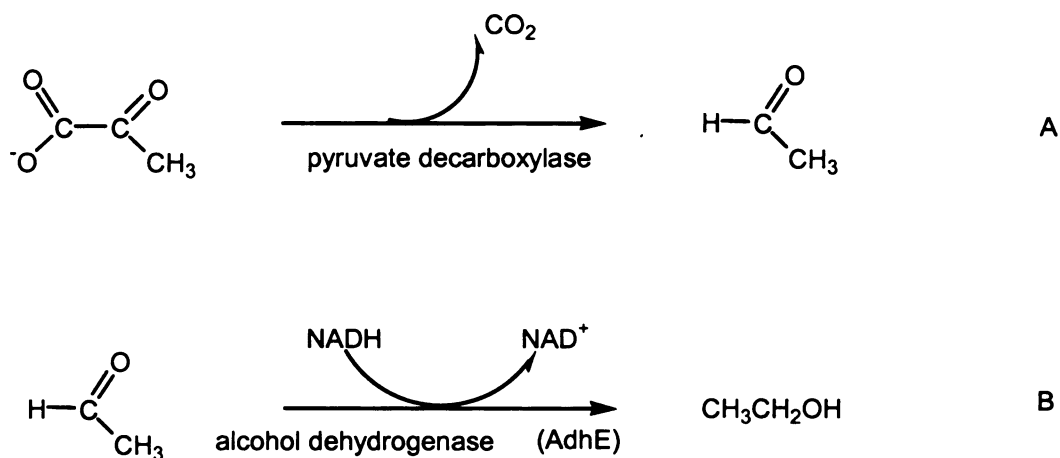
Scheme III.1. A Schematic of glycolysis showing the steps involved during the breakdown of glucose to pyruvate. The enzyme involved in each step is indicated on the side of the arrows in abbreviation. Two molecules of ATP are consumed during the first step and four are produced in the second part, thus yielding a net of two ATP molecules per molecule of glucose.



Scheme III.2. During aerobic growth, acetyl-CoA is fed into the TCA cycle wherein its oxidation is coupled to production of the reduced co-enzymes NADH and FADH₂.

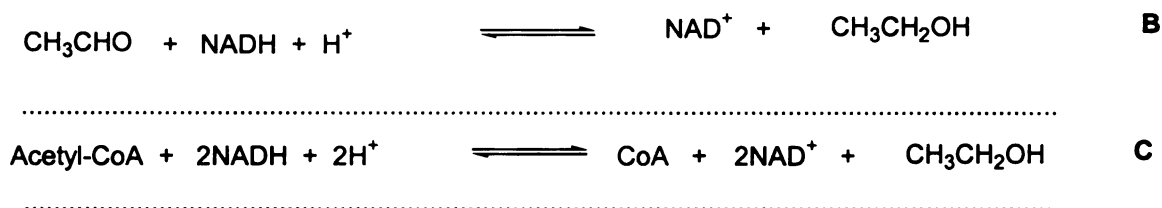
oxidative phosphorylation. During aerobic respiration, 38 ATP molecules are produced for every glucose molecule catabolyzed, and this mode of energy production is very efficient.

During anaerobic growth, however, glycolysis provides the only source of ATP for *E. coli*. One of the crucial steps in this catabolic process is the conversion of the isomers glyceraldehyde-3-phosphate (GAP) and dihydroxyacetone phosphate (DHAP) to two molecules of 1,3-biphosphoglycerate under the mediation of glyceraldehyde-3-phosphate dehydrogenase. This substrate-level phosphorylation step involves the consumption of two phosphates and reduction of two NAD^+ molecules to NADH. The NAD^+ necessary for this step is supplied by the reduction of pyruvate via a series of reactions starting with the decarboxylation of pyruvate to produce acetaldehyde (Scheme III.3). Acetaldehyde produced by pyruvate decarboxylase is reduced to ethanol by NADH under the catalysis of AdhE, and in the process, NAD^+ is cycled for the conversion of the GAP/DHAP pair to 1,3-BPG under the mediation of GAPDH. 1,3-BPG produced in this step, in the presence of ADP, is then acted upon by phosphoglycerate kinase (PGK) to generate more ATP and pyruvate. The alcoholic fermentation process is known to involve two steps as summarized in Scheme III.3. The first step (A) is the decarboxylation of pyruvate catalyzed by pyruvate decarboxylase, producing acetaldehyde as an intermediate. The second and final step is the reduction of acetaldehyde by NADH to ethanol, and this reaction is catalyzed by alcohol dehydrogenase (AdhE).



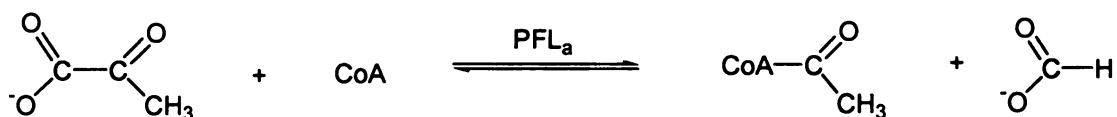
Scheme III.3. The two-step reduction of pyruvate to ethanol during alcoholic fermentation

During anaerobic growth and in the absence of exogenous electron acceptors, *E. coli* can produce any of a number of fermentation products, depending on the carbon source on which it is growing. Some of the possible products include ethanol (Scheme III.3), glycerol, formate, acetate, D-lactate, succinate, CO_2 and H_2 .¹ Under these conditions, AdhE is also able to reduce acetyl coenzyme A (acetyl-CoA) in a two-step process whereby two molecules of the reduced co-enzyme NADH are oxidized to two molecules of NAD^+ per turnover (Scheme III.4).²



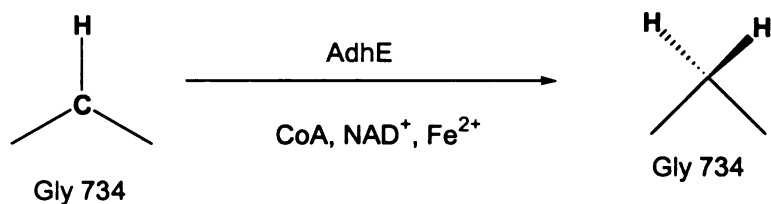
Scheme III.4. The reactions catalyzed by AdhE. The two steps (A and B) lead to the overall (C)

This fermentation route is of interest in relation to pyruvate formate-lyase (PFL), which, like AdhE, is an anaerobically induced and activated enzyme. In the presence of CoA, PFL mediates the homolytic cleavage of pyruvate producing acetyl-CoA and formate (Scheme III.5). Based on the two reactions above, it is notable that during anaerobiosis under conditions favoring the reduction of acetyl-CoA as depicted in Scheme III.4, PFL-mediated homolysis of pyruvate supplies the substrate for the fermentation reaction catalyzed by AdhE. There is therefore interesting cooperation between these two enzymes under anaerobic respiration, whereby the reduction of pyruvate to ethanol begins with employment of PFL but is finally mediated by AdhE.



Scheme III.5. The reaction catalyzed by PFL.

In addition to the alcohol dehydrogenase and acetaldehyde reductase activities, AdhE has been implicated in the deactivation of PFL, as shown by Scheme III.6.^{3,4}



Scheme III.6. The proposed role of AdhE as a PFL deactivase

This purported PFL deactivation activity is intriguing because it has to be invoked when conditions change from anaerobic to aerobic, whereas both enzymes are known to function under anaerobic conditions. PFL is translated in an inactive state and is then activated post-translationally under anaerobic conditions by an activating enzyme called PFL-activating enzyme (PFL-AE).⁵ Its active state comprises a free radical located on at Gly734,⁶⁻⁸ which has been demonstrated to be extremely sensitive to oxygen, undergoing oxygenolytic fragmentation within a few seconds of exposure to air.⁷ In order to be an effective deactivator of PFL, AdhE would have to do so very rapidly. It would also have to be able to sense small amounts of oxygen before it can destroy the very sensitive PFL radical. The PFL deactivase activity of this enzyme is, in part, the subject of this investigation. Recently, a novel antioxidant role of AdhE was discovered under aerobic conditions.⁹ If verified to be real, this activity adds valuable perspective towards elucidation of the roles that AdhE plays in both *E. coli* as well as other medically important facultative anaerobes, particularly those belonging to the family *Enterobacteriaceae*.

III.2. MATERIALS AND METHODS

III.2.1 Cloning of His₆-tagged AdhE

The gene sequence for *adhE* was obtained from the literature.¹⁰ The *adhE* gene was amplified by the standard polymerase chain reaction (PCR) technique using *E.coli* BL21(DE3)pLYS chromosomal DNA as a template. The synthetic oligonucleotide primers had the sequences shown in Figure III.1. The bold letters indicate the restriction enzyme recognition sequences, with the corresponding restriction enzyme used at each site indicated in italics above each restriction site sequence.

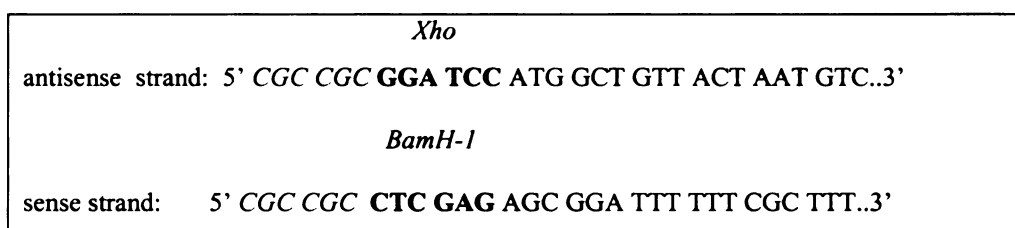


Figure III.1. The primers used to amplify the AdhE gene of *E. coli* by PCR. The restriction sites are shown in bold and were included to improve cloning efficiency.

The PCR product was digested with the restriction enzymes *BamH-1* and *Xho* and then cloned into a PET-21a(+) expression vector (Novagen), also digested with the same enzymes. The expression vector contains a His-tag sequence downstream of the *Xho* site. This tag attaches a chain of 6 histidines onto the C-terminus of the overexpressed protein. The recombinant DNA obtained from the cloning of the *adhE* gene into PET-21a(+) was first transformed into competent Epicurian XL1 Blue *E. coli* cells obtained from Novagen. The transformation mix was plated on LB-agar impregnated with 50µg/ml

ampicillin and incubated overnight at 37°C. Twelve colonies were identified and marked by circling over each on the cover plate of the petri dish. Using autoclaved toothpicks, about a quarter of each colony was used to inoculate a Falcon tube containing 5 ml of liquid LB medium to which was added 250 µg ampicillin. All twelve tubes were incubated overnight in a shaker at 250 rpm. The temperature was maintained at 37°C and each tube was covered so as to allow free diffusion of air into the cell suspension. After incubating overnight, all twelve tubes showed good growth, as indicated by the turbidity of the cell suspensions.

III.2.2 Extraction and analysis of PET-21^a (+)-adhE

From each of the overnight cultures, a total 1.5 ml was centrifuged in order to obtain a cell pellet. Plasmid DNA was then extracted from each cell pellet using a commercial DNA extraction kit (Stratagen™). The purity of the extracted DNA was determined by measuring the ratio of the absorbance due to DNA ($A_{260\text{nm}}$) and absorbance due to protein ($A_{280\text{nm}}$). An $A_{260\text{nm}} / A_{280\text{nm}}$ of 1.6 or greater was considered to indicate an acceptable level of DNA purity. In order to ascertain its genetic identity, the recombinant plasmid DNA purified as above was digested with *Xho* and *BAM-HI*, followed by electrophoretic analysis on 0.6% agarose gel impregnated with 10 µg ethidium bromide per mL. A 1kb ladder commercial DNA standard was used as a marker to establish the size of the fragments resulting from the restriction digest. Figure III.2 shows the fingerprints of DNA obtained from each of the 12 colonies.

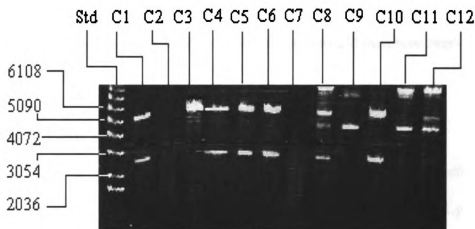


Figure III.2. DNA fingerprints of colonies 1 to 12 after digestion with *Xho* I and *Bam*H-I. The digested sample (10 μ L) was thoroughly mixed with approximately the same volume of loading buffer before loading into an agarose gel containing 10 μ g ml⁻¹ ethidium bromide. Lane 1 contains the DNA molecular weight marker and the molecular weights of the bands are shown on the side.

The expected size of the *adhE* gene is 2650 bp in size. The rest of the PET-21a(+)-*adhE* recombinant plasmid constitutes 5443 bp. Figure III.2 shows that DNA from colonies 1, 4, 5, 6 and 10 is cut into two fragments that correspond to the expected molecular weights. DNA from colonies 2 and 7 was not detectable, probably because of misloading of the wells. The band patterns from the other colonies also make sense. Colonies 8 and 12 were partially digested as evidenced by the appearance of two bands of identical masses to those seen with colonies 1, 4, 5, 6 and 10. The bands at ~4500 bp and ~8000 bp are probably due to supercoiled and nicked DNA respectively. Similarly, the bands observed for colonies 9 and 11 were interpreted as being due to nicked and supercoiled DNA. DNA from colony 3 was the most difficult to explain. A lone band of molecular weight corresponding to a PET21⁺ was observed for this colony. However, the fragment corresponding to the *adhE* PCR product is not observed, therefore suggesting that the band at ~5400 did not result from a double digest of PET-21a(+)-

adhE. Based on this interpretation, it was hypothesized that colonies 1, 4, 5, 6 and 10 and possibly 8, 9, 11 and 12 were successful transformants and would therefore over-express AdhE but colony 3 would not.

III.2.3. Transformation of BL21(DE3)pLysS with PET-21a(+)-adhE

The hypothesis proposed in section III.3.2 was tested by transforming recombinant plasmid DNA from colonies 3, 4, 5, 6 and 10 into BL21(DE3)pLysS and using the transformants to test for over-expression of the adhE gene product. Competent BL21(DE3)pLysS cells were obtained from Stratagen™. Following the prescribed protocol, 50 µL of competent cells was transformed using 2 µL of the test recombinant DNA. The transformed cells were then plated on LB/agar medium containing 10 µg of ampicillin per milliliter of medium and incubated at 37°C overnight. For each of the cell lines, the colonies obtained from the overnight culture plates were used to grow an overnight liquid culture of the transformants in 5mL of Luria-Bertini (LB) medium containing 10 µg of ampicillin per milliliter of medium. For each cell line, 50µl of the overnight cultures were used to inoculate two 50 ml LB cultures and the optical density of each culture was monitored at 600 nm (OD₆₀₀). At OD₆₀₀ = 0.5, only one of each pair of growths per cell line was induced by adding 1 M isopropyl β-D-thiogalactopyranoside (IPTG) to a final concentration of 1 mM. Both the induced and uninduced cells were allowed to grow for a further 2 hours before harvesting cell pellets from 1 mL of each of the cell suspensions. To test over-expression of AdhE, the cell pellets were denatured by boiling for 10 minutes in a sodium dodecyl sulfate (SDS) denaturing buffer (Maniatis). The denatured cells were then centrifuged at 12,000 rpm for 5 minutes and the

supernatant was loaded onto a 12% Tris-HCl electrophoresis gel purchased from BioRad™. Electrophoresis was run at a voltage of 250 mV and the protein bands were exposed with Coomassie stain.

III.2.4. Streaking of the glycerol stocks to obtain colonies

The process of growing the cells from the glycerol stocks involved lightly scraping the surface of a frozen stock of cells with a bacterial streaking needle and lightly streaking onto an ampicillin-impregnated agar culture medium contained in a bacterial culture plate. At all times the glycerol stock was prevented from thawing by keeping it in a Dewar flask chilled with liquid nitrogen and then putting it back into the freezer immediately after plating was completed. The streaked plate would then be incubated at 37°C overnight. At all times the working environment was kept sterile by applying ethanol to the workbench and then performing the streaking under a flame. Figure III.3 illustrates the streaking technique used. The streaking needle was sterilized in a flame and then cooled by touching it to the sides of the chilled micro tube containing the glycerol stock. The needle was lightly scraped on the surface of the frozen glycerol stock and then lightly streaked in different regions as illustrated in steps 1 to 3. The darkest streak (with an arrow) is the last one in each step and represents a progressively decreasing concentration of cells as streaking proceeds.

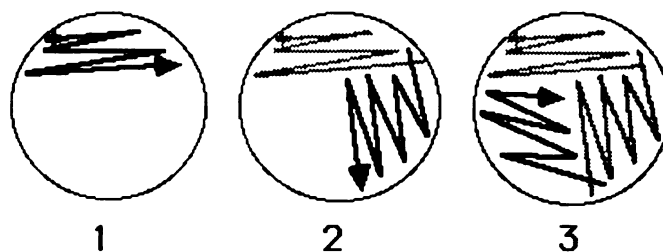


Figure III.3. Steps followed in streaking a glycerol stock onto an agar plate for overnight incubation.

Typically, several colonies were observed on the plate after 16 hours as illustrated in Figure III.4, and tended to be more isolated with the later streaks as shown in the boxed regions. Regions 1, 2 and 3 correspond to the streaking steps in Figure III.3.

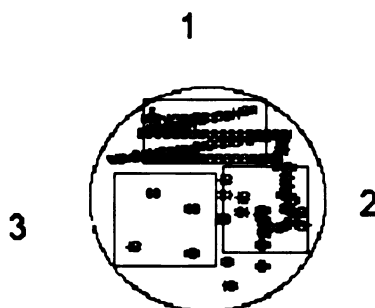


Figure III.4. The typical appearance of colonies on an agar plate after overnight incubation. Regions 1,2 and 3 (boxed) correspond to the streak steps in Figure III.4 and show stepwise dilution of the colonies with each subsequent streak step.

Since all the cells in the suspension used to prepare the glycerol stocks can be traced back to a single transformant cell, all of the colonies on the streaked overnight plate could reasonably be assumed to be isogenic. The choice of colony for the to be used for the overnight growth was usually based on the appearance of the colony. Only colonies that appeared healthy (not overgrown and having no satellite colonies around them) were used for overnight growths.

III.2.5. Growth, Harvesting and Lysis

Using a colony from a streaked plate prepared as in section III.3.4, a single colony was inoculated into a 50 mL of LB/Amp medium and incubated overnight in a shaker/incubator set at 37°C and 250 rpm. To a set of six 2.8 L Fernbach flasks containing ampicillin at a concentration of 50 µg/mL, 1 mL of the overnight culture was inoculated. The growth of the cells was monitored by measuring the optical density of each culture at 600 nm (OD₆₀₀). When OD₆₀₀ reached 0.5, the cells were induced by adding 1M isopropyl β-D-thiogalactopyranoside (IPTG) to a final concentration of 1mM and then allowed to grow for a further 2 hours.

After 2 hours, the cells were harvested in pre-weighed bottles by high-speed centrifugation using a Sorvall GS3 rotor at a speed of 8000 rpm for 5 minutes. The supernatant was then decanted and the wet cell pellet was drained by inverting the centrifuge bottles on absorptive paper for approximately 10 minutes. The bottles plus the drained cells were weighed and the mass of the cell pellets determined by difference. The cells were either lysed directly or stored at -80°C for later use. The lysis buffer consisted of 50 mM NaH₂PO₄, 10 mM imidazole and 300 mM NaCl, the whole mix adjusted to pH 8. To an average of 6 g of cells per harvest bottle, 20 mL of lysis buffer containing 8 mg lysozyme, 1 mM phenylmethylsulfonyl-sulfate (PMSF) and trace quantities (~0.1 mg) of each of RNase and DNase were added. The cell suspension was thoroughly mixed and then homogenized continuously with a magnetic stirrer at 4°C for approximately 2 hours. The lysed cell paste was centrifuged at 15,000 rpm using a Sorvall SS34 rotor for 30 minutes at 4°C. The supernatant containing the over expressed

AdhE was carefully pipetted into a 50 mL Falcon™ tube, flash-frozen in liquid nitrogen and stored at -80°C or used directly to purify AdhE.

III.2.6. Purification of His₆- AdhE

III.2.6.1. Purification Principle

The protein was purified using a commercial nickel nitrilotriacetic acid (Ni-NTA) immobilized metal affinity chromatography (IMAC) resin from QIAGEN®. This column consists of Ni²⁺ immobilized by a tetradentate nitriloacetic acid chelate in highly cross-linked 6% agarose beads on a superflow support. Figure III.5 is a schematic to show how Ni is immobilized by coordination to nitrilotriacetic acid (NTA).

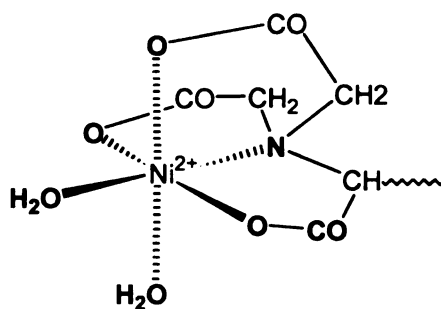


Figure III.5. Illustration of how immobilized Ni is coordinated to a nitrilotriacetic acid (NTA) support.

Upon loading the column, His-tagged AdhE protein displaces the water molecules and binds to the two remaining Ni²⁺ coordination sites via the nitrogen atoms on the imidazole rings of the histidine tag. The interactions between the NTA-immobilized Ni ion and two histidines of the tag are illustrated in Figure III.6. Once AdhE is bound as shown, all other proteins that do not specifically bind to the resin were washed out of the

column using a buffer containing mild concentrations (20 mM) of imidazole before eluting AdhE out with similarly constituted buffer containing a higher concentration (250 mM) of imidazole.

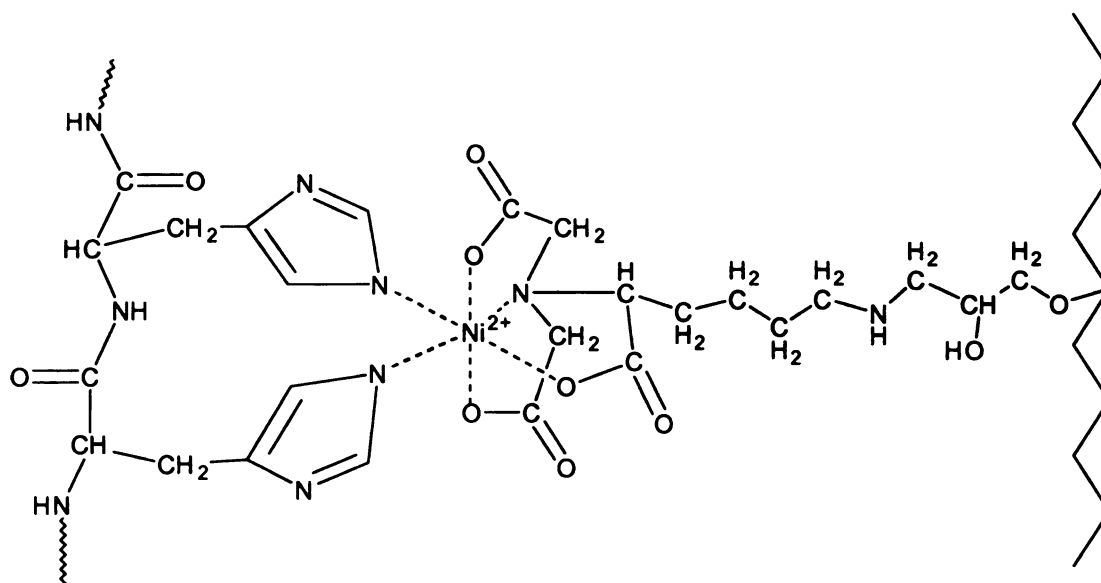


Figure III.6. Interactions between NTA-bound nickel and the two histidines from the His₆ affinity tag. The Ni²⁺ ion is held in place by nitrilotriacetic acid via tetradentate chelation resulting in a very stable complex. Under conditions of near neutral pH and prior to the introduction of imidazole or the histidines-rich tagged AdhE, two of the six coordination sites on Ni²⁺ are occupied by water molecules.

III.2.6.2 Purification and Analysis of His₆-tagged AdhE

The purification protocol entailed three major steps. 1) The crude lysate containing all the water-soluble proteins expressed by the bacterium was loaded onto the column in low-imidazole-concentration (lysis) buffer. 2) The loaded column was washed with medium-imidazole-concentration (wash) buffer to remove all components not specifically bound to the column. 3) The Ni-bound AdhE was eluted out of the column using a high-imidazole-concentration (elution) buffer. The lysis, wash and elution buffers all contained 50 mM NaH₂PO₄ and 300 mM NaCl and were adjusted to pH 8.

They only differed in the amount of imidazole they contained, that being 10, 20 and 250 mM for the lysis, wash and elution buffers respectively. The purification protocol was developed by first determining the column capacity with regard to protein load and the optimum pH for the elution buffer. The optimum buffer pH was established by eluting the protein with buffer of pH 6.9, 7.5, 7.6 and 8.0 and comparing the quality of elution in terms of both amount and purity of protein obtained. Using the buffer at pH 6.9 and 7.5, satisfactory and indistinguishable levels of enzyme purity were achieved (Figure III.7). However, in order to minimize Ni^{2+} leaching of the column due to protonation of NTA under acidic conditions, and thereby rapidly compromising the column's binding affinity, pH 7.5 was chosen for all subsequent purifications. After several trials were carried out, it was concluded that the optimal protein load of the fully regenerated and equilibrated column was maximally ~3 g of total protein per mL of resin. Each trial involved loading a known amount of total protein onto the column followed by several washes with pre-determined volumes of wash buffer. Fractions of equal volumes of wash buffer were collected and saved for analysis using SDS-PAGE. This was followed by eluting the protein with elution buffer in like manner and saving all elution fractions for subsequent analysis by SDS-PAGE. Figure III.8 shows a sample data obtained from such an analysis and the basis upon which the optimal conditions used to purify His₆-tagged AdhE were determined.

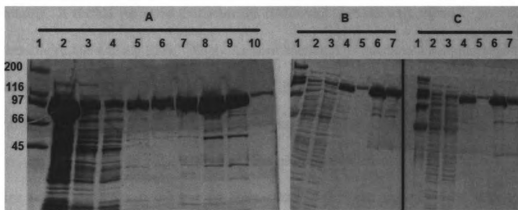


Figure III.7. Comparison of the effect of protein load on purification quality. The concentration of crude lysate was 6 mg/ml. In panel A, 2 ml of clear lysate were loaded onto 1.5 ml resin. Lane legend: 1: molecular weight marker (kDa), 2: crude lysate, 3: flow-through from loading, 4, 5, 6: first, second and third washes, 7, 8, 9, 10: elutions 1, 2, 3 and 4. In panel B 1ml clear lysate was loaded onto 1.5 ml resin. Panels B and C show data from purifications using elution buffers at pH 6.9 and 7.5 respectively. For both panels lane 1 is the molecular weight standard, lane 2 is the flow-through, lanes 3 and 4 are washes 1 and 2 respectively and lanes 5, 6 and 7 are elutions 1, 2 and 3 respectively. The lysis, wash and elution buffers all contained 50 mM NaH_2PO_4 and 300 mM NaCl and were adjusted to pH 8. They differed by containing 10, 20 and 250 mM imidazole respectively. The volume of the FT was 2 for panel A and 1 ml for panels B and C. All washes and elutions were done with 1 ml of buffer per fraction.

In panel A, lane 2 shows that AdhE was both very well over-expressed and soluble in the lysis buffer as evidenced by the very broad band at molecular weight 97 kDa. From the composition of the flow-through and first wash (lanes A3 and A4 respectively) it is evident that the majority of the proteins in the lysate did not interact with the column specifically, hence they passed right through the column with the loading (lysis) buffer (lane A3) and the remainder were washed out in the first wash (lane A4). Lanes A5 and A6 show that washes 2 and 3 contain AdhE almost exclusively, indicating that AdhE was overloaded to the column but was able to interact with the column sufficiently strongly to slow down its migration significantly compared to the

other proteins. It should be noted that after the fifth wash (not shown), virtually no AdhE was detectable in the wash buffer. When the concentration of imidazole was increased to 250 mM, essentially all AdhE was washed out of the column after 4 elutions (lanes A7 to A10). Panel A also shows a relatively significant co-expression of a protein of molecular weight of approximately 45 kDa. Most of this protein washes out with the rest of the impurities but a small amount of it co-elutes with AdhE but constitutes a relatively insignificant amount of impurity. Panels B and C show that loading 4 mg total protein per mL of resin resulted in improved retention of AdhE by the column as opposed to 8 mg total protein per mL of resin used in panel A. No AdhE was detectable in the flow through and first wash. It was not until the second wash that some AdhE was detected, thus showing improved AdhE retention by the column at a lower protein load. Comparison of lane 4, 5 and 6 in both panels B and C shows that a relatively large amount of AdhE washed out of the column after wash 2 (lane 4), following which relatively little AdhE came out in the first elution (lane 5), and then a large amount once again came out with the second and third elutions (lanes 6 and 7). Wash 2 (lane 4) probably contains AdhE that was specifically but weakly bound to the column due to saturation effects, resulting in dynamic exchanges between bound and unbound AdhE molecules. This would account for the delay of the AdhE detected in the second wash. However, when the “excess” AdhE molecules were washed out, the remaining AdhE molecules were more resistant to elution (lane 5) until a critical concentration of the competing imidazole was established (lanes 6 and 7).

After determining the optimum purification conditions, large-scale purification of the protein was carried out by applying 30 ml of 50% Ni-NTA/ethanol slurry to a 50 ml

Flex Column™. The column was equilibrated with 50 ml of lysis buffer at a rate of 2 ml/min, and 7ml of clear lysate (6mg/ml protein) were then applied. (The manufacturer recommends mass of protein loaded was within the range 5-10 mg protein / ml of resin). The level of AdhE purity achieved using the Ni-NTA IMAC purification technique was very good a will be shown in the “Results” section.

III.2.7. Cloning, Growth and Purification of untagged AdhE

III.2.7.1. PCR and ligation

In an effort to investigate the effect, if any, of the His₆-tag on the catalytic activity of AdhE, the *adhE* gene was cloned into a commercial vector that would allow expression of untagged AdhE. Primers were designed as described previously for the His₆-tagged AdhE. The oligonucleotide primers were ordered from Integrated DNA Technologies, INC, Coralville IA (Figure III.8) The antisense primer was 45 bases long, had a molecular weight of 13,837g/mol, and contained 65300 ng of DNA. The sense primer was also 45 bases long but had a molecular weight of 13,757 g/mol and contained 83100 ng of DNA.

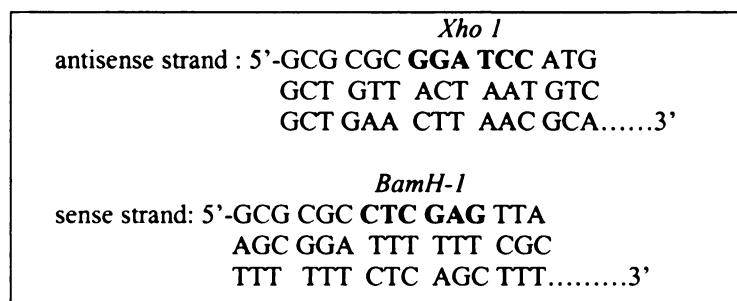


Figure III.8. The oligonucleotide primers used to amplify the AdhE gene for expression of the untagged enzyme. The bold sequences are the restriction sites and the restriction enzymes are shown in italics, each above its corresponding recognition site.

Based on the formula $T_m (^{\circ}\text{C}) = 2(N_A + N_T) + 4(N_G + N_C)$ obtained from the Stratagen Pfu DNA Polymerase Manual (2002), the melting points for both primers were calculated to be 90°C. For good yield of PCR product and to ensure high fidelity, between 25 and 30 cycles are generally used. The PCR thermocycler was therefore programmed to run 25 cycles before maintaining the reaction mix at 4°C. In addition, based on the guidelines from Stratagen (page 3 of Stratagen Pfu DNA Polymerase Instruction Manual (2000)), the extension time should be 1 minute per kb for vector targets up to 10 kb and genomic targets up to 6 kb. Since *adhE* is 2.65 kb long, an extension time of 3 minutes was used.

Genomic DNA was obtained from BL21 *E. coli* cells grown overnight at 37°C in LB medium, with shaking at 250/min to ensure good aeration. DNA was extracted using the Wizard® genomic DNA extraction kit from Promega. The genomic DNA obtained was analyzed both qualitatively and quantitatively by UV-visible spectroscopy. A 50x diluted sample was measured to simultaneously determine A_{260} (absorbance by DNA) and A_{280} (absorbance by protein impurities). The ratio A_{260}/A_{280} was measured in

duplicate and averaged 1.7. The absorbance at 260 nm (A_{260}) was 0.24. Using the relationship that 1 AU corresponds to 50 μ g/ml of DNA, and taking into account the dilution factor of 50, the concentration of the genomic DNA was calculated to be 600 ng/ μ l.

For the PCR reaction, the template DNA was diluted 6x to a final concentration of ~100 ng/ μ l. The mixes prepared for the PCR reaction are summarized Table III.1.

Table III.1. PCR Reaction Components

Cocktail 1		
<i>Component</i>	<i>Vol. (μl)</i>	<i>Amount in reaction</i>
H ₂ O	20	-
25mM dNTP	0.4	0.2 mM
70 ng/ μ l Atisense primer	1.9	133 ng
80 ng/ μ l Sense primer	1.7	136 ng
100 ng/ μ l Genomic DNA (template)	1	100 ng
Cocktail 2		
H ₂ O	20	-
10x Cloned Pfu DNA polymerase buffer	5	1x
2.5 U/ μ l Pfu Turbo DNA polymerase	1	2.5U

Cocktails 1 and 2 were mixed together immediately prior to being placed in the thermocycler. The program parameters of the thermocycler program were set as follows: Melting temperature, 90°C; Annealing temperature, 55°C; Polymerization temperature, 72°C; Extension time, 3 minutes; Number of cycles, 25.

Four reactions were carried out altogether. In the design of the primers, a Bam H1 restriction site was engineered immediately upstream of the start codon with a 6-base GC overhang immediately upstream of it. Correspondingly, a Xho restriction site was

inserted immediately downstream of the stop codon, followed by a 6-base GC overhang. Although blunt-end ligation was used for the untagged *adhE*, the restriction sites were engineered into the primers in order to provide an option for sticky-end ligation in case it became necessary. The *adhE* gene has 2650 base pairs. Taking into account the GC overhangs and the restriction sites, the total number of bases in the PCR product was expected to be $2650 + 24 = 2674$. Upon running an agarose gel, a band was therefore expected between the 3054 and 2036 base pair bands on the standard marker. The PCR band fell exactly where it was expected as shown in Figure III.9.

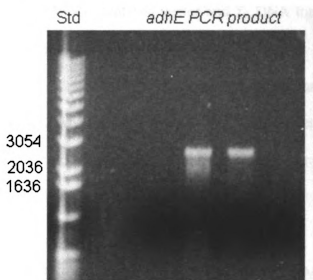


Figure III.9. The *adhE* PCR product for the untagged AdhE. The PCR product lies exactly where it is expected (2674 bp).

The *adhE* gene was ligated onto PETBlue, a blunt-end vector from Novagen™, according to the protocol prescribed. A positive control was included using an insert supplied in the commercial kit. The ligation procedure involved two steps.

- 1) *End-conversion*, in which the PCR product was reacted with a dephosphorylating agent in order to convert it to a form that will allow it to ligate through the loose triphosphate chain on the commercial vector
- 2) *Ligation to the vector*, whereby the end-modified PCR product was reacted with the blunt-end commercial vector PETBlue (Novagen).

For the first step, the mix was incubated for 2 hours at 22°C and the reaction was quenched by heating at 75°C for 5 minutes. The reaction mix was then cooled in ice for 2 minutes and then centrifuged for 5 minutes to collect the condensate. In the second step, 1 µl each of the commercial blunt-end vector and T₄ DNA ligase were added. For the positive control, a control insert supplied with the kit was used. The mixes were then incubated overnight at 16°C. It should be noted that blunt-end ligation does not require the inclusion of restriction sites on either end of the gene product as was done in this work. This was done as a back-up measure, providing an option for sticky-end ligation in the event that the blunt-end ligation was not successful.

III.2.7.2. Transformation, plating, DNA extraction and fingerprinting

III.2.7.2.1 Transformation

The overnight ligation mixes were transformed into NovaBlue cells according to the following protocol. Five tubes, previously stored at -80°C, each containing 25 µl of commercial (Novagen) competent cells, were thawed in ice for 5 minutes. To two of them were added 1 and 2 µl of control insert ligation mix respectively. To the remaining three were added 1, 2 and 5 µl of the experimental ligation mix respectively. After mixing well and leaving in ice for 5 minutes, the cells were heat-shocked for exactly 30

seconds at 42⁰C and placed in ice for two minutes. To each tube 250µl of SOC medium was added, followed by incubation for 30 minutes.

III.2.7.2.2. Plating

The ampicillin-impregnated medium to be used for plating had previously been treated to allow for white/blue screening of the bacterial colonies. To each plate, 20 µl of 100mM IPTG and 35 µl of 50 mg/ml X-galactose (X-gal) were added, spread and allowed to soak into the medium for 30 minutes. 50 µl of each of the transformation mixes were plated and incubated at 37⁰C overnight.

The principle behind the screening process is the following. Beta-galactosidase is one of the enzymes encoded by the LacZ operon of the PETBlue-1 plasmid vector *polylinker*. Beta-galactosidase metabolizes X-galactose to produce a blue product. When ampicillin is included in the growth medium, only cells that are resistant to the antibiotic (i.e., those containing the vector containing the ampicillin resistance gene) can grow. Of these, those without insert (containing an intact *polylinker*) will be blue due to breakdown of X-galactose. The cells containing an insert are not able to metabolize X-gal because the insert disrupts the expression of the LacZ operon thereby abolishing the expression of beta-galactosidase. The positive colonies are therefore white.

III.2.7.2.3. DNA Extraction

Both the positive control plates had over 1000 colonies and about 35% were white. Of the experimental plates, all had at least ~200 colonies but only about 3% were white. The positive colonies from the three experimental plates were numbered 1 to 16.

After labeling 15 ml Falcon tubes correspondingly and filling each with 5 ml of autoclaved LB medium containing 50 µg ampicillin / ml, an autoclaved tooth pick was used to transfer some cells from each colony into the medium. The cells were then grown overnight at 37°C and shaken at 250 rpm. Plasmid DNA was extracted from each of the overnight cultures. To recover a cell pellet of the putative PETBlue-1-adhE cells (#1 to #17), 2 ml of cell suspension were centrifuged. The DNA was extracted following the protocol in the commercial Plasmid DNA extraction kit from Promega.

III.2.7.2.3. Fingerprinting

The plasmid DNA extracted from each of the colonies was digested with *ScaI*, for which only one restriction site is known to occur on the vector, but not on the insert. Table III.2 shows an example of the mixes used for an experimental and control digest for each of the DNA extracts investigated.

Table III.2. Typical mixes for experimental and control restriction digest mixes for PETBlue-adhE fingerprinting.

	Plasmid (µl)	10x Buffer 6(µl)	H ₂ O (µl)	Sca I(µl)
Experimental	6	1	1.5	1.5
Control	6	1	3	0

After digesting for three hours at 37°C, the samples were analyzed by electrophoresis on 0.6% agarose gel containing 0.5 µg/ml ethidium bromide using a commercial DNA standard as a molecular weight marker. An exhaustive and systematic analysis of all 17 extracts was done. DNA from only one of the colonies showed bands consistent with PETBlue (3476 base pairs) with an adhE insert (2650 base pairs). A single cut with *ScaI* is expected to result in a band corresponding to linearized DNA of molecular weight in the region of 6126 base pairs. In addition, the control was expected

to migrate farther since it consisted of circular supercoiled DNA as demonstrated in Figure III.10.

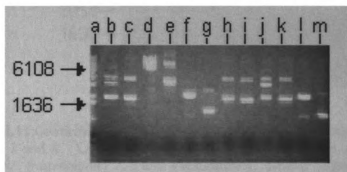


Figure III.10. Agarose gel of PETBlue-*adhE* recombinant plasmid digested with *Sca*I. Lane *a* is the molecular weight marker, lanes *b&c*, *d&e*, *f&g*, *h&i*, *j&k*, *l&m* show digested and undigested DNA extracted from colonies 2, 3, 4, 5, 6 and 17 respectively. Only DNA from colony 3 (*d&e*) showed bands that are consistent with the bands expected of singly digested and undigested PETBlue-*adhE*. The singly digested plasmid (lane *d*) shows a band at the expected molecular weight of ~6100bp. The two bands observed for the undigested plasmid (lane *e*) were probably due to supercoiled DNA (lined with ~4000bp marker) and nicked DNA (at ~6000bp).

In order to confirm the identity of the plasmid from colony 3, the DNA fingerprinting was repeated, but this time with 3 μ l of plasmid DNA instead of 6 μ l. DNA from colonies 2 and 4 was also included in the analysis to confirm the negative results from the first experiment. In addition, the PCR product was run together with the digested plasmid DNA in order to verify its molecular weight. The results previously obtained were reproduced and thus confirmed that only colony 3 contained PETBlue-*adhE*. The identity *adhE* PCR product was also confirmed (Figure III.11).

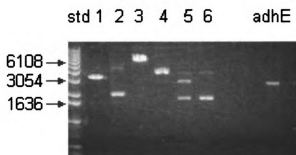


Figure III.11.Confirmatory DNA fingerprints of plasmids extracted from colonies 2, 3 and 4. Lanes 1&2, 3&4, 5&6 contain undigested and digested plasmid DNA from colonies 2, 3 and 4 respectively. Lane 3 (digested plasmid from colony 3) lines up with the 6000bp band of the molecular weight marker. The undigested plasmid from colony 3 migrated at the same rate the 4000bp marker. This is consistent with undigested and super-coiled DNA. The *adhE* PCR product corresponded with the expected molecular weight of 2674 bp.

III.2.7.3. Growth of Cell Cultures and Purification

III.2.7.3.1. Test Growths

After confirming the positive recombinant DNA from colony 3, 2 μ l of it was transformed into 50 μ l of Tuner (DE3) pLacI cells according to the transformation protocol described previously. The cell suspension (100 μ l) was plated in duplicate and incubated overnight at 37°C. After 20 hours, two colonies were observed on one of the plates. The colonies were given reference numbers labeled 1 and 2 respectively. Overnight cultures of both colonies were started in LB/Amp. The overnight cell suspensions (1mL) from each of colonies 1 and 2 were inoculated into each of two 250 mL flasks containing LB-Amp liquid medium. The cell suspension of each of colonies 1 and 2 was divided into two equal volumes that were grown in parallel. The optical density measured at 600nm (OD₆₀₀) was monitored over time and when it reached 0.66 and 0.65 for colonies 2 and 1 respectively, 50 μ l of a 1M solution of isopropyl- β -D-

thiogalactopyranoside (IPTG) was added to only one half of the growth to induce overexpression. All cell suspensions were allowed to grow for two hours post-induction.

Pellets from each of the four growths were made by centrifuging 3 ml of each suspension. The pellets were lysed according to standard protocols using SDS denaturing buffer containing 3.5% β -mercaptoethanol, followed by centrifugation for 5 minutes. For each sample, 10 and 15 μ l were loaded into 15 μ l wells of a 4-15% Tris-HCl gradient gel. Both colonies showed good over-expression in growths without IPTG but significantly decreased expression of AdhE in the growth to which IPTG was added, as can be seen in Figure III.12. Glycerol stocks were made by mixing the cell suspensions with autoclaved glycerol to 30% in a total volume of 1000 μ l. Curiously, repeated test growths using the glycerol stocks from colony 2 consistently showed no AdhE overexpression when growths were repeated. All subsequent growths of this cell line were therefore done with stocks from colony 1.

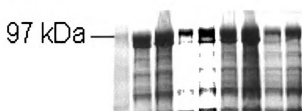


Figure III.12. Overexpression of untagged AdhE by colonies 1 and 2. The first lane is the molecular weight marker, the next four lanes are samples from colony 1 and the last four from colony 2. For each, the first pair of lanes are a duplicate from the uninduced growth and the second pair are from the induced growth.

In order to provide further proof that IPTG suppressed overexpression of AdhE in the Tuner (DE3) pLacI-adhE transformants, 5mL of an overnight culture cell

suspension were inoculated into two 2.8 L flasks each containing 1L of LB medium impregnated with ampicillin to a final concentration of 50 mg/ml. Both flasks were incubated at 37°C in a shaker incubator going at 250 shakes per minute. When the cell suspension reached an optical density (OD₆₀₀) of ~0.7 1 mL of 1M IPTG was added to flask 1. Both cell suspensions were allowed to incubate for a further two hours and then harvested. The wet cell masses were 6.07g and 5.85g for flask 1 and flask 2 respectively. Both were lysed with equal volumes of lysis buffer and the crude extract recovered by careful pipetting. Alcohol dehydrogenase activity of the crude extract was measured as an indirect means of determining the effect of IPTG on the expression of AdhE in Tuner (DE3) pLacI-adhE transformants. The results obtained are shown in Table III. 3.

Table III.3. Alcohol dehydrogenase activities of crude extracts from induced and uninduced Tuner (DE3) pLacI-adhE transformants

Measurement #	ADH, Flask 1 (nmolNADH/min)	ADH, Flask 2 (nmolNADH/min)
1	21.4	80.4
2	22.7	84.2
3	24.6	83.6

As shown in Table III.3, the AdhE suppression observed in the whole cell pellet (Figure III.12) was corroborated by a corresponding decrease in alcohol dehydrogenase activity of the crude lysate obtained from cells that had been “induced” by addition of IPTG during growth. The uninduced cells showed close to four times the activity, per gram of cells, than the induced cells. Based on these findings, all subsequent growth of these cells were done without addition of IPTG, and AdhE overexpressed well when the cells were grown up to the stationary phase.

III.2.7.3.2. Large Scale Growths

To prepare for a growth, glycerol stocks were routinely streaked on an LB-agar medium containing 50µg/ml ampicillin and incubated overnight at 37°C. An isolated colony was selected and transferred to LB liquid medium containing 50µg/ml ampicillin (LB-Amp) and again grown overnight at 37°C. For a large-scale growth, 5 ml of the overnight growth was transferred to 2.8 L flasks each containing 1.5 L of LB-Amp medium. The flasks were incubated in a shaker going at 250 rpm and maintained at 37°C until the optical density at 600 nm (OD₆₀₀) was 2.5. This tended to be the maximum attainable cell density, and it was reached within approximately 6 hours. Because addition of IPTG was found to suppress AdhE overproduction in Tuner (DE3) pLacI cells (Figure III.12), these cells were routinely grown to the stationary phase and then harvested without adding IPTG. Each growth was routinely checked for over-expression by spinning out a small pellet of cells, denaturing it by boiling in SDS denaturing buffer before loading the supernatant into a Tris-Cl polyacrylamide gel.

III.2.7.3.3. Cell Harvesting and Lysis

The cells were harvested by centrifugation at 8000rpm for 5 minutes in 500 ml pre-weighed polyethylene centrifuge bottles and after discarding the supernatant, the cell pellet was drained by inverting the bottles on tissue paper for about 10 minutes. The bottle plus the cells was then weighed and the difference from that of the empty bottle was recorded as the mass of the cells. In preparation for AdhE purification, the Tuner (DE3) pLacI-*adhE* cell pellets were lysed in a pH 7.5 buffer consisting of 50 mM Tris-sulfate (pH 7.5), 200mM NaCl, 1% TritonX-100, 5% glycerol, 10 mM MgCl₂, 1 mM

DTT, 1 mM PMSF, 8 mg of lysozyme and trace amounts (~0.1 mg) of each of DNase and RNase and incubated at 4°C for 2.5 to 3 hours. For each lysis batch, 1.5 mL of lysis buffer was used per gram of cell pellet. An average growth yielded a total of ~25 g of cell pellets. The cell paste resulting from enzymatic lysis was then centrifuged in a Sorvall™ super centrifuge equipped with an SS 34 rotor spinning at 18,000 rpm for 30 minutes. The supernatant was carefully decanted into 50 mL Falcon tubes and either flash frozen or directly used to purify AdhE.

III.2.7.3.4. Purification of untagged AdhE

The untagged AdhE protein was purified by size exclusion chromatography using a Superdex 75™ gel filtration column (5cm x 60cm). Typically approximately 40 to 50 mL of crude protein extract obtained as described in section III.3.7.3.3, were loaded onto the column at a rate of 3 mL per minute using Tris buffer. The optimization of the purification method was achieved by monitoring the change in absorbance at 280 nm as protein eluted out of the column. Fractions corresponding to the peaks observed were analyzed by SDS-PAGE to determine their composition by molecular weight. After identifying the peak corresponding to AdhE under the experimental conditions, the procedure was automated by writing a program that allowed fractions to be collected automatically in the chromatographic region spanning the AdhE peak. SDS-PAGE was routinely used to determine the composition of each of the fractions and to decide which fractions to pool for further purification. The purity of the protein was further improved by loading it onto an ion exchange column followed by gradient elution from low to high salt concentration. The low salt buffer consisted of 20mM HEPES containing 1 mM

DTT and adjusted to a pH of 7.2. The high salt buffer was similar, but also contained 200mM NaCl.

The overexpression of untagged AdhE in the Tuner (DE3) pLacI cells was poorer than that of His₆-tagged AdhE expressed in BL21 (DE3)pLysS, as seen by comparison of Figures III.13 and III.15. The untagged AdhE also proved to be more difficult to purify to homogeneity, even even after repeated trials. After carrying out SDS-PAGE on the fractions corresponding to the AdhE peak, those containing $\geq \sim 90\%$ wild type AdhE or $\geq \sim 95\%$ for the His₆-tagged AdhE were pooled together and concentrated using an Amicon™ concentrator equipped with a 50 kDa molecular weight cut-off (MWCO) point membrane purchased from Millipore™. The concentration of the protein was determined by the Bradford method. To prepare the standards, a series of microtubes containing various known volumes of a 0.119 mg/ml solution of bovine serum albumin. The volumes of the protein standard solution ranged from 0 to 60 μ l. To each of the tubes, enough sterilized water was added to make up the volume to 800 μ l. 200 μ l of the Bradford dye (obtained from BioRad™) were added to each of a series of microtubes to make up the volume to a total of 1000 μ l and to develop the spectrophotometrically active analytical complex. The tubes were then allowed to stand for 30 minutes to allow development of color. In parallel to the standards, a series of samples containing various volumes of diluted AdhE were prepared and incubated. The absorbance of the protein complex in each was measured at 595 nm and a calibration curve was plotted and used to calculate the concentration of AdhE in the samples.

III.2.7.4. Characterization of untagged AdhE

In order to ascertain that the observed over-expressed protein was indeed AdhE, a semi-quantitative analysis was carried out on AdhE fractions obtained from a partial purification of the untagged AdhE using gel filtration. The objective was to determine the correlation between the band at 97 kDa and the alcohol dehydrogenase activity. The fractions were collected such that they spanned the peak corresponding to the band at 97 kDa (as determined by SDS-PAGE). Crude extract from overexpressing cells was loaded onto a Superdex 75 gel filtration column, and fractions were collected for analysis by the alcohol dehydrogenase assay and by SDS-PAGE. Each fraction was assayed for alcohol dehydrogenase and the measured activity for each fraction was then compared to the corresponding height of the A_{280} peak. In a typical assay for each fraction, all components shown in Table III.4 (previously degassed and kept inside an anaerobic chamber) were mixed, except the sample from the fraction to be assayed. To a solution containing 300 mM K_2CO_3 (pH 10), 0.25 mM NAD^+ and 170 mM ethanol and an appropriate volume of purified (MilliQ) water, was added enough fraction volume to bring the total volume to 1mL. After rapid mixing, the rate of NADH production was measured spectrophotometrically by monitoring the rate of increase of absorbance at 340 nm. The rate of NADH production was measured as a function of both the fraction volume and the substrate ethanol.

Table III. 4. Typical composition of mixes used for ADH activity of AdhE

17 M EtOH (μ l)	500mM K_2CO_3 , pH 10 (μ l)	25 mM NAD^+ (μ l)	Fraction (μ l)	H ₂ O
10	600	10	30	350

The results (Figure III.16) showed a direct correlation between the alcohol dehydrogenase activity (nmolNADH/min) and the intensity of the band at 97 kDa.

III.2.7.5. Characterization of the His₆-tagged AdhE

III.2.7.5.1. Identification of AdhE by mass spectrometry

His₆-AdhE, purified as outlined in section III.3.6.2, was concentrated using an Amicon™ concentrator equipped with a 30 kDa molecular weight cut off membrane from Millipore™. The concentration of the protein was measured by using the Bradford method, using bovine serum albumin (Sigma) as a standard and a commercial protein dye from BioRad™. The protein was dialyzed into water (previously adjusted to pH 7.2) to remove all elements of buffer and salts. A sample of the protein (in water) was then submitted to the Macromolecular Facility in the biochemistry department at Michigan State University for analysis by matrix assisted laser desorption ionization mass spectrometry (MS-MALDI). The molecular ion of 97 kDa was positively identified with greater than 90% confidence to be AdhE.

III.2.7.5.2. Alcohol dehydrogenase assay

The alcohol dehydrogenase activity of AdhE is the reverse of the reaction represented by Scheme III.7. The activity was measured by monitoring the rate of change of NADH absorbance at 340 nm. The assay was carried out as described in section III.2.7.4.



Scheme III.7. The alcohol dehydrogenase/acetaldehyde reductase reaction catalyzed by AdhE.

First the concentration of AdhE was held constant while that of EtOH was varied and vice versa (Table III.5) In either case, the species under study was added last. All components were first degassed and kept inside an anaerobic chamber before mixing them in a 1mL quartz cuvette equipped with a screw-on air tight rubber septum. The component under investigation (AdhE or EtOH) was added last, using a Hamilton syringe. After two quick inversions to mix the components, the automated kinetic program was immediately started to monitor absorbance at 340 nm using a Model 8453 Hewlett Parckard spectrophotometer.

Table III.5 Typical composition of mixes for alcohol dehydrogenase activity assay

17 M EtOH (μl)	500mM K ₂ CO ₃ (μl)	25 mM NAD ⁺	98 μM AdhE	H ₂ O
10	600	10	0	380
10	600	10	10	370
10	600	10	20	360
5	600	10	40	345
10	600	10	40	340
15	600	10	40	335

III.2.7.5.3. Acetaldehyde reductase assay

This activity is responsible for the forward reaction of Scheme III.7 as written. In this case, the activity was measured as the rate of NADH consumption (as measured by the rate of decrease of A₃₄₀). Similarly to the case of the alcohol dehydrogenase activity, the rate was measured with respect to the concentration of each of the substrate (acetaldehyde) and the enzyme (AdhE) in turn. Table III.6 shows a typical mix reaction

mix used for this assay. To a cuvette containing 50 mM Tris-HCl (pH 7.6), 0.256 μ M NADH, 100mM acetaldehyde and an appropriate volume of purified water (MilliQ) was added varying amounts of AdhE, ranging from 0 to approximately 4 μ M. The total volume of the assay mix was always fixed at 1mL. After quick mixing, the rate of consumption of NADH was measured by automatic measurement of the rate of decrease of absorbance at 340nm. Measurements were also made with the concentration of AdhE held constant and varying that of acetaldehyde.

Table III. 6.Typical composition of mixes used for acetaldehyde assay

1M Tris-HCl, pH 7.6 (μ l)	98 μ M AdhE (μ l)	10M CH ₃ CHO	256 μ M NADH	H ₂ O
50	0	10	10	930
50	20	10	10	910
50	40	10	10	890
50	30	20	10	890
50	30	30	10	880
50	30	40	10	870

III.2.7.5.4. Iron analysis

In order to calculate the mole ratio of iron in AdhE, fractions were collected during elution from the Ni-NTA column. After washing the loaded lysate with approximately 50mL of wash buffer, the samples were eluted with elution buffer containing 250 mM imidazole. Each fraction was analysed for AdhE and Fe, in order to determine if there was correlation between Fe and AdhE. Protein was determined using the Bradford method as described in Section III.4.2.2. Fe was determined spectrophotometrically using bathophenanthroline as the complexing agent. The basic procedure involved preparation of a series of standards using a commercial solution of Fe²⁺ dissolved in sulfuric acid. The volume of standard used ranged from 0 to 200 μ l.

The volume was then made up to 1000 μl with MQ water. 500 μl of a solution comprising 4.5% w/v KmnO_4 and 12N HCl was then added to each tube. The purpose of this step is to denature the protein and oxidize iron to Fe^{3+} in order to facilitate its release from the protein matrix. After heating for 2 hours at 65°C , 100 μl of a solution consisting of 9.7 g ammonium acetate, 8.8 g ascorbic acid, 80 g of each of neocuprine and ferrozine, all dissolved in a total of 45 mL of filtered (MilliQ) water. After standing for 30 minutes to allow for complete complexation, the absorbance of the standards and samples were read at 562 nm. A calibration curve was plotted and used to calculate the concentration of Fe in the samples.

III.2.7.5.5. Calculation of activity from kinetic data

The kinetics program used to measure the rate of change in NADH absorbance as a function of active PFL measures the change in absorbance per second. However, the program also makes provision for multiplication of the measured rate by any constant and the choice of units to be used for the output. Most of the PFL and AdhE activities are measured based on the rate of consumption of NAD^+ , and are reported in units of nano moles of NADH produced per minute. We therefore conformed to this norm and took advantage of the program to command the computer to convert absorbance units/s to $\text{nmolNADH}/\text{min}$. We accomplished this by converting absorbance units to nmoles of NADH though the Beer-Lambert law, $A = \epsilon bc$, where ϵ , b and c are the molar absorptivity of NADH, the cuvette path length and concentration of NADH, respectively. Using the cuvette path length of 1 cm and the molar absorptivity of $6270 \text{ M}^{-1}\text{cm}^{-1}$, conversion factor of 9569.4 was calculated and used to calibrate the program to report the rates in $\text{nmolNADH}/\text{min}$.

III.3. RESULTS

III.3.1. Over-expression and Characterization of Untagged AdhE

III.3.1.1. Overexpression of untagged AdhE

A typical whole cell SDS-PAGE analytical gel for Tuner (DE3) pLacI-*adhE* is shown in Figure III.15. Expression of untagged AdhE was suppressed by addition of IPTG and therefore all growths were done without induction. Comparison of Figures III.15 to Figure III.13 also reveals that the crude lysate of BL21 (DE3)pLysS-PET21a⁺-*adhE* cells was cleaner than that of Tuner(DE3)LacI-PetBlue-*adhE* cells. Consequently, it was easier to purify the tagged AdhE to homogeneity than it was the untagged protein (compare Figures III.14 and III.16).

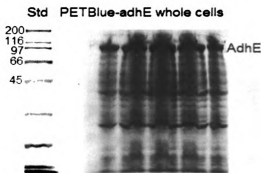


Figure III.13. Results from whole cell SDS-PAGE of Tuner (DE3) pLacI-*adhE* cells grown to stationary phase in LB/Amp. The cells were grown to an OD₆₀₀ of ~2.5 and then a cell pellet was prepared by centrifuging 1 mL of cell suspension in a 1.5 mL micro tube. The pellet was suspended in equal volumes of SDS denaturing buffer containing 3.5% 2-mercaptoethanol and water to make a total volume of 60µl. The cell suspension was then boiled for 10 minutes and then centrifuged at 12,000 rpm to separate out particulate matter from the mixture of denatured protein. 10µl of supernatant containing denature dissolved proteins was loaded into a commercial (BioRad™) 4-15% Tris-Cl polyacrylamide gel.

III.3.1.2. Characterization of untagged AdhE

III.3.1.2.1. Correspondence of untagged AdhE activity to the 97 kDa band

The results presented in Figure III.16 demonstrate a strong correlation between AdhE activity and the protein band at approximately 97 kDa, thus proving that we have successfully overproduced native AdhE.

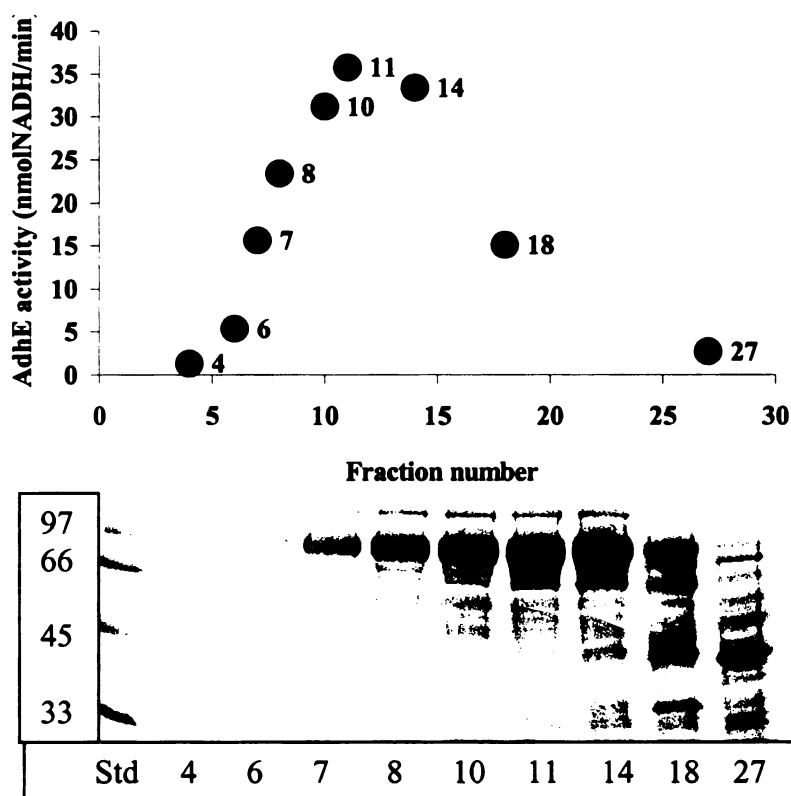


Figure III.14. AdhE lacking a His₆ tag was partially purified by gel filtration using an AP-5 Superdex 75 gel filtration column (5cm x 60 cm). Fractions were assayed for alcohol dehydrogenase activity. The results show a direct correlation between the intensity of the band at 97 kDa and alcohol dehydrogenase activity. This provided additional evidence that the overexpressed protein is AdhE.

III.3.2. Over-expression and Purification of His₆-AdhE

III.3.2.1. Test growths

Based on DNA analysis (Figure III.2) four small growths from different colonies were of cells transformed with PET21a⁺-adhE were grown in LB-Amp medium. The results (Figure III.13) were consistent with the DNA fingerprints, showing good overexpression of the His₆-AdhE. As shown in Figure III.15, colony number 3 showed no over-expression in either the induced or uninduced growth. In contrast, colonies 5, 6 and 10 show a dramatic difference between the induced and uninduced growths.

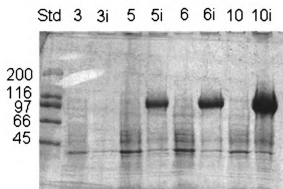


Figure III.15. Sodium dodecyl sulfate polyacrylamide gel electrophoresis (SDS-PAGE) of cell pellets of colonies 3, 5, 6 and 10 from a plate of BL21(DE3)pLysS transformed with PET21a⁽⁺⁾-adhE encoding His₆-tagged AdhE. The colonies were inoculated and grown in duplicates whereby X and X_i denote uninduced and induced colony X respectively. Whereas colony 3 did not show any AdhE over-expression both in the absence and in the presence of IPTG, colonies 5, 6 and 10 showed a marked response to IPTG, over-expressing AdhE almost exclusively when IPTG was added.

Whereas the uninduced growths for these colonies are indistinguishable from colony 3, the induced growths show a very intense band at molecular weight of ~97 kDa, corresponding to the molecular weight expected for AdhE tagged with six histidine residues. Notably, the intensity of the band appearing below 45 kDa was observed to be

lower in the induced growths than in the uninduced ones for each of the colonies. This was consistent with the expectation that upon induction with IPTG, the energy of the cells will almost exclusively be directed towards the production of AdhE. The uninduced cell suspension from colony 10 was used to prepare glycerol stocks by mixing equal volumes of autoclaved glycerol and the cell suspension in capped micro tubes. The 1:1 glycerol stocks were kept at -80°C and were used to grow *BL21(DE3)pLysS-PET-21^a(+)-adhE* bacterial colonies on ampicillin-impregnated (50 µg/mL) agar plates whenever needed. Large-scale growths from these glycerol stocks showed similar levels of overexpression as the test growths illustrated in Figure III.13.

III.3.2.2. Purification

As outlined in the previous section, the His₆-tagged AdhE was purified using a Ni-NTA affinity column. The crude extract was obtained by lysing the cells in phosphate buffer containing imidazole, lysozyme, DNase, RNase and PMSF. The crude extract was then loaded onto the column and then washed with low imidazole buffer, followed by elution with the same buffer, but containing a higher concentration of imidazole. The flow-through, the wash and the elution fractions were all collected and analyzed for protein using SDS-PAGE. Figure III.14 shows gels of fractions collected during purification using the Ni-NTA affinity column.

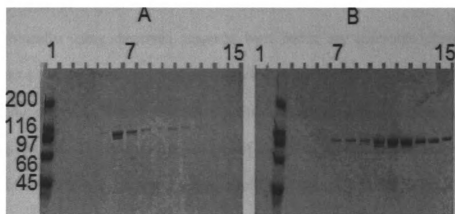


Figure III.16. Gels showing the level of purity achieved for His₆-tagged AdhE by using a Ni-NTA affinity column to purify the protein. For gel A lane 1 contains the standard molecular weight marker, lane 2 contains the flow through from loading the Ni-NTA column and the subsequent lanes contain washes 1 to 11. Lanes 14 and 15 were not used. For gel B, lane 1 was not used. Lanes 2 and 3 contain the first eluted fraction the standard molecular weight marker respectively. The rest contain elution fractions 2 to 13.

His₆-tagged AdhE showed very specific affinity for the Ni-NTA column and was therefore purified to homogeneity. Virtually all impurities were removed by washing with buffer containing 20 mM Imidazole (Figure III.14). Typical yields of purified AdhE were between 50 and 60 mg of purified protein per liter of bacterial culture.

III.3.2.3. Alcohol Dehydrogenase Activities

Alcohol dehydrogenase activity was measured as described in sections III.2.7.4 and III.2.7.5. In one experiment, the concentration of the substrate (ethanol) was held constant and that of AdhE varied. The activity was measured by observing the increase in NADH absorbance at 340 nm. In the second experiment, the concentration of AdhE was held constant and the increase in NADH absorbance at 340 nm observed as a function of the change in the amount of ethanol. The total volume of the reaction mix

was 1000 μl . A typical mix was as shown in Table III.4. The reactions were carried out anaerobically using degassed reagents kept inside an anaerobic chamber. All components except enzyme or substrate were mixed together into a quartz cuvette inside the anaerobic chamber. The cuvette was then sealed with a screw-on rubber stopper such that it was airtight. The appropriate volume of substrate or enzyme was then transferred into and held inside a Hamilton syringe. Both the syringe and the cuvette were then brought out of the chamber and the cuvette placed into the UV-vis instrument. The enzyme (or substrate) was then released into the reaction mix through the rubber stopper and quickly mixed by inverting the cuvette twice. For each of the forward and reverse reactions (Scheme III.7), the reaction was first carried out with the enzyme held constant and then with the substrate held constant. The results of the assays are shown in Figures III.17 (reverse reaction) and III.18 (forward reaction).

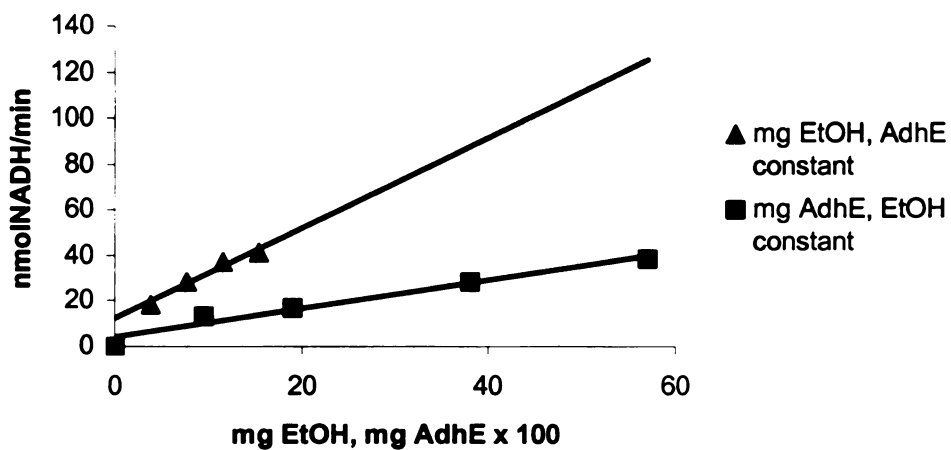


Figure III.17. Alcohol dehydrogenase catalyzed by AdhE. The rate of production of NADH was measured as a function of the amount of AdhE or EtOH, respectively, during the alcohol dehydrogenase reaction. The constant [EtOH] assays were done at 7.7 mg/ml. The constant [AdhE] assays were done at 0.38 mg/ml. Reactions were monitored spectrophotometrically at 340 nm. The data shown was obtained using His₆-tagged AdhE. The untagged AdhE similarly showed alcohol dehydrogenase activity.

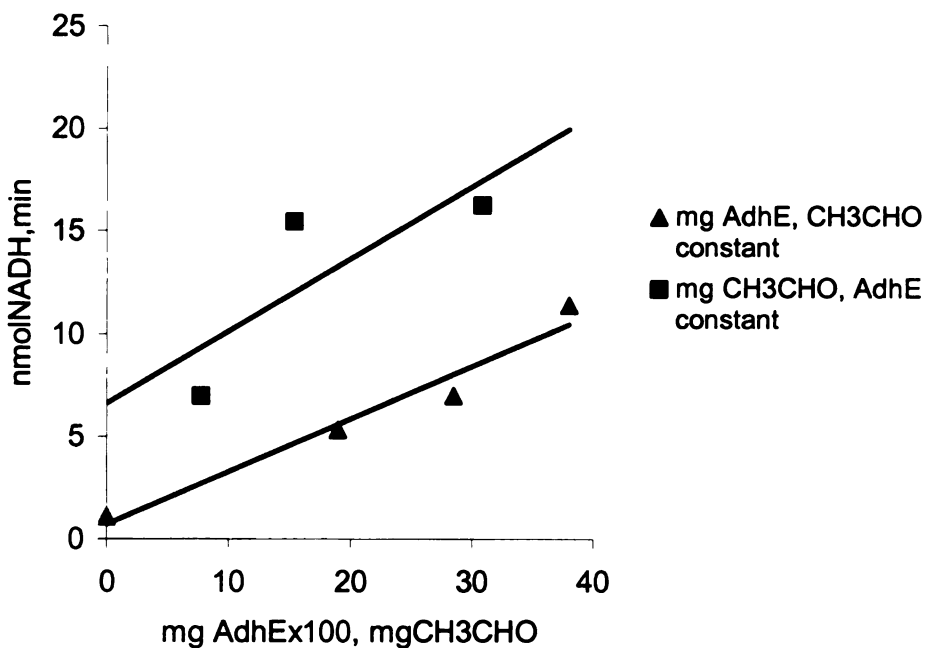


Figure III.18. Acetaldehyde reductase activity of AdhE was measured by monitoring the decrease in NADH absorbance at 340 nm. The graph shows the rate of decrease of absorbance plotted as a function of the amount of AdhE or the substrate acetaldehyde, respectively, during the acetaldehyde reductase reaction. The constant [AdhE] assays were done at 0.29 mg/ml. The constant [CH₃CHO] assays were done at 7.7 mg/ml.

These results demonstrated that the His₆-tagged AdhE indeed harbors the expected activities. Based on the enzyme concentration of 0.3 μ M (Figure III.17) and the activities observed, the calculated specific alcohol dehydrogenase activity for AdhE 63 nmolNADH/min/mgAdhE. The specific acetaldehyde reductase activity was calculated as 26 nmolNADH/min/mgAdhE. This compares very favorably with values published in the literature^{11, 12}.

III.3.2.4. Iron Content of AdhE

The data presented in Figure III.19 shows a correlation between Fe concentrations and the AdhE peak. Each fraction was analyzed with respect to the concentration of both AdhE and Fe. The concentration of each was plotted as a function of the volume of eluent passed over the column. Figure III.19 shows the plot of concentration as a function of fraction number for both Fe and AdhE. The peaks for both Fe and AdhE coincide with each other, suggesting that the Fe is associated with AdhE in a specific fashion. The calculated Fe: AdhE mole ratio ranged from 0.25 to 1.25. The iron of the purified enzyme averaged approximately 0.6 Fe/AdhE, again confirming the identity of AdhE.

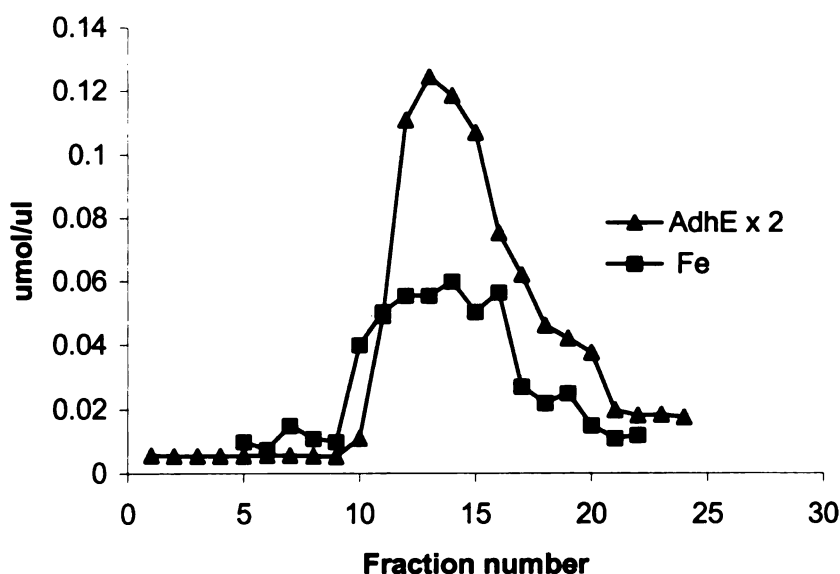


Figure III.19. Correlation between the amount of AdhE and Fe in successive fractions collected during purification of His₆-tagged AdhE using a Ni-NTA affinity column.

The observations in Figure III.19 are consistent with those previously reported in the literature in which it was found that there is 1 Fe ion per molecule of AdhE.³ In our hands, the Fe:AdhE of purified His-tagged AdhE ranges from ~ 0.2 to ~0.6.

III.3.2.5. Comparison of “as isolated” and iron-stripped AdhE activities

A comparison of the specific activities of apo- and holo- enzyme was made by calculating the change in the rate of production of NADH during the alcohol dehydrogenase assay as a function of the concentration of enzyme used in the assay. The holo- enzyme was the His₆-tagged enzyme as-isolated from the Ni-NTA column, and contained 0.6 moles Fe per mole of AdhE. The apo- form of the enzyme was generated by incubating the “as-isolated” enzyme for 45 minutes in 1mM EDTA to complex out Fe²⁺. At the end of the incubation period, the protein was passed through a PD-10 gel filtration column to separate the protein from the Fe-EDTA complex. Iron content of the apo-AdhE proved to be below the detection limit for the complexometric method. Alcohol dehydrogenase activity was then measured as a function of protein volume. The specific activity was calculated as the slope of the plot of rate of NADH production (in nanomoles per minute) vs mg of protein in the assay. Figure III.20 is a graphical depiction of the results obtained. The slopes of the graphs give the specific activities of the respective forms of AdhE, with the specific activity of holo-AdhE being 28 nmolNADH/min/mg compared to 12 nmolNADH/min/mg for apo-AdhE. The results indicate that the specific activity of the as isolated enzyme was more than twice that of the Fe-depleted form. This is consistent with the previous reports that the alcohol dehydrogenase activity is dependent on the presence of Fe²⁺.¹

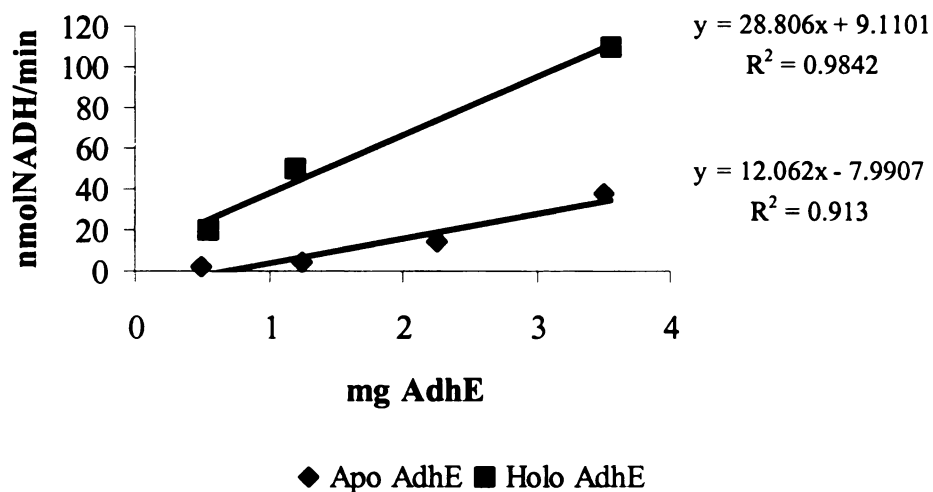


Figure III.20. Comparison of specific activity of EDTA-treated (apo-) AdhE and as-isolated (holo-) AdhE . A decrease in specific activity was observed when AdhE was incubated in EDTA and gel filtered, suggesting that the Fe in the enzyme is important for the alcohol dehydrogenase activity. The activity assays were carried out aerobically.

III.3.2.6. Effect of Fe^{2+} on the alcohol dehydrogenase activity of AdhE

In order to further investigate the effect of Fe on the alcohol dehydrogenase activity of AdhE, an approximately stoichiometric amount of Fe^{2+} was added to each of the EDTA-treated and the “as-isolated” AdhE. The alcohol dehydrogenase activity was then determined as a function of protein concentration. For each of the EDTA-treated and the “as-isolated” samples, enzyme assays were done on both before and after iron addition.

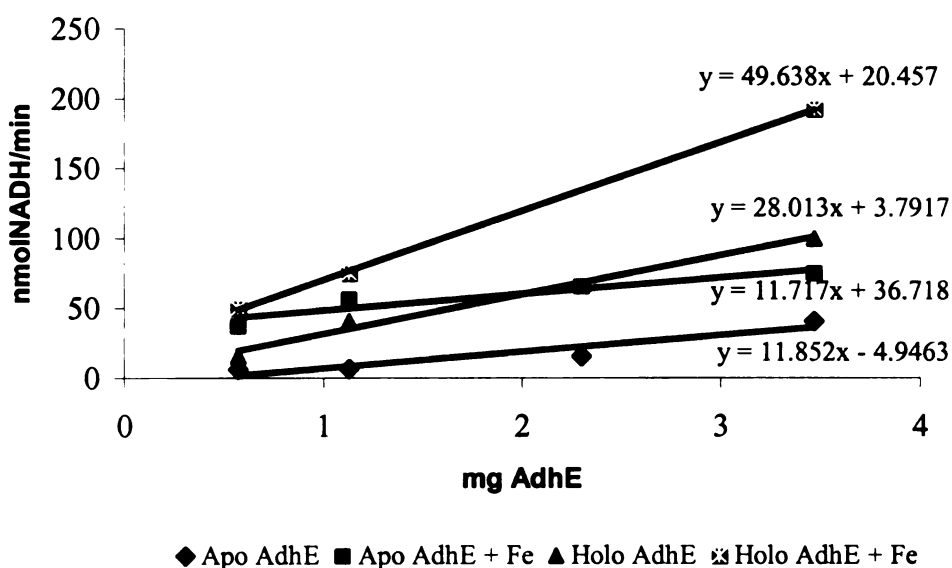


Figure III.21. Effect of Fe^{2+} on the alcohol dehydrogenase activity of holo- and apo-AdhE. Overall, holo-AdhE has a higher specific activity than apo-AdhE as determined by the slopes of the linear fit of the data points. The calculated specific activities are 12 nmolNADH/min/mg AdhE for both apo- and apo+Fe, and 28 and 50 nmolNADH/min/mgAdhE for holo- and holo + Fe respectively.

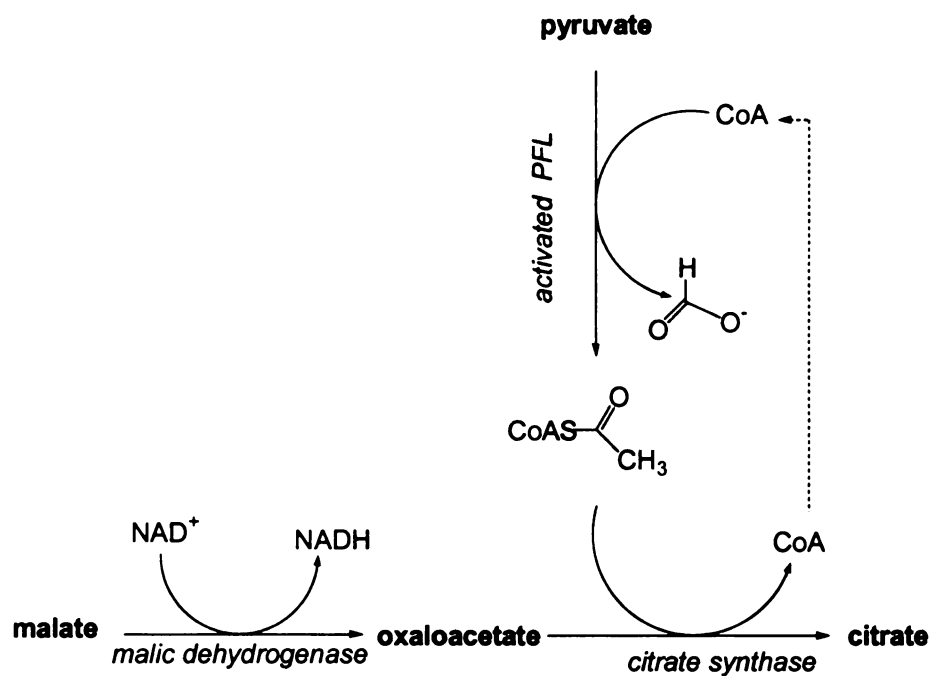
The results in Figure III.21 show that the “as-isolated” enzyme is more active than the EDTA-treated enzyme, consistently with the results obtained in Figure III.20 above. Interestingly, the specific activity of the Fe^{2+} -supplemented and unsupplemented

apo-AdhE is essentially identical. On the other hand, alcohol dehydrogenase activity of the Fe-supplemented “as-isolated” enzyme increased dramatically over that of the unsupplemented enzyme.

The specific activities observed here are within the same order of magnitude as those in the literature.¹⁰ It is noteworthy that the activity of holo-AdhE without added iron was found to have similar activity to the “as-isolated” AdhE in Figure III.20. Our data also shows that when Fe was removed from AdhE the specific activity was not restored to that of the “as isolated” enzyme, remaining practically the same both with and without iron supplementation. The data also suggests that once Fe is stripped out of the enzyme, it becomes more difficult to re-incorporate back into the enzyme than into AdhE that already has occupied sites. This apparent lack of sensitivity of the apo-AdhE to iron supplementation may be a result of failure of the enzyme to reconstitute the iron active site due to conformational changes resulting from EDTA treatment. For the “as isolated” enzyme, however, there was a dramatic increase in the specific activity after incubating with Fe^{2+} . This suggested that the “as isolated” AdhE still had the capacity to incorporate more iron, presumably into vacant active sites. That there could have been some vacant Fe-coordinating sites is plausible since the measured AdhE: Fe ratio for purified His₆-AdhE was determined to be ~0.6. If such incorporation of iron does indeed occur, it would explain the dramatic increase in the specific activity of the enzyme. It would therefore appear that the presence of some Fe in AdhE primes it for further incorporation of Fe. It is also plausible, however, that the observed decrease response to EDTA by AdhE results from denaturation of AdhE by EDTA.

III.3.2.7. Investigation of PFL deactivation

AdhE has also been reported to harbor PFL deactivase as a third activity in addition to ADH and acetaldehyde reductase.^{3, 4, 12} One of the reports further asserts that in order to carry out deactivation of PFL, AdhE required NAD^+ , Fe^{2+} and CoA as cofactors.³ In this study the putative PFL deactivase activity was investigated by preparing a series of reactions in which activated PFL was incubated in the presence of different combinations of AdhE and cofactors. All the reactions were carried out inside an anaerobic chamber. After incubating activated PFL with a given combination of cofactors and AdhE, the residual activity of PFL was followed periodically using the coupled enzymatic assay shown in Scheme III.8, in which the PFL-catalyzed formation of acetyl-CoA is coupled to the reduction of NAD^+ , which can be monitored spectrophotometrically. The first set of PFL deactivation experiments was done using AdhE and various combinations of the other purported cofactors. Although no correlation could be seen between the rate of PFL deactivation and AdhE, there appeared to be a correlation with CoA, as illustrated in Figure III.22.



Scheme III.8. The coupled enzymatic assay used to measure the activity of PFL.

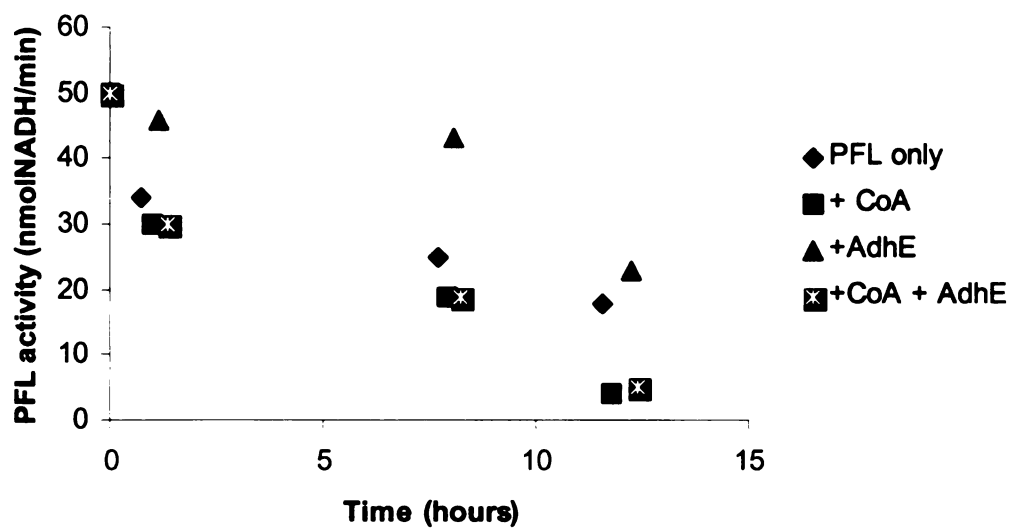


Figure III.22. Some correlation was observed between CoA and PFL deactivation

Following on this observation, the investigation of the cofactors was carried out further to try to ascertain the effect, if any, of the cofactors by themselves and in the presence of AdhE, on the activity of PFL. Table III.7 shows an example of reaction mixes used to carry out this investigation. The first set consisted of activated PFL incubated with AdhE and all three putative cofactors. In the second set, active PFL was incubated with the cofactors only and in the third set of reactions activated PFL was incubated with “as isolated” AdhE only. The reactions were carried out under strictly anaerobic conditions.

Table III.7. The components of the mix used to investigate PFL deactivation

Reaction component	React 1 (μl)	React 2 (μl)	React 3 (μl)
1M Tris, pH 7.5	100	100	100
20 mM NAD ⁺	30	30	0
10 mM CoA	30	30	0
160 nM Fe ²⁺	30	30	0
694 μM PFL	100	100	100
100 μM AdhE	10	0	10
H ₂ O	60	70	150

Representative results are shown in Figure III.23. These results demonstrate clearly that AdhE by itself does not deactivate PFL. Furthermore, the mixture of cofactors by themselves steadily and systematically deactivated PFL over several hours of incubation. The reaction mix containing AdhE in the presence of the cofactors showed an identical effect to the one containing the cofactors alone. These results therefore indicate that either one or a combination of the cofactors NAD⁺, Fe²⁺ and CoA deactivates PFL. Also, the observation that when AdhE was introduced to the reaction

mix, exactly the same rate of PFL deactivation was observed proved that AdhE plays no role in the deactivation process in this experiment.

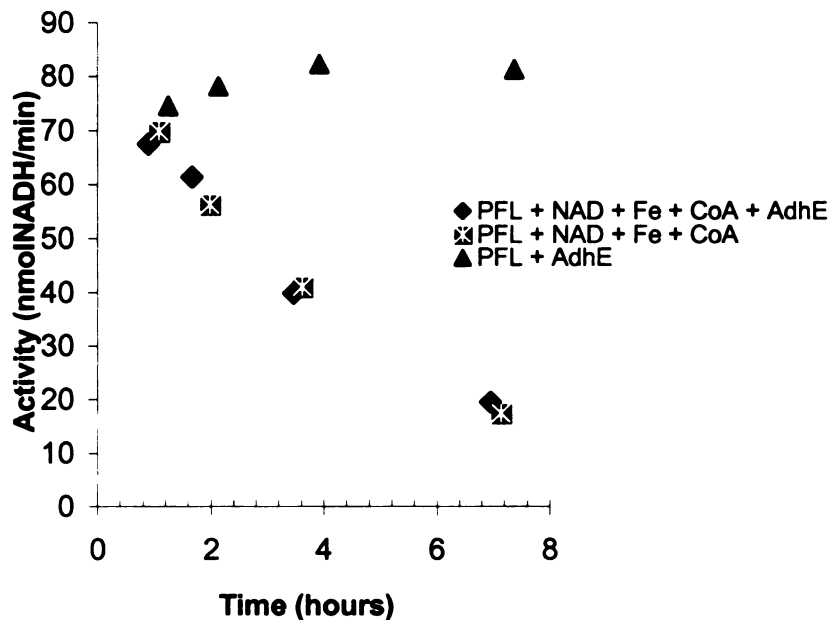


Figure III.23. AdhE, the cofactors NAD^+ , Fe^{2+} and CoA and a combination of both AdhE and the cofactors. All the reaction mixes were of a total volume of 360 μl . The final PFL concentration was 193 μM . Where applicable the final concentrations of each reactant were; AdhE: 3 μM , NAD^+ : 0.2 mM, CoA: 0.1 mM, Fe^{2+} : 1 mM, respectively.

The experiment illustrated in Figure III.23 was repeated but this time the amount of AdhE in the mix was doubled. The trend (Figure III.24) was found to be identical to that observed previously, again indicating that the observed deactivation was due to the effect of at least one of the components on activated PFL, and that AdhE was not that component. Moreover, it was yet again shown that AdhE does not make any difference to the rate of deactivation of PFL.

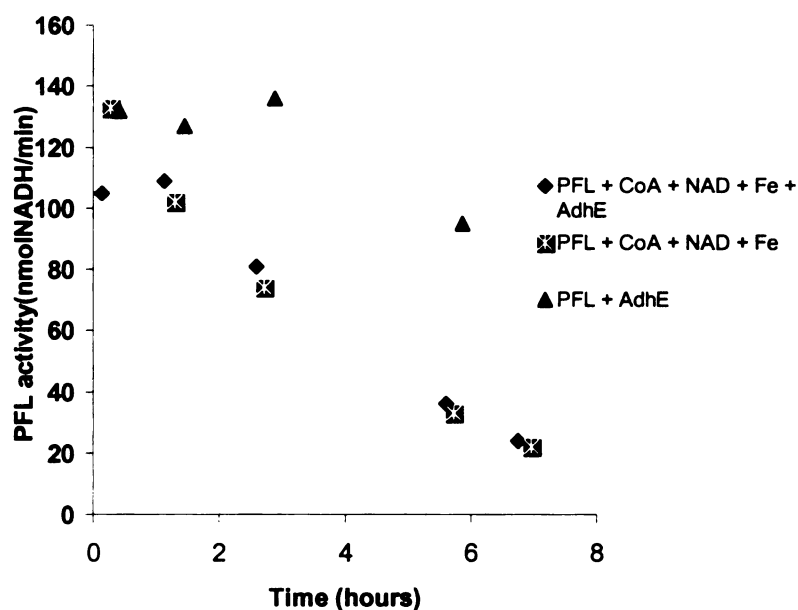


Figure III.24. A time course of PFL deactivation in reaction mixes containing AdhE, the cofactors NAD^+ , Fe^{2+} , CoA, and a combination of both AdhE and the cofactors.

All the reaction mixes were identical to those in Figure III.23, except that the concentration of AdhE was doubled to 6 μM . Further experiments were carried out in an attempt to isolate the cofactor(s) responsible for the observed deactivation, and the mixes for this series of experiments were prepared as shown in Table III.8. The total concentrations of NAD^+ , CoA and Fe in the reaction mixes were 3, 3 and 4 mM respectively. All the reaction mixes were incubated inside an anaerobic chamber at a temperature of approximately 24°C , and the residual activity was determined over time.

All of the experimental mixes containing various combinations of AdhE, CoA, NAD^+ and Fe^{2+} exhibited virtually identical behavior (Figure III.25). All showed a higher rate of PFL deactivation than the control and did so at essentially the same rate.

These results were interpreted as suggesting that at least two of the putative AdhE cofactors are able to deactivate PFL, since the absence of all (PFL only) resulted in a somewhat decreased rate of PFL deactivation, whereas systematic exclusion of one at a time results in essentially identical rates of PFL deactivation, as when all components are present.

Table III.8. Compositions of the reaction mixes used to investigate PFL deactivation under anaerobic conditions

Component	React 1 (μ l)	React 2 (μ l)	React 3 (μ l)	React 4 (μ l)	React 5 (μ l)	React 6 (μ l)
1M Tris-Cl	100	100	100	100	100	100
0.03 M NAD ⁺	30	30	0	30	30	0
0.03 M CoA	30	30	30	0	30	0
0.4 M Fe ²⁺	30	30	30	30	0	0
55 μ M PFL _a	100	100	100	100	100	100
139 μ M AdhE	20	0	20	20	20	0
H ₂ O	0	20	30	30	30	110

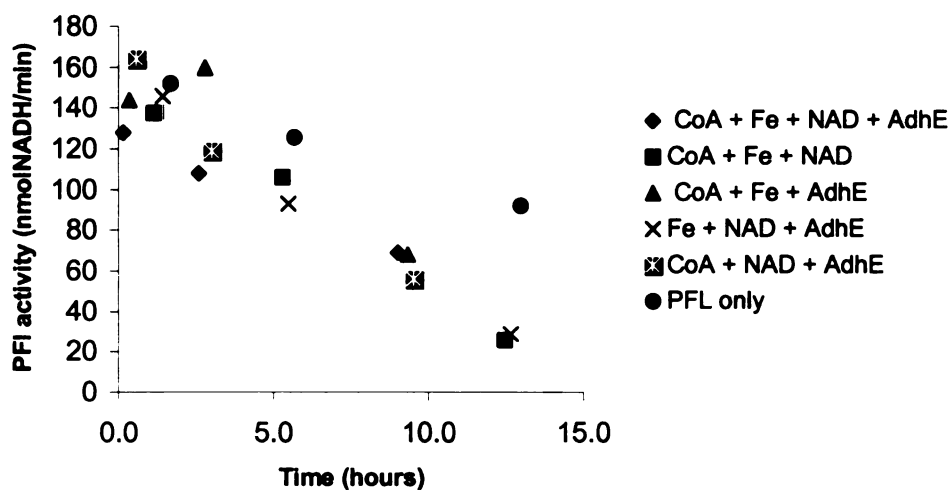


Figure III.25. Graph of PFL deactivation using various combinations of cofactors and AdhE. The control showed relatively slow but steady deactivation over an extended period of time, making analysis of deactivation more difficult.

To further pursue this question, more deactivation studies were done using more cofactor combinations. Each cofactor was also tested individually in order to determine which of the cofactors was sufficient to effect PFL deactivation by itself. The reaction mixes investigated are listed in Table III.9. All the components were added to Tris buffer in a reaction vial inside an anaerobic chamber and were well mixed. Active PFL was then quickly added to each of the vials before sealing the vials with screw-on cap equipped with an airtight rubber septum. The time at which PFL was added to the reaction mix was noted and recorded. The residual PFL activity in each mix was monitored by periodically removing 5 μ l of the reaction mix and placing it carefully on the inside wall of a cuvette containing 995 μ l of the PFL activity assay mix (see page 132, Scheme III.8). The cuvette was then sealed with an air-tight screw-on rubber septum, brought out of the chamber, quickly shaken to wash down the reaction mix containing active PFL and immediately placed in the UV-vis instrument. The rate of production of NADH was then monitored over a period of 60-120 seconds. The rate of NADH production is directly correlated to the concentration of active PFL in the reaction. The instrument is programmed to record the rate of NADH production in units of Au/s. The conversion factor from Au/s to nmol/min was calculated from the Beer-Lambert Law using the cell path length of 1 cm and the molar absorptivity of NADH as $6270 \text{ M}^{-1}\text{cm}^{-1}$. The results obtained are presented in Figure III.26.

Table III.9. Composition of mixes used to isolate the species responsible for PFL deactivation. The concentrations of the stock solutions used to prepare the mixes are indicated.

Component	React 1 (μ l)	React 2 (μ l)	React 3 (μ l)	React 4 (μ l)	React 5 (μ l)	React 6 (μ l)
1M Tris-Cl	100	100	100	100	100	100
46 mM NAD ⁺	0	0	0	30	0	30
42 mM CoA	0	0	0	0	0	30
170 mM Fe ²⁺	0	30	0	0	30	30
694 μ M PFL _a	100	100	100	100	100	100
139 μ M AdhE	0	0	30	30	30	30
H ₂ O	120	90	90	60	60	0

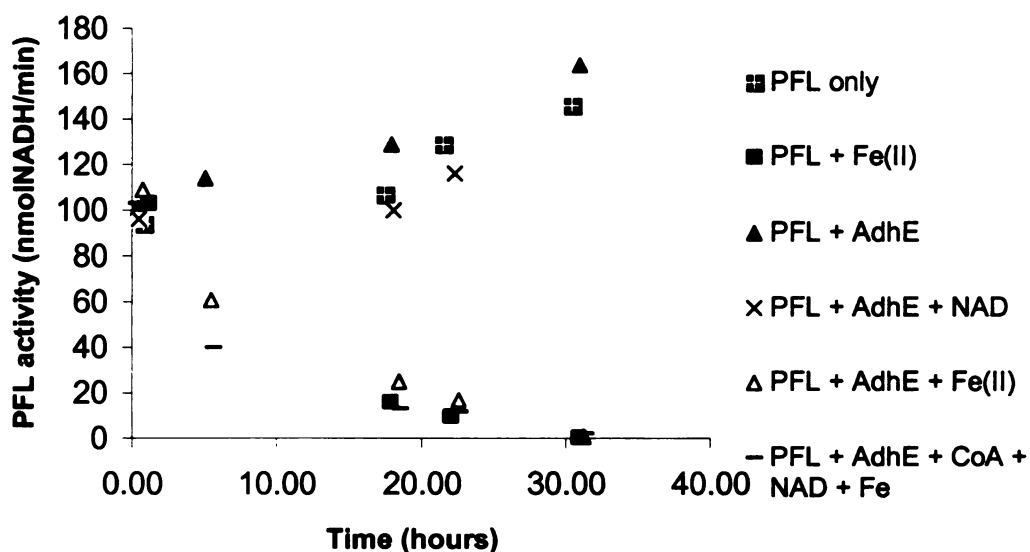


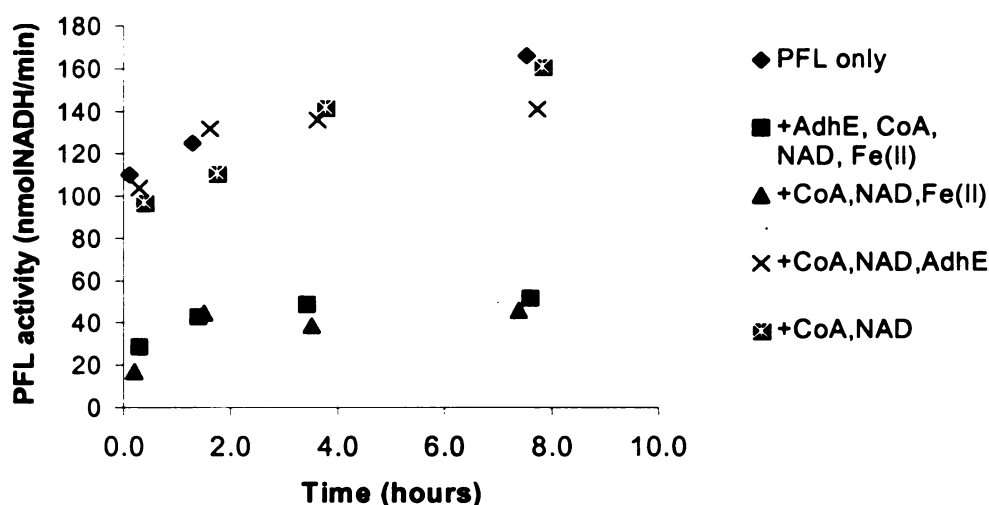
Figure III.26. The effect of various combinations of components used to isolate the component responsible for PFL deactivation.

The data falls into two distinct groups. The first group comprises three reactions showing an increase in the activity of PFL over time, whereas the other group shows a steady decrease in PFL activity over the same period. The only common distinguishing feature between these two groups is the presence or absence of Fe(II). All of the reactions

that contain Fe(II) also show systematic deactivation of PFL, while those containing no Fe (II) show no deactivation. Notably, the reaction mix in which active PFL was incubated with only Fe(II) exhibited deactivation kinetics that are indistinguishable from those containing Fe(II) and other components such as AdhE. These results are consistent with our previous findings suggesting that AdhE has no effect on PFL deactivation. However, intriguingly, Fe (II) appears to deactivate PFL. In fact, the reactions without Fe (II) showed an increase in PFL activity over the course of the experiment. The observed increase in the activity of PFL in the mixes without Fe (II) suggested that PFL could be activated further by exposure to ambient light in the presence of traces of the initial activation components. To test this hypothesis, activated PFL mixes containing different combinations of the putative cofactors were prepared as given in Table III.10, except SAM and AE were excluded. Iron was included in reactions 2 and 3 but not in the other three, which included the control. After incubating for approximately 18 hours, PFL-AE and SAM (both of which are essential components for the activation of PFL), were added as indicated in Table 10. The activity of PFL in each of the reaction mixes was then monitored periodically using the coupled enzymatic assay. The experiment was carried out under strictly anaerobic conditions. The results are obtained are summarized in Figure III.27.

Table III.10 . Effect of Fe(II) on Extent of PFL Activation

Component	React 1 (μl)	React 2 (μl)	React 3 (μl)	React 4 (μl)	React 5 (μl)
1M Tris-Cl	100	96	100	100	100
46 mM NAD ⁺	0	30	30	30	30
42 mM CoA	0	30	30	30	30
170 mM Fe ²⁺	0	30	30	0	0
694 μM PFL _a	100	100	100	100	100
139 μM AdhE	0	30	0	30	0
H ₂ O	116	0	26	26	56
700 μM AE	2	2	2	2	2
10 mM SAM	2	2	2	2	2

**Figure III.27. Effect of Fe (II) on the reactivation of PFL**

These results showed a very interesting and consistent behaviour when compared to Figure III.26. As expected based on the results from Figure III.26, the initial PFL activities in the mixes containing Fe (II) were both low (~20 nmolNADH/min) compared to those without Fe (II) (~100 nmolNADH/min). This was consistent with the previously observed PFL deactivation by Fe (II) in Figure III.26. Whereas the reactions without Fe showed a steady increase in activity to approximately 160 nmolNADH/min, those to

which Fe was added showed marginal activation to ~45 nmolNADH/min in ~8 hours. The monitoring of activity was not continued to saturation under the experimental conditions. However, these results prove that Fe (II) does deactivate active PFL in a systematic way.

III.4. DISCUSSION

The multiplicity of enzymatic functions harbored by AdhE is now commonly accepted within the fields of biochemistry and bioinorganic chemistry. Specifically, this enzyme is believed to be a triple function enzyme, mediating alcohol dehydrogenase, acetyl-CoA reductase and pyruvate formate-lyase (PFL) deactivase. Indeed recently it was reported that AdhE also exhibits antioxidant activity ⁹. Our lab has been involved with the investigation of the interaction between the activating enzyme of PFL (PFL-AE) with both the co-substrate S-adenosyl-L-methionine and the substrate PFL for some time.¹⁴ One of the objectives has been to understand the nature of the interaction among these three by employing various physical methods in order to elucidate the mechanism by which AE achieves the generation of a glycy radical on PFL.

In this study, our interest in AdhE was with regard to its purported PFL deactivase activity. Taken together with the understanding of the chemistry of the activation process mediated by PFL-AE, elucidation of the chemical mechanism of the deactivation process catalyzed by AdhE would shed light on the bigger picture regarding the PFL activation-deactivation system. An understanding of the interconversion of PFL between the radical and non-radical forms could be seminal since there are several other enzymes that are similar to PFL in that they bear a glycy radical co-factor that is similarly generated by an activating enzyme. PFL is up-regulated under anaerobic conditions when pyruvate has to be turned over anaerobically. Activated PFL, however, is rapidly cleaved by exposure to oxygen *in vitro*, suggesting that PFL is either inactivated or deactivated as conditions become more aerobic. Under anaerobic conditions, AdhE is also expressed and used to convert acetyl-CoA to ethanol and CoA by alcoholic fermentation. Notably, the acetyl-

CoA is a by-product of the PFL reaction. That AdhE should also function to deactivate PFL was a very intriguing proposal as it suggested that AdhE somehow acts as both a microaerophilic sensor and a deactivator of PFL, and thus protects it from oxygenolytic degradation. The fact that AdhE is known to have a mononuclear iron (II) center led us to hypothesize that it is probably this iron that provides the electron necessary to quench the glycyl radical. We therefore set out to investigate the role of this iron in the PFL deactivation reaction and to seek to understand the mechanism by which the deactivation process proceeds.

To that end, the AdhE gene was successfully cloned onto a PET21^(a)+ vector and the protein was subsequently overexpressed in BL21 (DE3) pLysS and purified to homogeneity using an Ni-NTA affinity chromatographic column. Enzymatic assays confirmed the presence of both the alcohol dehydrogenase and acetyl-CoA reductase activities in AdhE and this corroborated the positive identification of the enzyme using gel electrophoresis. However, repeated attempts to reproduce the AdhE-catalyzed PFL deactivation reported in the literature all led to negative results. Whereas it was easily demonstrable that AdhE cloned and isolated in our laboratory harbors both of the other known activities, no association could be made between PFL deactivation and the presence of AdhE. Indeed the rate of PFL deactivation in the reactions containing AdhE was consistently similar to that of the control experiment in which only buffer and PFL were present. On the other hand, of the reactions containing the purported cofactors NAD⁺, CoA and Fe²⁺, those containing Fe²⁺ showed a consistent enhancement in deactivation relative to the control. The presence of NAD⁺ alone showed no discernible effect on the rate of PFL deactivation. Based on the observations made in this study,

Fe^{2+} , and to some measurable degree CoA, was found to be capable of deactivating PFL either by itself or in the presence of other co-factors. The presence or absence of AdhE did not have any effect in this deactivation, thus causing us to put to question its role in the previously reported PFL deactivation, particularly considering that the reactions were done in the presence of Fe^{2+} . Other experiments (data not shown) also showed that CoA deactivates PFL at a significant rate relative to background deactivation observed in activated PFL alone.

It is noteworthy that the deactivation observed in all of these reactions did not show enzymatic behavior, occurring over a period of many hours. The deactivation kinetics are consistent with behavior that one would expect from the quenching of the PFL radical by a small non-enzymatic molecule. On that basis, the deactivation of PFL in these reactions was attributed to the action of Fe^{2+} or CoA. However, it was clear that this same explanation could not be immediately used to account for the deactivation reported in the literature because in that case the deactivation was complete within 30 minutes,³ which is much faster than we have observed. We also noted that the deactivation mixes used by Knappe and Kessler in all their experiments contained DTT in large excess over PFL.³ Having tentatively ascribed the observed deactivation by CoA to the thiol group, we postulated that DTT, also being a thiol, would likewise deactivate PFL by quenching of the glycyl radical at Gly734. We further postulated that the deactivation previously ascribed to AdhE was probably due to the combined contributions of Fe^{2+} and DTT. The tentative implication of DTT was in part predicated upon previous reports of glycyl radical quenching by thiols.¹³ The effect of thiols on the activity of PFL is further pursued in Chapter 4.

III.5. CONCLUSIONS

AdhE from *Escherichia coli* was successfully cloned, overexpressed and purified to homogeneity. Analysis by sodium dodecyl sulfate polyacrylamide gel electrophoresis (SDS-PAGE), enzymatic assays for alcohol dehydrogenase, acetaldehyde reductase, DNA fingerprinting using restriction enzymes, partial sequencing of the adhE PCR gene product, and MS-MALDI of the AdhE gene product were all used to confirm the identity of the AdhE. Iron analysis using complexometric photometry corroborated previous reports that AdhE harbors one Fe atom per molecule of the enzyme.

Several attempts to reproduce the reported PFL deactivase activity, which has been reported as one of the activities harbored by AdhE, consistently showed that AdhE does not have any role in PFL deactivation. On the other hand, the reactions containing Fe^{2+} (and to a lesser extent CoA) always showed an increased rate of deactivation relative to the control. However, this deactivation was clearly not enzymatic as it occurred over several hours. These observations have therefore led us to conclude that AdhE is not a PFL deactivase as previously reported, but that the deactivation that was observed was likely due to one or any combination of Fe^{2+} , CoA and DTT, all of which constituted part of the assay mix used in the deactivation studies.

REFERENCES

1. Clark, D.P. **1989**, *FEMS Microbiol. Lett.* 63, 223-234.
2. Goodlove, P.E. **1989**, *Gene* 85, 209-214
3. Kessler, D and Knappe, J. 1992, *J. Biol. Chem.* 267, 25, 18073-18079.
4. Kessler, D.; Leibrecht, I.; Knappe, J. **1991**. *FEBS Lett.* 281, 59-63
5. Frey, M.; Rothe, M.; Wagner, A.F.V.; Knappe, J. **1994**, *J. Biol.Chem.* 269, 17, 12432-12437.
6. Knappe, J.; Neugebauer, F.A.; Blachskowski, H.P.; Ganzler, M. **1984**, *Proc. Natl. Acad. Sci. USA*, 81, 1332-1335.
7. Wagner, A.F.V.; Frey, M.; Neugebauer, F.A.; Schafer, W.; Knappe, J. **1992**, *Proc. Natl. Acad. Sci.U.S.A* 89, 996-1000.
8. Unkrig, V.; Neugebauer, F.A.; Knappe, J. **1989**, *Eur. J. Biochem.* 184, 723-728.
9. Echave, P.; Tamarit, Jordi.; Cabiscol, E.; Ros, J. **2003**, *J. Biol. Chem.* 278, 30193-30198.
10. Holland-Stanley, C.A.; Lee, K.; Clark, D.P.; Cunningham, P.R. **2000**, *J.Bacteriol.* 182, 6049-6054.
11. Membrillo-Hernandez, J.; Echave, P.; Cabiscol, E.; Tamarit, Jordi.; Ros, J.; Lin, E.C.C. **2000**. *J. Biol. Chem.* 275, 33869-33875.
12. Knappe, J.; Sawers, G. **1990**. *FEMS. Microbiol. Rev.* 75, 383-398.
13. Armstrong, D.A.; Yu, D.; Rauk, A. **1998**. *J.Am. Chem. Soc.* 120, 8848-8855.

CHAPTER IV

DEACTIVATION OF PFL BY SMALL MOLECULES

ABSTRACT

Several small molecules were studied with respect to their ability to deactivate PFL. Based on preliminary findings indicating that the presence of CoA resulted in a measurable and reproducible increase in the rate of PFL deactivation relative to the control, we carried out a systematic investigation of several small molecules. Based on the hypothesis that the thiol group was responsible for PFL deactivation, the initial set of molecules studied were all thiols. All showed a similar effect as CoA, with the rate of deactivation generally proving to be more rapid for the smaller molecules. Whereas DTT, 2-mercaptoethanol and ethanethiol all deactivated PFL in a systematic manner, they all did so at a markedly higher rate than CoA. Among these compounds, the rate of PFL deactivation showed a correlation to the size of the thiol, with the smaller thiols showing a generally higher rate of PFL glycy radical quenching. In order to determine whether the observed PFL deactivation by thiols was an inherent property of the thiol functionality or whether thiols were exerting their property as reducing agents in general, other biological reducing agents were also studied to determine their effect on active PFL. All the reducing agents studied proved to be capable of deactivating PFL.

IV.1. INTRODUCTION

Upon observing that CoA deactivates PFL, we were intrigued to further investigate the effect of thiols on the activity of PFL. Our hypothesis was that the glycyl radical of activated PFL was quenched by the thiol group of CoA, as that was the most plausible functional group by which CoA could supply the hydrogen atom required to quench the glycyl radical. Thiols have been shown to quench glycyl radicals¹. However, in previous studies done on PFL, as indeed is the case with most other enzymes studied in research laboratories, small molecule thiols were used routinely as components of the buffers. Dithiothreitol (DTT), for example, is the most common thiolic reductant used in enzymatic assays and is routinely used as a component of lysis buffers and buffers used during protein purifications. Following the observation that CoA slowly inactivates PFL, a number of thiols were systematically studied, with the aim to investigate the effect of thiol size and structure on the rate of deactivation. Other small molecule reducing agents relevant to biological systems were also studied in order to determine whether the observed activity of the compounds containing a thiol group is specific to the thiol group, or whether it can be extended to reducing agents in general. Because the glycyl radical of active PFL is known to be buried within the structure of the protein, it was expected that the rate of PFL deactivation would be sensitive to the size of the reducing species. This would be so particularly if there was direct hydrogen transfer from the reductant to the glycyl radical of active PFL. In this chapter, the effect of several small molecules on active PFL was investigated systematically in order to shed some more light on the properties of active PFL, particularly with regard to its stability.

IV.2. MATERIALS AND METHODS

IV.2.1. Materials

All the chemicals used in these experiments were of the highest quality commercially available. Dithiothreitol was obtained from American Bioanalytical, and 2-mercaptoethanol, ethanethiol, cysteine, homocysteine, glutathione and methionine were obtained from Sigma. The enzymes and reagents used in the coupling assay were purchased from Sigma. PFL was purified and activated as described in Chapter 2. The structures of the compounds investigated in the study are shown in Figure IV.1.

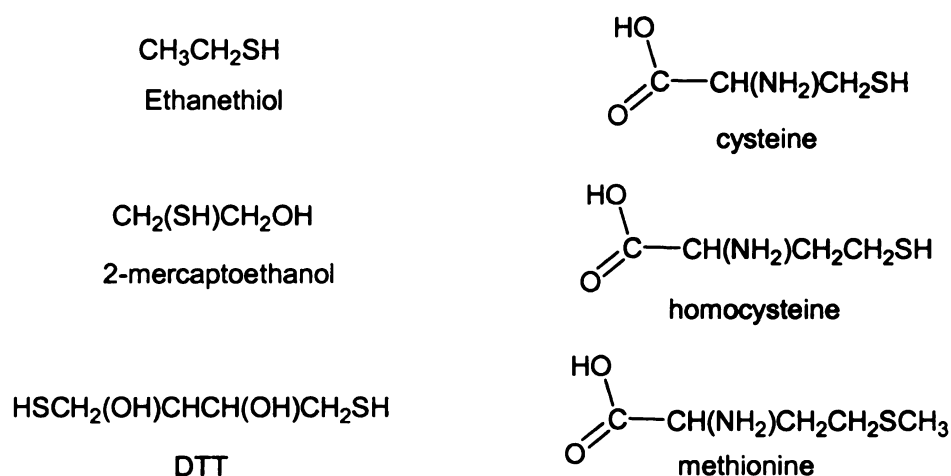
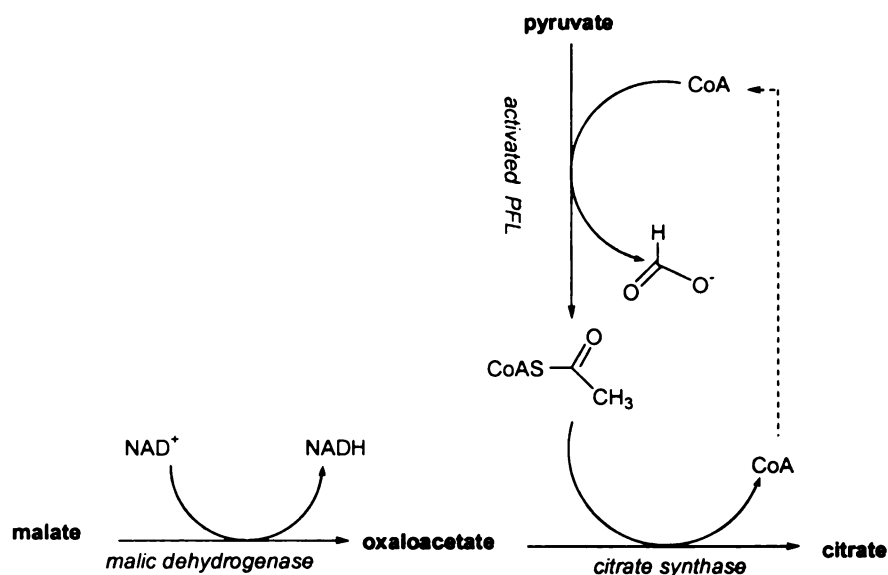


Figure IV.1. Structures of the small molecules used in PFL deactivation studies

IV.2.2. The PFL deactivation experiment

For each deactivation carried out, the active PFL in 300 mM Tris-HCl buffer, pH 8.5, was incubated in an anaerobic chamber (Mbraun) with a known concentration of the reagent under investigation. The residual PFL activity was determined periodically by transferring 2 μ l of the deactivation mix into 698 μ l of the coupling reaction mix as previously described in Chapter II. To avoid reaction while transporting the reaction mix from the anaerobic chamber to the spectrophotometer (HP Model 8543), the 2 μ l of the PFL deactivation mix was carefully deposited on the inside wall of the cuvette. Care was taken to ensure that there was no contact between the deactivation mix and the assay mix. The cuvette containing the activity mix was made airtight by sealing it with a screw-on septum prior to bringing it out of the anaerobic chamber. The deactivation mix and the assay mix were then quickly mixed by rapidly and vigorously shaking the cuvette so that the 2 μ l of deactivation mix (containing residual active PFL) was washed into the bulk of the assay mix. The cuvette was rapidly placed in the instrument and the residual PFL activity was measured by monitoring the production of NADH as a function of time. The activity assay is summarized in Scheme IV.1.



Scheme IV.1. Enzymatic activity assay used to monitor residual activity of PFL in the deactivation reactions.

As summarized in Scheme IV.1, in the presence of CoA, active PFL mediates homolysis of pyruvate between C1 and C2 and transfer of the acetyl group to CoA to produce acetyl-CoA. In the presence of oxaloacetate, citrate synthase then converts acetyl-CoA back to CoA and in the process produces citrate. CoA produced in this step is fed back to the pyruvate-PFL reaction and produces more acetyl-CoA. Meanwhile, oxaloacetate is replenished by the conversion of malate (in the presence of NAD^+) by malic dehydrogenase. Provided NAD^+ and malate are in excess, the concentration of oxaloacetate is essentially constant. The rate of consumption of oxaloacetate (and indirectly NAD^+) under such conditions is directly proportional to the activity of PFL, provided that pyruvate is also present in excess. The rate at which the reactions in the coupled assay proceed can therefore be measured by the rate of production of NADH. This is the principle upon which the coupled enzymatic assay is based.

IV.3. RESULTS

IV.3.1. Deactivation by DTT and β -ME

Based on the observation that CoA showed measurable deactivation of PFL, and the hypothesis that this deactivation was due to thiol moiety of CoA, we decided to investigate the effect of small molecule thiols on PFL activity. Since dithiothreitol (DTT) was routinely used as a reductant in the lysis and purification buffers for PFL, it was one of the first small molecules investigated. For comparison, 2-mercaptoethanol (β -ME) was also tested. β -ME is structurally similar to DTT and is also a thiol. Like DTT, this compound is routinely added to buffers used during protein purifications and handling. With regard to PFL, it is important to establish whether the presence of β -ME in solution had any effect on the lifetime of the glycyl radical. The experiment was carried out by incubating activated PFL (0.14 mM) with 0.14 M β -ME and 0.10 M DTT and measuring the residual PFL activity over time, using the enzymatic assay represented in Scheme IV.1. The control consisted of replacement of the thiol with water followed by similar treatment as the experimental. The preparation and the incubation of the deactivation mixes were done inside an anaerobic chamber, with oxygen concentration maintained at less than 2 ppm. Each deactivation mix was prepared by transferring 90 μ L of activated PFL into a reaction vial equipped with a cap bearing an air tight rubber septum. The volume was made up to 100 μ L with the thiol under study, or water in the case of the control, mixed thoroughly, and then aliquots were taken periodically to check for residual activity. Representative results are shown in Figure IV.2. The activity of PFL in the control remained constant over the entire duration of the experiment, whereas the activity of PFL incubated with DTT showed a slight downward trend over the time of the

experiment, but was only marginally different from that observed for the control. β -ME, on the other hand, completely deactivated PFL within 1 hour.

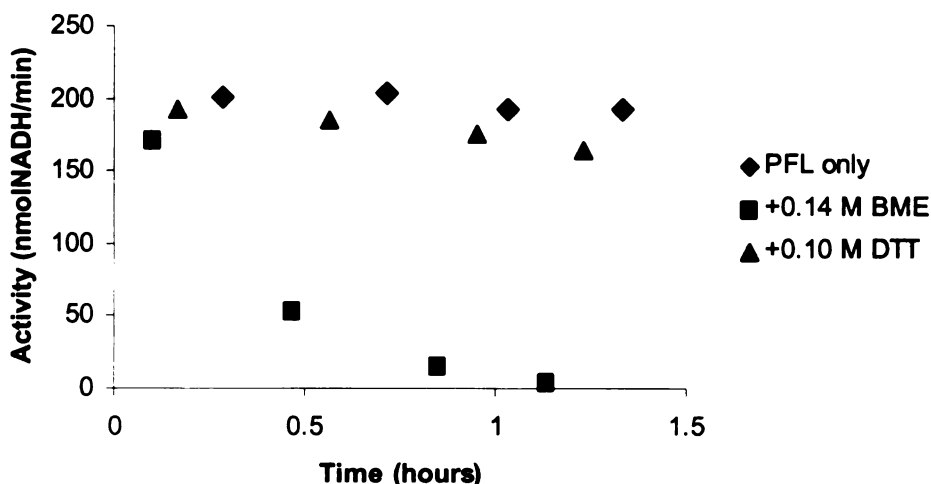


Figure IV.2. The effect of DTT and β -ME on the activity of PFL as determined by the enzymatic assay shown in Scheme IV.3.1. Conditions: [PFL] = 125 μ M; [DTT] = 100 mM; [β -ME] = 140 mM; buffer is 300 mM Tris, pH 8.5.

The results in Figure IV.2 demonstrate that PFL by itself remained active and stable over the entire period of the experiment. It is also evident that β -ME rapidly deactivates PFL. Although the PFL activity in the presence of DTT showed a downward trend, the activity was too close to that of the control to allow any concrete conclusion to be made. In order to investigate this further, the deactivation experiment was repeated, but carried out for a longer time. The concentration of DTT was maintained at 1 mM as in the first experiment, in order to make a direct comparison of the results obtained from the two experiments. The results in Figure IV.2 illustrate the effect of DTT on PFL

activity over a longer period. The effect of DTT on the activity of PFL in the first hour in Figure IV.3 is identical to that shown in Figure IV.2. After about 7.5 hours, the effect of DTT became more apparent in that the PFL activity in the experimental mix was virtually all gone, whereas the control showed activity at a similar level to those at the beginning of the experiment. Remarkably whereas no PFL activity was detectable in the experimental mix after 24 hours, the control retained 90% of the highest measured activity within that period, thus attesting to the stability of the PFL radical.

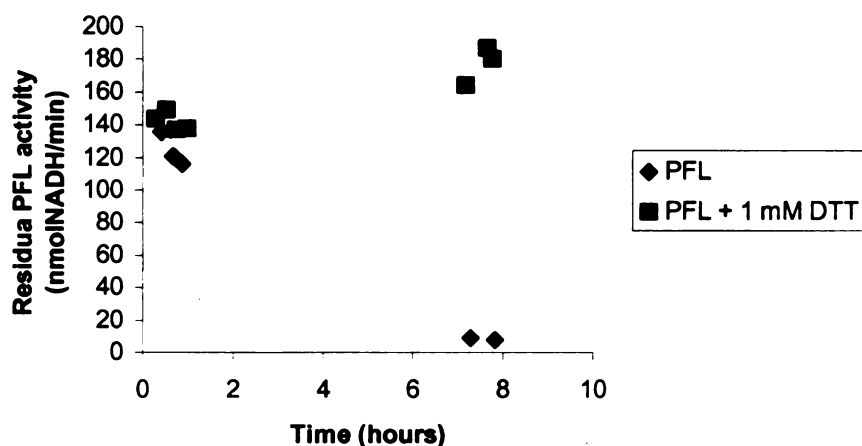


Figure IV.3. The effect of DTT on the activity of PFL over an extended period of time. After seven hours of incubation, the control shows PFL activity at similar levels as at the beginning of the experiment, whereas the activity of the reaction to which DTT was added to a concentration of 1 mM showed virtually no activity after the same period of time. Conditions were as in Figure IV.2.

IV.3.2. Effects of Illumination on the deactivation of PFL

In some of our previous experiments it was observed that when the deactivation was carried out under ambient light, the activity of PFL in the control

reaction steadily increased over time (see, for example, Figure III.26). In the current experiments similar observations were made (Figure IV.3). The activity of PFL increases both in the control and in the presence of DTT, although the activity of the reaction containing DTT increased at a slower rate than the control. In the presence of β -ME, the activity still decreased over time. Whereas β -ME deactivated PFL rather rapidly (about 80% in 20 minutes), the activity in the presence of DTT steadily increased similarly to, but at a slightly slower rate than that of the control.

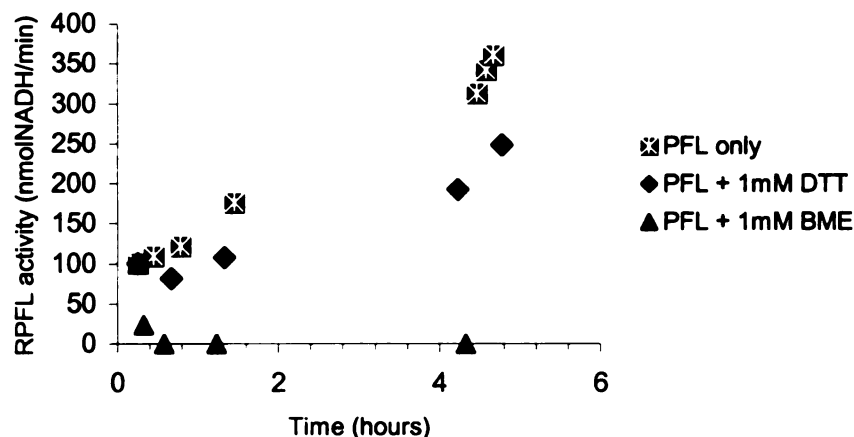


Figure IV.4. Effect of DTT and β -ME on the activity of PFL when exposed to ambient light. Conditions: [PFL] = 98 μ M; [DTT] = 10 mM; [β -ME] = 10mM; buffer was 300 mM Tris, pH 8.5. The reactions also contained quantities of PFL-AE (4.5 μ M), SAM (0.7 mM) and deazariboflavin (10 μ M) left over from the activation of PFL.

The observation of steady increase in activity of the control (and to a lesser extent the reaction containing 1 mM DTT), suggested that the PFL was not fully activated prior to initiating the deactivation experiments, and thus, that PFL activation was competing with deactivation. The on-going activation was presumably occurring due to the

presence of small quantities of PFL-AE (2 μ M), AdoMet (700 μ M) and deazariboflavin (140 μ M), which were not removed from the activated PFL prior to initiating deactivation studies. Since deazariboflavin is a photoreductant used as the electron donor in activating PFL, it appeared that the ambient lighting was sufficient to drive further PFL activation. This finding was surprising, given that previously PFL activations were carried out using an intense 300W halogen lamp.²

In order to test our hypothesis that activation by ambient light was competing with deactivation, the stock solution of previously activated PFL was incubated in ambient light for about five hours and then used to carry out the deactivation studies. The PFL thus treated exhibited significantly higher activity, and subsequent deactivation experiments showed identical results, regardless of whether the experiment was carried out in the dark or under ambient light (Figure IV.5). No increase in control PFL activity was observed even under ambient light, showing that after reactivation of PFL by ambient light, PFL had been activated to the maximum extent. It is particularly noteworthy that activated PFL proved exceedingly stable, maintaining its activity over an extended period at average temperatures ranging from 22-23°C; this proved to be of great experimental advantage for these studies. The data illustrate again that β -ME causes rapid deactivation of active PFL, reducing the activity by ~80% within 6 seconds, while for the DTT-treated sample no detectable decrease was observed until after ~2 hours of incubation. Notably, the initial activity of PFL was more than 120% greater after reactivation than before reactivation (~230 vs ~100 nmol NADH/min) and remained virtually constant in the control over the six hours of incubation. PFL activity in the reaction mix containing DTT decreased relatively slowly (by ~ 60% of the initial) during

the same period. This was consistent with previous observations that showed that at the given relative concentration, DTT deactivates PFL rather slowly (hours). The activity in the mix containing a similar concentration of β -ME on the other hand was completely quenched within 25 minutes.

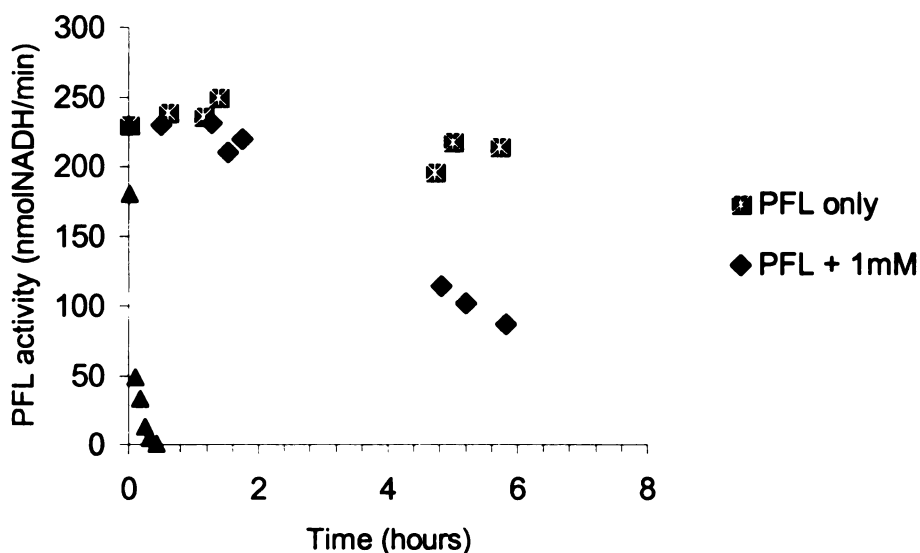


Figure IV.5. Deactivation of PFL fully activated by exposure to ambient light for about 6 hours before deactivating with 1 mM of each of β -ME and DTT. Experimental conditions were as outlined under Figure IV.4.

IV.3.3. Deactivation of PFL by other thiols and small molecules

Other small molecules and thiols were also investigated in order to determine whether the observed deactivation was particularly a thiol effect, or whether it was due to some other more general property of these small molecules. Specifically, it was of interest whether the observed deactivation by DTT and β -ME was a result of the presence of the thiol functional group in these molecules, or whether it was their capacity as reducing agents that conferred on them the capacity to deactivate PFL. Figure IV.6 shows data obtained from experiments conducted to compare DTT, β -ME and ethanethiol ($\text{C}_2\text{H}_5\text{SH}$), all of which showed systematic PFL deactivation.

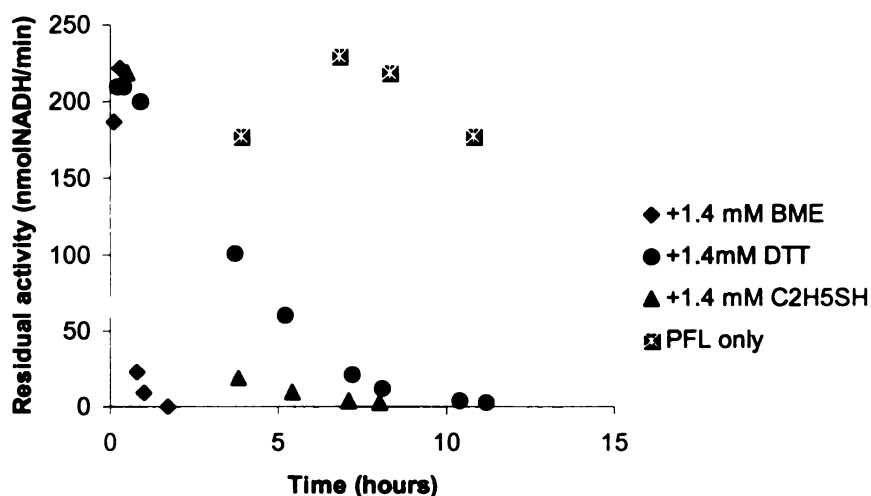


Figure IV.6. Comparison of the PFL deactivation properties of ethanethiol, DTT, and β -ME. Ethanethiol showed similar deactivation kinetics to DTT and β -ME. Conditions: [PFL] = 98 μM ; [thiol] = as shown above; buffer is 300 mM Tris, pH 8.5.

IV.3.4. Investigation of PFL deactivation by other small molecules

In order to gain a broader view of the nature of the reaction responsible for PFL deactivation by the small molecules, we expanded the investigation to include glutathione, methionine, cysteine and homocysteine. There were three basic reasons for choosing this particular set of small molecules. Firstly, these molecules are very common in biological systems and are therefore physiologically relevant molecules. Methionine and cysteine are amino acids and are synthesized regularly by bacteria in order to be incorporated into various types of polypeptides, including enzymes and structural proteins. Cysteine is also credited with the ability to strengthen the antioxidant capability within the living cell, particularly by mitigating the harmful effects of heavy metals.^{3,4} Homocysteine is generally associated with the risk of heart disease⁵ in humans, and is therefore of general biological interest. It was included because of its structural and chemical similarity to cysteine. Glutathione is most commonly known for its involvement in detoxification, transforming toxins such as heavy metals, solvents, and pesticides into a form that can be excreted in urine or bile.⁶ Glutathione is also an important antioxidant and is now known to protect against toxic chemicals in the brain, hence an increased interest in it by researchers in Alzheimer's disease.⁷

Secondly, we wanted to determine whether there was a correlation between the size of the thiol and the rate of PFL deactivation. If deactivation required direct interaction between the small molecule and the active site radical of PFL, then the rate of deactivation would show a direct correlation with the size of the small molecule, such that the smaller molecules would deactivate PFL more efficiently than the larger ones.

The third reason for choosing these molecules was to determine whether or not the deactivation of PFL previously observed during investigation of Fe^{2+} , DTT, CoA and β -ME was due to the specific involvement of the thiol moiety, or whether it was due to the general property of these molecules as reducing agents. If the deactivation was a specific function of the thiol group, methionine would not deactivate PFL. Each compound was prepared such that its effective concentration in the deactivation mix was 4 mM. The results of this investigation are presented in Figure IV.4.7.

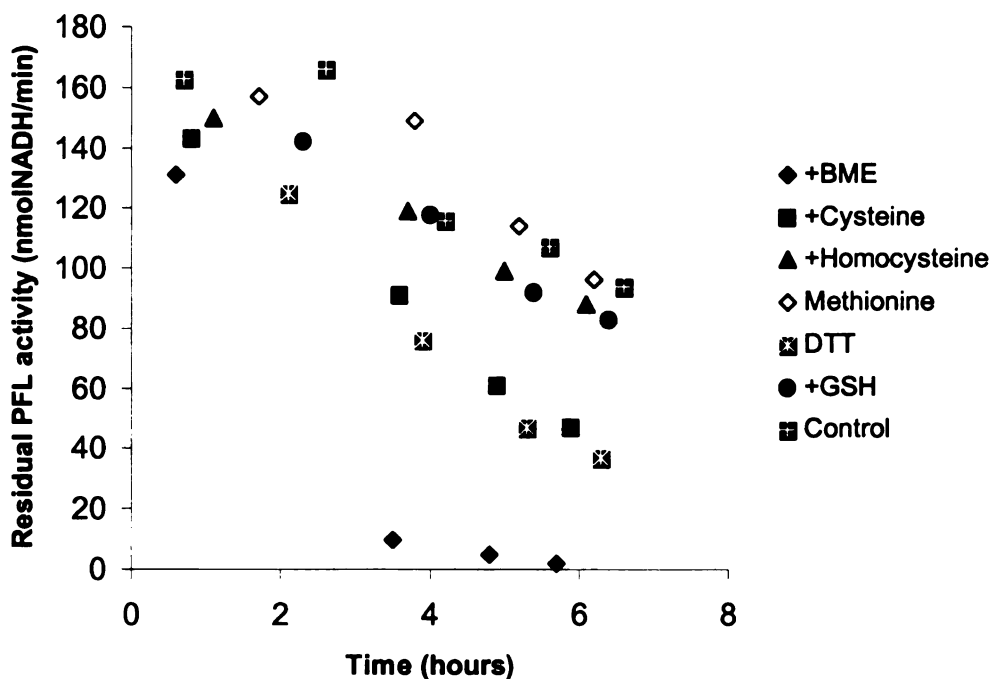


Figure IV.7. Comparison of deactivation rates of various thiols and small molecules. The concentration of each of the components was 4 mM. Conditions: [PFL] = 370 μM ; [small molecule] = 4 mM; [Deazaroboflavin] = 10 μM ; [AE] = 35 μM ; Buffer is 300 mM Tris, pH 8.5.

Among the molecules shown in Figure IV. 7, β -ME showed the most rapid deactivation, achieving half of the original activity within two hours. DTT and cysteine showed comparable rates of deactivation, decreasing the activity of PFL by half within ~3.5 hours. Glutathione showed rather marginal deactivation compared to the control, bringing the activity of PFL to half its maximum in approximately 6 hour. Within the same period, the control retained ~65% of its original activity. Methionine, the only molecule without a thiol group among those investigated here, showed virtually identical kinetics to the control, suggesting that it was not capable of deactivating PFL. The PFL activities measured in the mixes containing each of the species after ~ 6 hours are listed Table IV. 1.

Table IV.1 Residual PFL activities of PFL in deactivation mixes containing some small molecules

Species studied	Residual PFL activity
Control	101
Homocysteine	88
Methionine	98
Glutathione	81
Cysteine	47
DTT	37
β -ME	0

Relative to the control, methionine proved virtually ineffective with regard to PFL deactivation. Homocysteine and glutathione were comparable in their degree of PFL deactivation in 6 hours. Cysteine proved to be relatively effective, deactivating ~80% of PFL within the same period. As observed before, DTT and β -ME deactivated PFL relatively rapidly, with β -ME doing so a lot faster.

IV.3.5. Comparison of methionine and cysteine

Following on the results presented in Figure IV.7, the deactivation experiment was repeated using only methionine and cysteine, in order to ascertain that indeed methionine, as hypothesized based on its lack of a thiol functional group, does not deactivate PFL, whereas cysteine does. The concentration of each amino acid was increased to 4 mM for ease of comparison. The results of this investigation (Figure IV.8) provide further and more convincing support for the deactivation of PFL by cysteine.

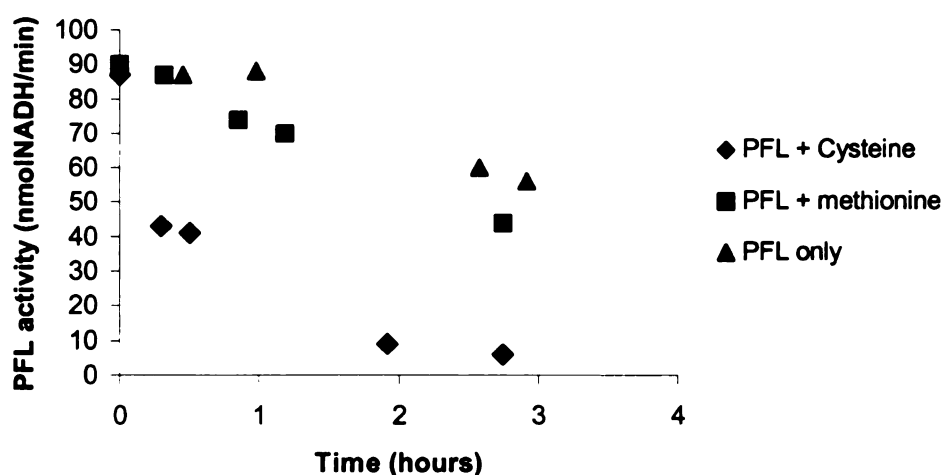


Figure IV.8. Comparison of methionine and cysteine as PFL deactivators. Conditions: As in Figure IV.7.

Within the time frame of the experiment, methionine proved to be a much less effective quencher of the glycy radical of PFL than cysteine, consistent with our previous observations.

IV.3.6. Other non-thiol reducing agents

Previous studies (Chapter III) had shown that Fe (II) deactivates active PFL in a systematic manner, and within a similar time frame as was observed with some of the thiols investigated in this study, therefore suggesting that the quenching of the glycy radical in active PFL might be a function of the presence of any species capable of providing reducing equivalents. Following that line of reasoning, ascorbic acid and dithionite were the chosen candidates of study in order to address this question. Figure IV.9 gives the results obtained from the investigation. Although the initial activity of the PFL used in this experiment was lower than in the previous ones, the activity of the control was steady for the entire 5 hours for which the experiment was run. At the end of the experiment, all of the experimental runs showed markedly reduced PFL activities compared to the control. The experimental reaction containing dithionite contained no detectable PFL activity after the same incubation period as that containing ascorbic acid.

Based on the hypothesis that the observed deactivation of PFL was due to the participation of the thiol functionality in the small molecules studied, we had predicted that ascorbic acid and dithionite might not deactivate PFL. That these molecules also proved to be capable of deactivating PFL was interesting, and led us to propose that the capacity to deactivate PFL, exhibited by the molecules investigated in this study, was a property of reductants in general. This proposal is supported by the observation that dithionite, a strong reducing agent without a thiol group, actually deactivated PFL more ascorbic acid. This was also

consistent with the observation that Fe(II) also proved to be an effective deactivator of PFL (Figure III.25).

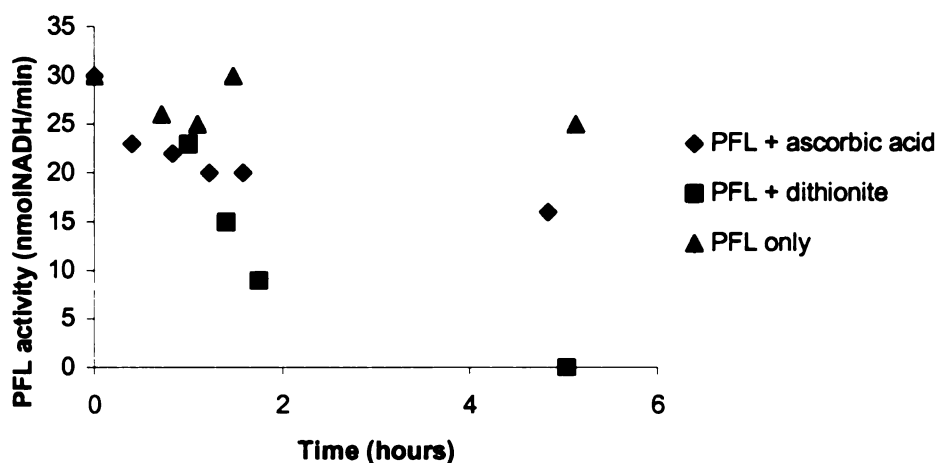


Figure IV.9. Effect of non-thiolic reductants on the activity of PFL. A 1 μL aliquot of an 400 mM solution of each was transferred to a final solution of 90 μL of active PFL and the volume made up to 100 μL with ultra pure water. Reaction conditions: As in Figures IV.7. and IV.8.

IV.3.7. Deactivation of PFL by β -ME is reversible

A crucial question arising from all of the fore-going observations was whether the observed loss of PFL activity was due to deactivation or inactivation. In other words, was active PFL being converted to its native non-radical state by the quenching of the radical at glycine 734, such that it could once again be activated under the right conditions ('deactivation'), or was the loss of activity associated with a permanent chemical or conformational change that rendered PFL unactivatable ('inactivation')?

To address this question, active PFL was reacted with β -ME as described previously. Activated PFL was diluted 2x with ultra pure and degassed water that had

been kept inside an MBraun™ anaerobic chamber. To 990 μL of active PFL, 30 μL of a 1.4M $\beta\text{-ME}$ stock solution was added. The solution was mixed well to ensure homogeneity. A control was prepared by using water in the place of $\beta\text{-ME}$. The residual PFL activity was then monitored as a function of time using the coupled enzymatic assay shown in Scheme IV.1. The results in Figure IV.10 show that after 3 hours the activity of PFL in the control had increased slightly upon incubation in ambient light (~ 120 to 160 nmol NADH/min), the average temperature being 23°C . In the next 7 hours the activity decreased by less than 10% (~ 160 to ~ 150 nmol NADH/min). During the same period (7 hours), the activity of PFL containing $\beta\text{-ME}$ decreased by over 99%. These results were consistent with those made previously.

At 10 hours, 500 μg of PFL-AE and 385 μg deazariboflavin were added to each of the control and experimental samples (double arrow) and illuminated with a 300-watt halogen lamp for 30 minutes. During illumination, both samples were kept in ice water in order to keep the temperature of the reactions within the stability range of the proteins. The activity of PFL in both samples was then monitored as before over a time range of spanning 30 hours.

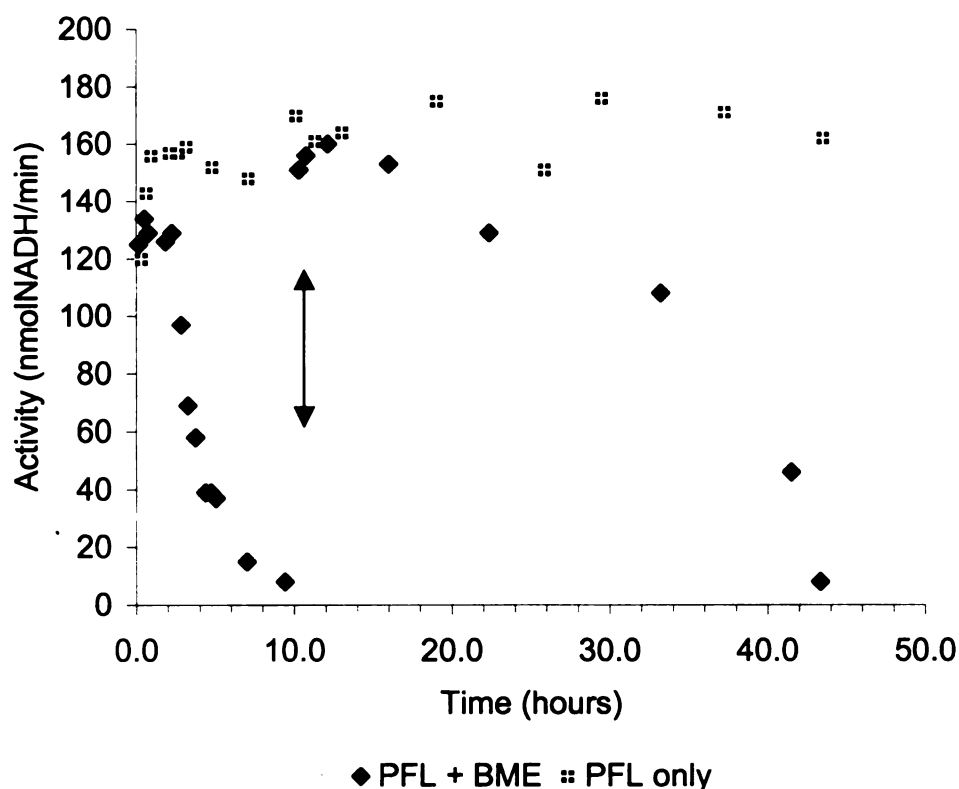


Figure IV.10. PFL deactivation by β -ME. After 10 hours, only 12% of PFL activity remained in the experimental sample, whereas the control sample still had 93% of PFL activity remaining. Conditions: [PFL] = 125 μ M; [β -ME] = 140 mM; buffer is 300 mM Tris, pH 8.5. Also present from original PFL activation: AE, 20 μ M; SAM, 1 mM; deazariboflavin, 10 μ M. At 10 hours deazariboflavin was added to a final concentration of 20 μ M. The reaction was then illuminated for 30 minutes and PFL activity monitored over time.

Following addition of PFL-AE and deazariboflavin, and illuminating for 30 minutes, the activity of PFL in the “+ β -ME” reaction increased more than 10-fold from ~15 to ~160 nmol NADH/min within 2 hours. The activity of PFL in the control

increased by only 19% from ~148 to ~176 nmol NADH/min and remained stable at about the same level for the entire duration of the experiment. Notably, the maximum PFL activity achieved after additional activation of PFL in the control reaction is essentially the same as that attained after reactivation of PFL in the experimental reaction.

Our interpretation of these results is that under the initial activation conditions, PFL was activated to about 75% of the maximum possible (~130 nmolNADH/min). In the control sample, additional activation to ~90% of maximal occurred due to ambient lighting. This additional activation of previously activated PFL was also observed in previous experiments. The addition of 41 mM of β -ME resulted in the deactivation of almost 90% of the active PFL within 10 hours while essentially no deactivation was observed in the absence of β -ME (control). Upon addition of the PFL activating enzyme and deazariboflavin to both reactions, the deactivated PFL in the experimental reaction was reactivated to slightly over its original level. The activity of PFL in the control, however, had already been close to the maximum attainable under the conditions of the experiment and therefore increased only slightly upon illumination.

Another way to interpret these results is that the addition of PFL-AE and illumination simply activates PFL that had not been previously activated. However, in this case we would expect to see additional activation in the control as well, unless the observed activities are artificially limited by the experimental conditions. Using the coupled PFL activity assay described previously under similar conditions, we have consistently measured PFL activities that are well over 500 nmol NADH/min. The possibility that the observed maximal activity measured in this experiment is artificially limited by the experimental conditions can therefore be ruled out. So, had the dramatic

increase in PFL activity observed for the test reaction been due only to previously unactivated PFL, the same increase in activity would also have been observed in the control reaction, giving NADH production rates in the region of 350 nmol/min for the control. Taken together, these results suggest that the increase in activity of PFL observed in the experimental reaction resulted from the β -ME-deactivated PFL, and thus we conclude that deactivation of PFL by β -ME is reversible.

It is also of interest to note that shortly after reaching the maximum activity of ~ 160 nmol NADH/min, the activity of the reactivated PFL begins to decrease relatively rapidly in the reaction mix containing β -ME (Figure IV.10). The kinetics of this second deactivation phase are noticeably different from those of the first. Whereas the first deactivation phase showed the typical decreasing rate of deactivation (concave curve), the second phase shows a steadily increasing rate of deactivation. The significance of this difference is not clear at present, but it is noteworthy.

IV.3.8. Effect of the NADH/NAD⁺ Ratio on PFL Deactivation by ADHE

Previous studies have shown that overexpression of AdhE is directly correlated with the NADH/NAD⁺ ratio.⁸ Since the NADH/NAD⁺ ratio is a function of the redox status of the cell, it is expected that the expression of redox-sensitive or redox-responsive enzymes will be correlated to this ratio, and therefore the observed correlation makes sense. The ratio of NAD⁺ to NADH in *E. coli* is sensitive to the growth conditions. The efficiency of reoxidation of NADH produced by glycolysis varies depending on whether it is carried out by electron acceptor via the electron transport chain (aerobic growth), or

through fermentation (anaerobic growth). Previous studies have also shown that AdhE is translated under both aerobic and anaerobic conditions, but that its translation under aerobic conditions is considerably less than under anaerobic conditions. As a PFL deactivase, AdhE would express this activity during the transition from anaerobic to aerobic growth. However, during anaerobic growth the two enzymes coexist, as they are both required for mixed acid fermentation. In order to change its role from alcohol fermentation to PFL deactivation, and to prevent PFL deactivation under conditions where active PFL is needed, AdhE would have to switch to the appropriate mode in response to cellular signals.

This intriguing possibility was investigated by carrying out deactivation studies aimed at determining the effect of the NADH/NAD⁺ ratio on the putative PFL deactivase activity of AdhE. Different ratios of NADH to NAD⁺ were studied and each of the experimental runs was controlled by running a parallel reaction in which AdhE was excluded. The concentrations of NADH used in the reactions were 0.0128 μmol/μL for Reaction 1 and 0.128 μmol/μL for Reactions 2 and 3. For NAD⁺, the concentration of the stock solution was 1 μmol/μL. The mixes used in the experiment are listed in Table IV.2. All the mixes were prepared under strictly anaerobic conditions, inside an anaerobic chamber.

Table IV.2. The mixes prepared to investigate whether the NADH/ NAD⁺ ratio (\bar{x}) affects the putative PFL deactivase of AdhE.

		NADH	NAD ⁺ (1M)	MOPS (500 mM)	PFL _a (75 μ M)	AdhE (123 μ M)	\bar{x}
Volumes transferred (μ L)							
Rxn 1	Mix 1	6.25	3.92	34.8	50	5	.02
Rxn 2	Mix 2	5.2	3.33	36.5	50	5	.2
Rxn 3	Mix 3	13.4	2.29	29.3	50	5	.75
Ctrl 1	Mix 4	0	0	45	50	5	-
Ctrl 2	Mix 5	0	0	50	50	0	-
Ctrl 3	Mix 6	13.4	2.29	34.3	50	0	.75

Activated PFL was the last component to be added to each of the mixes, the total time needed for addition and mixing being ~ 10 seconds. The reaction vials (all covered with air tight rubber septa) were incubated inside the chamber and the residual activity of PFL was measured as a function of time, as described in the preceding sections. The results of this experiment are shown in Figure IV.11.

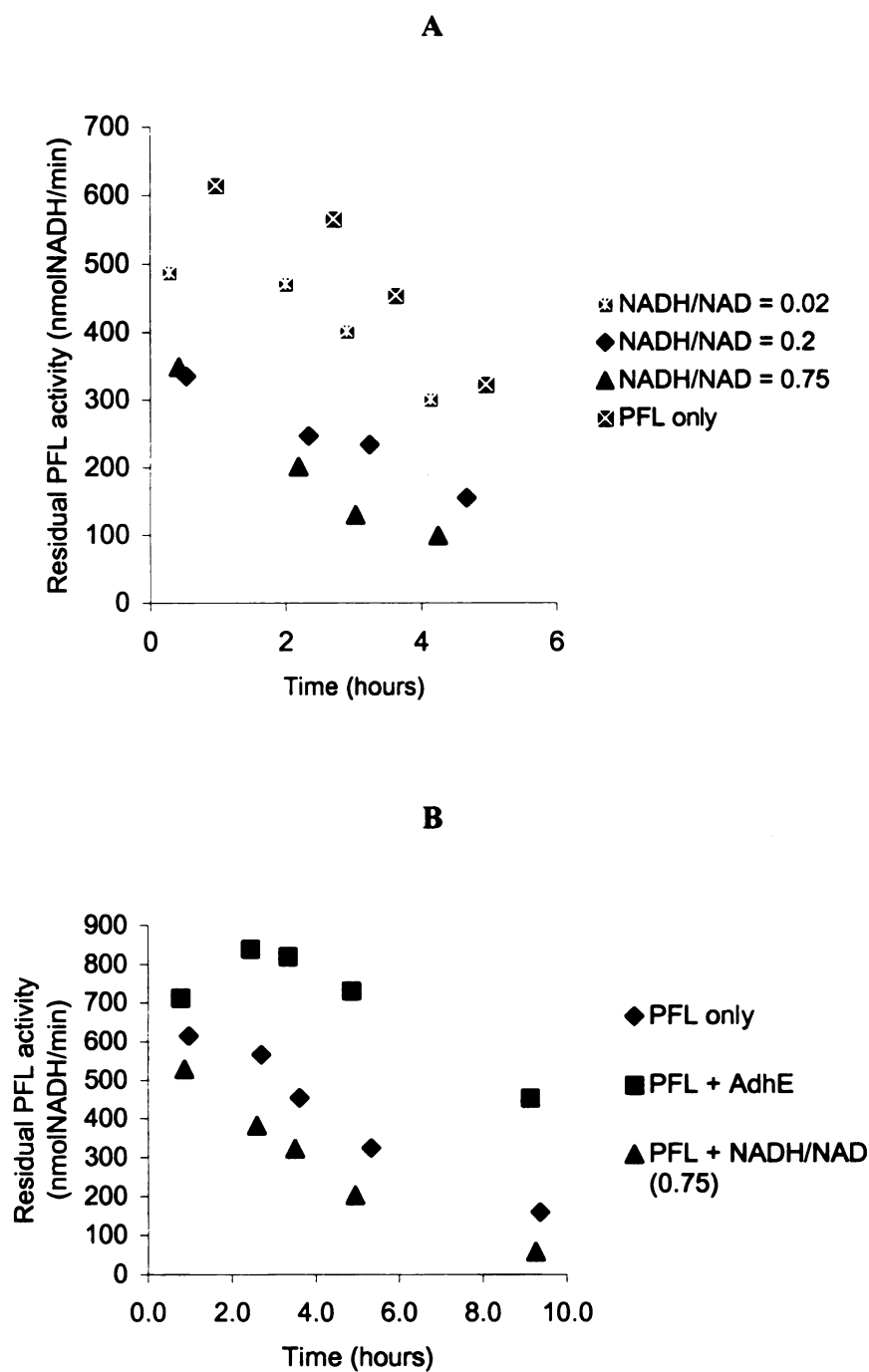


Figure IV.11. Comparison of the effect of different NADH/NAD⁺ ratios and AdhE on the activity of PFL. Panel A shows the effect in the presence of AdhE. Panel B shows a set of controls as outlined in Table IV.2. Conditions are as outlined in Table IV.2

The data (Figure IV.11) shows that the rate of PFL deactivation is directly correlated with the NADH/NAD⁺(A). All of the samples in Figure IV.11A, except the control, contained AdhE, together with NAD⁺ and NADH in the indicated ratios. The data shows that the PFL activity remaining in the mixes containing AdhE plus NADH and NAD⁺ decreased with increasing NADH/NAD⁺ ratios. From the data on IV.10A, alone it was not possible to determine which one of AdhE, NADH, or NAD⁺, or combination of the components was responsible for the observed PFL deactivation. The answer to this question was provided, in part, by the data from the controls (Figure IV.11B). These showed that even in the absence of AdhE, PFL activity decreased more rapidly in the reaction containing the NADH/NAD⁺ mixture than in the control. Interestingly, it was also observed that in the reaction containing PFL and AdhE only, the activity of PFL remained at about the initial level for up to 5 hours after the beginning of the experiment, even though the activity in the “PFL only” control decreased somewhat. After nine hours, the residual PFL activity in the respective control mixes were; ~16% for the reaction containing NADH and NAD⁺, ~31% for the reaction containing PFL only and ~77% in the reaction containing PFL and AdhE only. These results showed that in the presence of NADH and NAD⁺ the deactivation of PFL took place more rapidly. Intriguingly, active PFL appeared to be more stable when AdhE was present. This finding suggested that AdhE stabilizes active PFL. Another view of these results is provided in Figure IV.12.

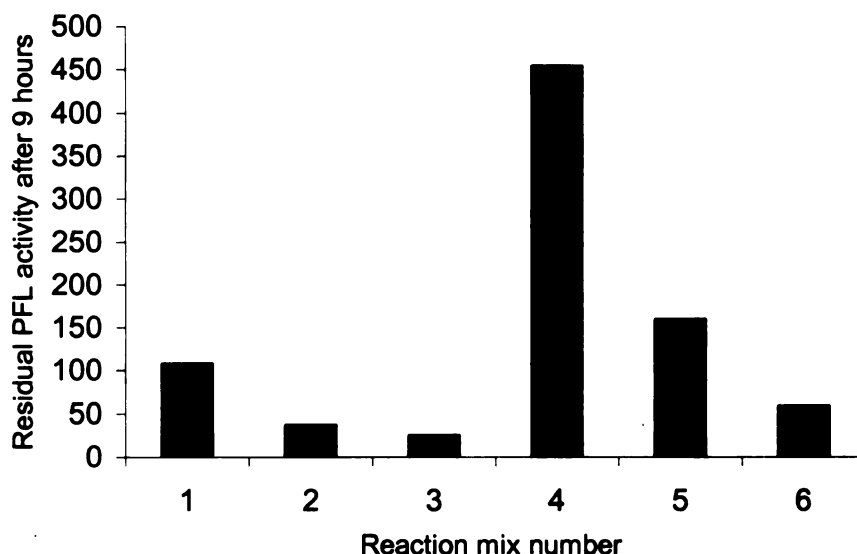


Figure IV.12. The residual PFL activity in each of the reaction mixes (Table IV.2) after 9 hours of incubation. Mix numbers 1, 2 and 3 correspond to experimental mixes containing AdhE in the presence of NADH/NAD⁺ ratios of 0.02, 0.2 and 0.75, respectively, as given in Table IV.1. Mix numbers 4, 5 and 6 correspond to the controls reactions containing PFL+AdhE only, PFL alone and PFL+NADH/NAD⁺ (= 0.75), respectively, as shown in the same table.

The increase in PFL deactivation could not be conclusively correlated to the increase in the ratio NADH/NAD⁺ *per se*, as the increase in the ratio was directly proportional to an increase of NADH in solution. However, the results from controls 1, 2 and 3, respectively, show that AdhE appears to confer greater stability to PFL. The residual PFL activity of the mix containing PFL and AdhE was approximately 3x higher than that of PFL alone (Figure IV.12). The results from control 3 also showed that the deactivations observed in reactions 1 to 3 were due to the effect of at least one of the components of the NADH-NAD⁺ mix, but independent of AdhE. In order to investigate their behaviour further, the reactions were left overnight inside the anaerobic chamber, and then the activity of PFL in each mix was measured. Though the activity in all of the

mixes had decreased considerably, the relative magnitudes were similar to those measured after nine hours of incubation (Figure IV.13). To each of the reaction mixes, 1 μ L of each of SAM, PFL-AE and deazariboflavin was added and incubated inside the anaerobic chamber to bring the total concentrations to 0.5, 0.02 and 0.1 mM respectively. The PFL activity in each was measured after 4 and then again after 6 hours of incubation in ambient light. The mixes were then left overnight for the second time. The activities were again measured and reactivation repeated by adding SAM, PFL-AE and deazariboflavin. The activity profiles of the mixes are summarized in Figure IV.13.

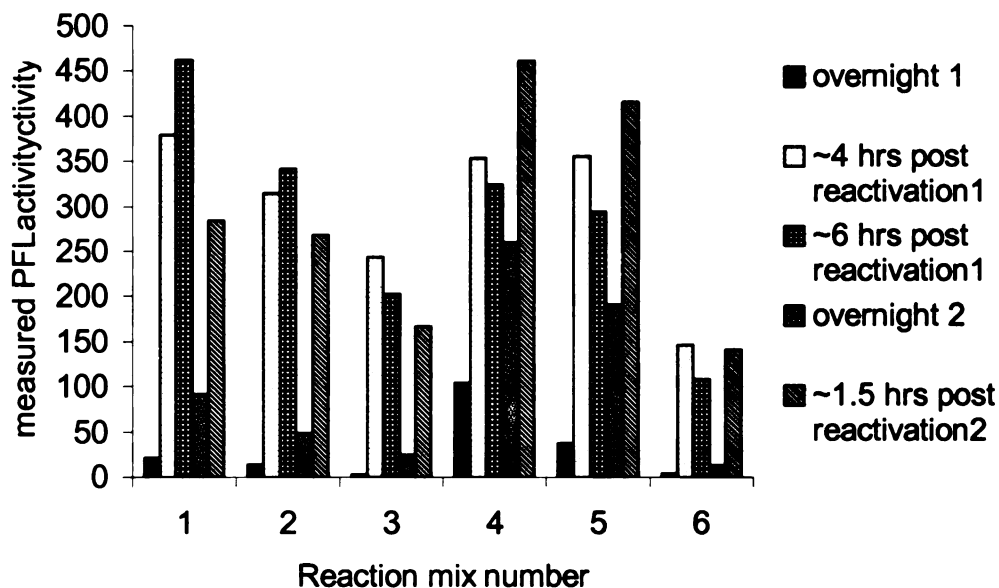


Figure IV.13. PFL activation-deactivation cycles in the reaction mixes. The composition of the mixes is as indicated in Table IV.10.

The first three reaction mixes show that the higher the proportion of NADH in the mix, the greater the extent of deactivation, as shown by the activities measured after both overnight incubations. The data also shows that the degree of PFL reactivation decreased

when the NADH/NAD⁺ ratio was higher, as shown by both “reactivation 1” and “reactivation 2”. The data from reactions 4 and 5 (controls 1 and 2, respectively), demonstrate that when AdhE is present, the rate of PFL deactivation is significantly reduced. AdhE also appears to increase the degree of PFL reactivation as shown by comparison of data from “post reactivation 2” for these reactions. Comparison of data for reaction 3 (mix #3) and control 3 (mix #6) also supports this observation. Both of these reactions contain NADH and NAD⁺ in a ratio of 0.75, but reaction 3 also contains 6μM of AdhE. The residual PFL activity measured after reactivation and after the second overnight incubation for reaction 3 (+AdhE), were all higher than the corresponding measurements for control 3 (-AdhE). This strongly suggested that AdhE plays a role in both the enhancement of PFL activation and the stabilization of the PFL radical once it is generated.

Chemical intuition, our experience with other reductants, and these observations, together led to the hypothesis that the deactivation seen in these experiments was due to the action of NADH, and that NAD⁺ does not play an active role in the process. We proceeded to test this hypothesis by preparing the series of reaction mixes (Table IV.3) inside an anaerobic chamber and monitored their PFL activity over time. Reactions 1 and 4 together were used to test if NADH does indeed deactivate PFL, whereas 1 and 2 were used to address the question about the effect of AdhE on the rate of such PFL deactivation by NADH, as would be expected based on previous observations.

Table IV.3. The reaction mixes used to investigate the effect of NADH and AdhE during PFL deactivation

Mix #	0.0128 M NADH	500 mM MOPS	75 μ M PFL _a	123 μ M AdhE
	Volumes transferred (μ l)			
1	8	14.5	25	2.5
2	8	17	25	0
3	0	25	25	0
4	0	22.5	25	2.5

Reaction 3 was the control, in which only PFL and buffer were incubated. Reactions 3 and 4 together were used to investigate whether AdhE confers greater stability to active PFL. The results of this investigation are shown in Figure IV.14. These results confirm that the deactivation observed in the previous experiments was indeed due to the action of NADH, rather than the combined action of NADH and NAD⁺. This was demonstrated by the fact that reactions 1 and 2 consistently showed lower activities than reactions 3 and 4. Based on reactions 1 and 2, it is concluded that AdhE counteracts the deactivation of active PFL by NADH, as demonstrated by the consistently higher activity of PFL in reaction 2. The samples containing NADH (1 and 2) lost $\geq 90\%$ of PFL activity within 7 hours. On the other hand, PFL activity in the samples without NADH was virtually unchanged within same period (191 vs 180 nmol/min for reaction 3 and 183 vs 194 nmol/min for reaction 4). Whereas the PFL activity in mixes 1 and 2 decreased within the first three hours, the activity increased in reactions 3 and 4 within the same period. AdhE also appeared to preserve PFL activity in the absence of NADH, as shown by the data for reactions 3 and 4 over time. The compositions of the two reaction mixes were identical, except that AdhE was added to reaction mix 4 but not to reaction mix 3. At this

point the main observations made were that 1) the amount of residual PFL activity at any given time tended to be higher in the mix containing AdhE, and 2) the extent of PFL reactivatability, tended to be higher in the mix containing AdhE.

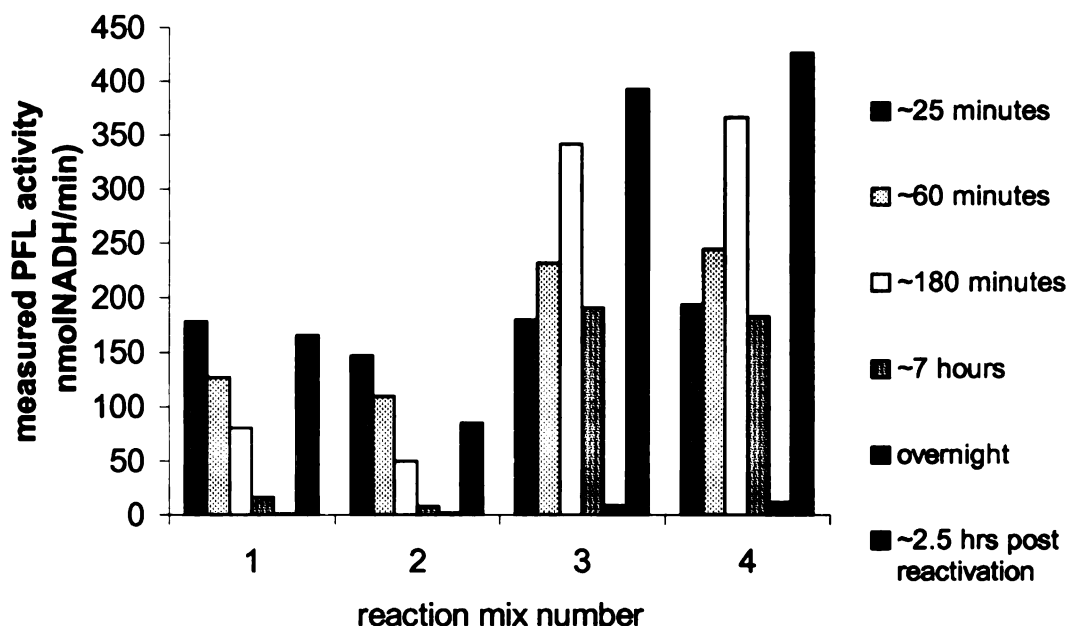


Figure IV.14. The effect of NADH and AdhE on the activity of PFL. The mixes were prepared as in Table IV.2 and the residual PFL activity measured at various time intervals as indicated in the legend.

IV.4. DISCUSSION AND CONCLUSIONS

Several small molecule thiols were investigated with the aim to establish their role in the deactivation of the active (radical) form of PFL. All of the thiols studied showed a measurable deactivation of active PFL, with the capacity of such deactivation (measured by the extent of deactivation within a given time), showing a general correlation to the size of the thiol. In order to determine whether this capacity to deactivate PFL was a function of the thiol functionality, or whether it was exhibited as a property of reducing agents in general, other small molecule reductants were similarly investigated. The results of these investigations revealed that non-thiol biological reducing agents also deactivate PFL at a significant rate.

Investigation of the effect of the NADH/NAD⁺ ratio and NADH by itself revealed that this ubiquitous biological reductant also deactivates PFL with fast kinetics relative to the background deactivation observed in the control. The alcohol dehydrogenase multifunction enzyme (AdhE), whose overexpression is known to be up-regulated similarly to PFL during anaerobic growth, was found to stabilize active PFL. In the presence of AdhE, the activity of PFL was greater than in the absence of AdhE. In addition, deactivation of PFL by NADH was measurably slower in the presence of AdhE than when AdhE was absent. Considering the findings of other investigators which showed that PFL and AdhE expression both respond to an increase in the ratio NADH/NAD⁺, this apparent protective role of AdhE is intriguing. It is when *E. coli* is growing anaerobically that it deploys PFL for post-glycolytic catabolism of pyruvate. PFL so deployed has to be in the active (radical) form in order to act on its substrate pyruvate, in the presence of the co-substrate coenzyme A. Under the same conditions,

NADH is present at concentrations comparable to those of the other products of glycolysis, having been a product of one of the steps in glycolysis. The observation that NADH is effective at deactivating PFL suggests that under conditions in which both exist simultaneously, a mechanism must be present by which active PFL is protected against deactivation by NADH. Based on our observations herein, we propose that the multifunction enzyme AdhE provides such protection.

Regarding the role of reducing agents in general, it is significant that the thiols, particularly β -ME and DTT, have proven to be relatively potent deactivators of PFL. Both of these reductants are very routinely used during enzyme purification in order to provide the reducing conditions necessary to avoid denaturation of the proteins under study. It would appear that it is necessary to only use minimal concentrations of each of these reductants to prevent protein denaturation, without significantly counteracting the activation of PFL. What that concentration should be can only be established by systematic study. Interestingly, DTT is required in small concentrations during PFL activation. Determination of the optimum DTT concentration necessary to facilitate PFL activation without compromising the stability of the same would provide valuable information for any research involving PFL activation. Several theoretical studies on protein radicals have demonstrated that the activation enthalpy for the transfer of a hydrogen atom from a thiol to a C-based radical is in the region of $\sim 12 \text{ kJ mol}^{-1}$.^{9,10} The observation of deactivation by thiols is therefore consistent with predictions made from theoretical studies.

We also find it fascinating that cysteine deactivates PFL, because there are two cysteine residues (C418 and C419) at the active site of PFL. Given the high effective

concentration of cysteine in the vicinity of the PFL glycyl radical, and based on our findings, it is conceivable that the glycyl radical would be rapidly deactivated shortly after formation. However, this is not found to be the case. One of the active site cysteines does, however, “quench” the glycyl radical during the PFL-catalyzed reaction, as the glycyl radical is transferred to Cys419.¹¹

REFERENCES

1. Rabek, J. F. **1987**, *Mechanisms of Photophysical Processes and Photochemical Reactions in Polymers. Theory and Applications*, Chichester, New York, Brisbane, Toronto, Singapore: Wiley.
2. Broderick, J.B.; Henshaw, T.F.; Cheek, J.; Wojtuszewski, K.; Smith, S.R.; Trojan, M.R.; McGhan, R.M.; Kopf, A.; Kibbey, M.; Broderick, W.E. **2000**. *Biochem. Biophys. Res. Commun.* 269, 451-456.
3. Droge W. **1993**. *Pharmacol.* 46(2):61-5.
4. Quig D. **1998**. *Altern Med Rev.* 3(4):262-70.
5. Alftan, G.; Aro, A.; Gey, K.F. **1997**. *Lancet* 349: 397.
6. Dorval, J.; Hontela, A. **2003**. *Toxicol. Appl. Pharmacol.* 192(2):191-200.
7. Li, Y.J.; Oliveira, S.A.; Xu, P.; Martin, E.R.; Stenger, J.E.; Scherzer, C.R.; Hauser, M.A.; Scott, W.K.; Small, G.W.; Nance, M.A.; Watts, R.L.; Hubble, J.P.; Koller, W.C.; Pahwa, R.; Stern, M.B.; Hiner, B.C.; Jankovic, J.; Goetz, C.G.; Mastaglia, F.; Middleton, L.T.; Roses, A.D.; Saunders, A.M.; Schmechel, D.E.; Gullans, S.R.; Haines, J.L.; Gilbert, J.R.; Vance, J.M.; Pericak-Vance, M.A. **2003**. *Hum Mol Genet.* Dec 15; 12(24):3259-67.
8. Leonardo, L.R.; Dailly, Y.; Clark, D.P. **1996**, *J. Bacteriol.*, 178, 20, 6013-6018.
9. Armstrong, D.A.; Yu, D.; Rauk, A. **1998**. *J. Am. Chem. Soc.* 120, 8848-8855
10. Reid, D.L.; Shustov, D.A.; Armstrong, A.; Rauk, A.; Schuchmann, M.N.; Akhlaq, M.S.; von Sonntag, C. *Phys. Chem. Chem. Phys.*
11. Becker, A.; Fritz-Wolf, K.; Kabsch, W.; Knappe, J.; Schultz, S.; Wagner, A.F.V. **1999**, *Nature: Struct. Biol.* 6 (10), 969-975.

CHAPTER V

MOTIVATION FOR THIS STUDY, SUMMARY OF FINDINGS AND FURTHER INVESTIGATIONS

V.1. MOTIVATION FOR THIS STUDY

At the onset of this research project, our aim was to study the Fe(II) alcohol dehydrogenase from *E. coli* (AdhE) with respect to its purported deactivase activity on pyruvate formate-lyase. This would include the characterization of the Fe (II) center in terms of the identity of the ligands directly coordinated to Fe (II), using a number of techniques, including Mossbauer, XAS and EXAFS spectroscopies. The second part of the project would then be to investigate the mechanism by which AdhE accomplishes the deactivation of PFL. The activation of PFL, which involves the generation of a glyceryl radical on a glycine residue at position 734 of the PFL polypeptide, has received a great deal of attention from numerous researchers.¹⁻³

Based on a wealth of data collected over the years, the basic mechanism by which the activation of PFL is accomplished, as well as the co-factors involved in the process are now known.⁴⁻⁶ Indeed the knowledge base for the activation reaction is now at a point where the focus is now on trying to understand how the co-factors and enzymes involved in the activation interact with one another in order to achieve the generation of the radical co-factor on the PFL backbone. The correct determination of the mechanism by which the activation of PFL proceeds derives importance from the fact that many vital bacterial enzymes are now known that are characterized by the generation of a radical co-factor mediated by another enzyme, analogously to PFL-AE on PFL.^{7,8} Also, it is now known that PFL-AE belongs to a super family of enzymes collectively known as the radical SAM super family, all of which use SAM to generate a radical co-factor on another enzyme or at another site on the same enzyme.⁹ It is therefore conceivable that the mechanism of generation of the radical co-factors in these enzymes would be similar.

Whereas the activation of PFL and the components involved therein have received considerable attention, the reverse reaction, which is purported to be mediated by AdhE, has never been investigated further since the publication of 2 papers by one research group over a decade ago.^{10,11} This is in spite of the fact that virtually every publication on AdhE since around 1992 attributes its reference to AdhE as a PFL deactivase to the same.¹²⁻¹⁶ The fact that the PFL deactivase activity of AdhE was reported by only one research group, and given the potential applicability of the deactivation as a model reaction for at least some of the radical SAM enzymes, we sought to better understand this fascinating reaction. However, before embarking on a study of the metal center of AdhE and the mechanism of PFL deactivation by AdhE, we considered it logical to first establish whether AdhE indeed contained deactivase activity, hence the deactivation studies.

V.2. ACTIVATION AND STABILITY OF PFL

V.2.1. *Some Philosophical and Practical Considerations on Activation*

The classical challenge facing any researchers in the areas of biochemistry and bioinorganic chemistry is the difficulty of creating experimental conditions *in vitro*, that approximate those found within the living cells closely enough, such that the observations made therein and conclusions drawn therefrom can be applicable to the real life situation. The disparity between the conditions under which PFL has been activated in all previous studies, and those that actually obtain within the cell, dictates that the extrapolation of any findings made *in vitro* to what happens within the cell, be considered with caution. Any modification of the experimental conditions that reduces the disparity between the *in vitro* and *in vivo* situation with regard to the identity and nature of the components involved, however, renders the conclusions drawn from the biochemical study concerned more applicable to the real situation.

It is against such a background that the activation of PFL by illumination with a high intensity halogen lamp has always been of concern to us. It is known that *in vivo*, the activation reaction employs flavodoxin/flavodoxin reductase as the reductant. Understandably, this system does not require light, as many of the anaerobic environments in which *E. coli* is found, such as in the stomach, are actually dark, therefore light activation is artificial. Also, it is extremely difficult to maintain constant temperature during activation while illuminating the sample with a high intensity lamp. The addition of ice to the cooling water tends to cause a drastic drop in temperature initially, followed by a steady increase between ice additions. The kinetics of PFL

activation under these conditions, therefore, can be difficult to control and to analyze, and are certainly not comparable to those inside the cell.

V.2.2. Activation Without Intense Illumination is Advantageous

Our discovery that PFL can be activated without the need for high intensity illumination enabled us to perform the activation at a constant temperature of approximately 23°C. This temperature much more closely approximates temperatures of the natural habitats of *E. coli*, relative to the wide range from < 10°C to ~23°C observed during intense illumination experiments. Another advantage offered by activation without illumination is that sample handling becomes greatly simplified, as it is no longer necessary to try to control the temperature of the activation reaction by periodically adding ice to the water bath. This also minimizes fluctuations of the oxygen concentration inside the anaerobic chamber, which tended to be common when ice was brought into the chamber, sometimes in spite of care having been taken to thoroughly evacuate the ice prior to bringing it into the chamber.

V.2.3. In vivo PFL Activation Employs A light-independent Reductant

As indicated, the (anaerobic) conditions under which *E. coli* requires the use of active PFL tend to be dark, and yet *E. coli* is able to metabolize glucose. PFL-AE is able to activate PFL under such conditions because the flavodoxin/flavodoxin reductase system responsible for providing the required reducing equivalents is not light induced. We therefore set out to attempt to carry out PFL activation under conditions that more closely approximate those prevailing in an *E. coli* cell carrying out anaerobic metabolism.

As a first step, PFL was activated under ambient light and temperature. The activation mix was prepared as described previously but, instead of illuminating with a high intensity lamp and cooling the activation mix with ice-water, the mix was incubated inside the anaerobic chamber maintained at ~23°C. All the light in the box was from a fluorescent bulb inside the box and from those in those in the lab. As was shown in Chapter II, PFL activity in the activation mix increased steadily up to a threshold level comparable to (and sometimes higher than) that obtained when using the usual illumination method. In effect, therefore, the variable that was made to approximate the *in vivo* situation more closely was the temperature, but not light, since the photoreductant was still exposed to light, only at lower intensity.

A closer approximation of the situation *in vivo* for *E. coli* would be achieved by using a biological reductant that is capable of generating active PFL under anaerobic conditions, room temperature, and in the absence of light. Within the cells, such a reductant would more closely model the flavodoxin/flaxodoxin reductase system involved in the PFL/PFL-AE activation mechanism. Successful activation of PFL without intense illumination, achieved in this study, was only a step towards this goal because the photoreductant used was exposed to light, albeit at lower intensity.

V.3. STUDIES OF THE DEACTIVATION OF PFL BY ADHE

Kessler et al. have published work in which they indicate that AdhE is a deactivase for PFL, namely, that it mediates enzymatic and non-destructive conversion of PFL from the radical form to the non-radical form.^{10,11} These workers therefore assert that AdhE catalyzes the reverse reaction to that catalyzed by PFL-AE, thus completing an interconversion cycle between active and inactive PFL. We found this report very intriguing, as it proposed an elegant mechanism by which *E. coli* apparently avoids oxidative destruction of PFL upon environmental change from anaerobic to aerobic. This made sense, since by conservatively converting PFL from the active to the inactive form, this bacterium would save a considerable amount of energy required synthesizing new PFL when conditions again become anaerobic. According to these workers, AdhE achieves the radical quenching in cooperation with NAD^+ , Fe^{2+} and CoA as cofactors.

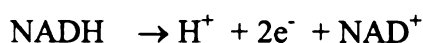
We therefore set out to first confirm these reported findings by repeating the deactivation experiments under similar conditions as those described by Kessler et al.¹¹ Interestingly, our findings were at variance with the reported data. Based on our study, the rate of deactivation of active PFL samples to which known amounts of DTT, Fe^{2+} and CoA (all components of the AdhE assays of Knappe and Kessler¹¹) were added, was found to be systematic and to proceed at rates significantly higher than that of the control containing PFL alone. Surprisingly, AdhE was found to protect active PFL from inactivation in the presence of a deactivator and to confer PFL with greater stability compared to a negative control in which AdhE was excluded. From their study, Kessler and co-workers noted that during the deactivation of PFL by AdhE, NAD^+ was not replaceable by non-reducible analogs, and on that basis they reasoned that NAD^+

therefore directly participates as an oxidant.¹¹ They also noted that there was a net increase in the amount of NADH in solution during PFL deactivation and that addition of NADH inhibited PFL deactivation.

From a chemical standpoint, it is not immediately clear how NAD^+ would be involved in the quenching of the glycy radical of active PFL. The quenching reaction effectively involves the addition of a hydrogen atom at Gly-734 of active PFL, which is a reduction reaction. It is therefore not conceivable that NAD^+ would be able to achieve this reaction, directly or indirectly. Their observation of an increase in NADH during PFL deactivation may be explained by a side reaction between NAD^+ and another reductant in solution, particularly since the reaction was carried out under reducing conditions. These workers also noted that the production of NADH was concomitant with and correlated to the amount of PFL deactivated, and that the background amount of NADH was essentially constant when inactive PFL was used. They therefore argued that this provided further proof that NAD^+ was being reduced in the process of PFL deactivation. It should be noted, however, that the activated PFL used by these workers contained several components, including reducing agents such as Fe^{2+} and DTT. Under such reducing conditions, NAD^+ could be reduced to NADH detected in the mix. The more activated PFL transferred, therefore, the larger the amount of reducing equivalents and so the amount of NAD^+ reduced. Unactivated PFL, on the other hand, contained much lower concentrations of the reducing agents found in the active PFL mix, particularly Fe^{2+} .

As additional proof that NAD^+ was directly involved as an oxidant, these workers report that it was “not replaceable by non-reducible analogs”¹¹. In the absence of the data

based upon which this conclusion was drawn, it is difficult to comment on what might have led to the said observations. Whereas these workers report that NADH proved to be a competitive inhibitor, our findings show that NADH deactivated PFL quite effectively, relative to a negative control. This is also amenable with the chemical properties of both NADH and active PFL. NADH is a ubiquitous biological reductant and readily reduces biological oxidants and is converted to NAD^+ in the process. The quenching of active PFL effectively entails addition of a proton and an electron at the radical-bearing carbon of glycine-734. The conversion of NADH to NAD^+ can be visualized as



Therefore, in NADH-mediated deactivation of PFL, the hydrogen atom would be transferred to the radical center and the electron transferred to an oxidant in solution. We presently do not have sufficient data to provide more details regarding the mechanism by which this deactivation proceeds. However, in a subsequent section we propose some experiments that can be carried out in order to preliminarily test if there is direct interaction between active PFL and NADH.

It is also intriguing that even though Knappe and co-workers reported that CoA was required for the deactivation of PFL, they also report that it did not undergo any detectable chemical modification.¹¹ However, they observed that CoA was probably directly involved in the deactivation through the thiol group because the desulfo analog of CoA competitively inhibited deactivation. Our findings are consistent with these reported observations, except that we find PFL deactivation to be independent of AdhE.

V. 4. CONTEXT, RELEVANCE AND OTHER STUDIES

In order to develop a perspective of the role of AdhE within the context of the metabolic machinery of the organism, particularly *E. coli*, a brief discussion of some findings from the literature will first be presented. *E. coli* is able to survive and thrive under very adverse conditions because it has evolved mechanisms to allow it to cope with a wide range of environmental conditions. Such conditions may vary widely in terms of factors such as pH and oxygen availability. The adaptability of this organism can be traced to its ability to express its genes selectively depending on environmental demands.¹⁷ This organism is a facultative anaerobe and controls gene expression by using a combination of transcription factors that respond to the overall oxygen status of the growth environment.¹⁷ Fumarate and nitrate reduction regulator (FNR) is one of the most important transcription regulators responsible for turning on the expression of most of the enzymes needed for anaerobic growth.¹⁷ The sensing mechanism of FNR under anaerobic conditions involves the acquisition of an oxygen-labile [4Fe-4S] cluster, which triggers the dimerization of FNR, thereby enhancing site-specific DNA binding.¹⁸⁻²⁰

The *pflB* gene encoding PFL is FNR-regulated. Recently Green and co-workers discovered that another FNR-regulated enzyme, YfiD, bears very close sequence homology (77% homology over a 64 amino acid overlap) to the C-terminal region of pyruvate formate-lyase (PFL).²¹ Based on its strong homology to pyruvate formate-lyase (PFL), these workers predicted that YfiD would also be a radical-containing enzyme. They not only confirmed that to be so, but also found that PFL-AE is able to introduce the radical on YfiD, similarly to PFL. Based on the PFL deactivase activity of AdhE reported in the literature, it was expected that AdhE would quench the radical generated

on YfiD during its activation by PFL-AE. All attempts to identify the reverse activity, under the mediation of AdhE, however, gave negative results.²¹

The genes for aerobic metabolism are regulated by the O₂-responsive Arc system, comprising two enzymes ArcA and ArcB.^{22,23} ArcB is a membrane protein and primarily plays a sensory role, while ArcA is the response regulator. The expression of PFL and AdhE under conditions ranging from aerobic through microaerobic to anaerobic have been studied quite extensively. Many of these studies have ranged in detail from O₂-responsive transcriptional regulators,²⁴⁻²⁶ to the genes targeted by those regulators,²⁷ the promoter structures involved,²⁸ and the mode by which the system senses oxygen.²⁹

In their study of the effect of oxygen tension on the expression of anaerobic enzymes and their metabolic products, Becker and co-workers found that AdhE expression was more sensitive than PFL to oxygen tension.³⁰ These workers defined pO_{0.5} as the oxygen tension required to bring down protein or metabolite synthesis to half the maximum observed under anaerobic conditions. Using this operational definition, they measured pO_{0.5} for the fermentation products of PFL and AdhE, as well as for the enzymes themselves. They observed that the general trend was that the pO_{0.5} for the synthesis of the fermentation products acetate, ethanol, lactate and succinate, fell within the narrow range from 0.2-0.4 mbar. The exception to this was formate, which was found to have a pO_{0.5} value of 1 mbar. What these findings suggested was that during the change from aerobic to anaerobic metabolism, formate is formed earlier than the other products. Also, for PFL and AdhE, pO_{0.5} was measured to be 5 and 0.8 mbar O₂, respectively, while the corresponding pO_{0.5} for the formate and ethanol were 1 and 0.4 mbar O₂. In metabolic terms, these findings indicate that during the transition from

aerobiosis (high pO_2) to anaerobiosis (lower pO_2), PFL is deployed earlier than AdhE, hence the detection of its metabolic product, formate, earlier than the metabolic product of AdhE, ethanol. The interpretation offered by these workers is that the earlier deployment of PFL could be because it has to be post-translationally modified (activated) prior to catalysis. The limitation of this interpretation, however, is that both the activating enzyme (PFL-AE) and activated PFL are highly sensitive to oxygen *in vivo* and would therefore be expected to operate only at lower oxygen tensions, which is later in the transition from aerobiosis to anaerobiosis.

Notably, deletion mutations at the ubiquinone synthase and quinoloxidase loci, both of which are members of the electron transport chain, resulted in a shift of both formate and ethanol production to higher pO_2 values, suggesting that both PFL and AdhE become operational earlier during the shift from aerobic to anaerobic metabolism.¹⁶ Removal of some of the members of the electron transport chain is expected to lead to accumulation of NADH, since the mechanism of disposal of reducing equivalents is no longer available. Previous studies had shown that accumulation of NADH inhibits pyruvate dehydrogenase (PDH).³¹ It is therefore conceivable that under those conditions pyruvate metabolism would shift towards PFL, since it is the other of two systems available to metabolize pyruvate to acetyl-CoA. Notably, accumulation of NADH also stimulates NADH reoxidation by alcoholic fermentation, a reaction that requires AdhE.³² Based on the fore-going analysis, it is therefore sensible that both PFL and AdhE and their corresponding metabolic products would shift towards higher pO_2 values when the electron transport chain enzymes are either removed or inactivated. However, this has to be reconciled with the fact that PFL and its activating enzyme are very sensitive to

oxygen *in vitro*. Based on our observation that AdhE appears to confer greater stability to active PFL, we propose that the observed shift of PFL and AdhE expression towards more aerobic conditions when the electron transport activities are not present, is induced by metabolic necessity and made possible by the protective role of AdhE for active PFL.

More recently, Teixeira de Mattos and co-workers investigated the metabolic response of *E. coli* to varying oxygen availability and found that PFL was active at low oxygen concentrations.³² Their measurements show that even under microaerobic conditions, when respiration is at half its maximal rate, the processing of as much as half of pyruvate is due to PFL, showing that both the pyruvate dehydrogenase system and the PFL system are operational under these conditions. They further proposed that PFL is stabilized by *cytochrome bd* through rapid consumption of oxygen via uncoupled respiration.³² In their review, Poole and Hill note that *cytochrome bd* has been discovered to be the terminal oxidase responsible for protecting oxygen-labile nitrogenase during nitrogen fixation in *Azotobacter vinelandii*.³³ The discovery of this protective role of *cytochrome bd* for nitrogenase removed the paradox of aerobic nitrogen fixation in prokaryotes, a process mediated by a very air-sensitive enzyme. The implication of *cytochrome bd* as a protector of PFL during microaerobic respiration was previously suggested by Becker and co-workers, who found *cytochrome bd* to be maximally expressed under microaerobic conditions, similarly to PFL.³³ Since PFL is known to be extremely sensitive to oxygen, and yet it is found to be active under conditions of relatively high oxygen tension, this is strongly suggestive of an agent that protects it against oxygenolytic destruction, a fate that it suffers almost instantly *in vitro* when exposed to air.³³ Our finding that AdhE appears to stabilize active PFL, and that of

Echave et al.¹², who found AdhE to have some antioxidant properties has lead us to suggest that the presence of AdhE allows PFL to be able to operate under microaerophilic conditions.

The co-expression of AdhE and PFL, observed by several researchers,^{12,24-33} is also consistent with the fact that both enzymes are sequentially involved in the processing of pyruvate to ethanol under anaerobic growth. The suppression of pyruvate dehydrogenase resulting from the accumulation of NADH would necessitate the deployment of PFL, which would, in turn, require activation to convert it to the catalytic state. Since the acetyl-CoA produced by the PFL reaction with pyruvate and CoA is a substrate for AdhE, it also makes sense that AdhE should be co-expressed with PFL. Furthermore, alcoholic fermentation mediated by AdhE consumes NADH, which accumulates under microoxic conditions. Under this set of conditions, the multifunctional role of AdhE as an alcohol dehydrogenase participating in the fermentation reaction, while at the same time protecting active PFL against oxygen, makes sense.

The PFL protective role proposed for AdhE is not only consistent with the precedence of the apparent PFL protection by *cytochrome bd* mentioned above,³² but also with the reported antioxidant properties of AdhE.¹² The latter results showed that *E. coli* cells with an AdhE knockout were not able to grow aerobically in minimum medium. It was also noted that these cells were particularly prone to oxidative stress, but reintroduction of the *adhE* gene into the mutants restored the cells' ability to grow aerobically.¹² AdhE purified from the *adhE*⁺ cells was found to undergo metal catalyzed oxidation (mco) very rapidly when exposed to H₂O₂ leading to inactivation of the

enzyme.¹² Upon substitution of Zn for Fe in the AdhE, no metal catalyzed oxidation was observed. The Zn-substituted AdhE also led to reduced cell viability compared to the Fe AdhE. These observations led to the conclusion that AdhE was acting as an antioxidant and that Fe²⁺ was essential for the antioxidant activity.

In conclusion, the following observations have been made in the studies of AdhE and related enzymes carried out by a number of workers:

1. Although it is generally known to be an anaerobically active enzyme, AdhE is expressed under aerobic conditions as well.
2. AdhE and PFL are expressed to comparable levels during microaerobiosis, under which conditions PFL is found to be active, despite its high sensitivity to oxygen.
3. Cytochrome bd, a terminal oxidase found to be effective in protecting nitrogenase against oxidative degradation, is also found to be present in higher concentrations under microoxic growth conditions.
4. AdhE was discovered to protect growing bacterial cells against hydrogen peroxide.
5. In our work, AdhE was found to confer greater stability to active PFL and to protect it against deactivation.
6. In our work, NADH, which accumulates both under microoxic conditions and in mutants devoid of terminal quinone oxidases, was found to deactivate PFL.

These findings, among others (Chapter III) put to question the assertion that AdhE is a PFL deactivase. Deactivase properties would not be consistent with the finding that

under microoxic conditions AdhE and PFL are co-expressed and that PFL is active under the same conditions. This is inconsistent because

- i) active PFL would either be destructively inactivated by oxygen or
- ii) active PFL would be deactivated by AdhE

With what we now know of the effect of NADH on active PFL, its accumulation under microaerobic growth would also contribute towards PFL deactivation and thus render fermentative metabolism impossible. The case of YfiD is also instructive. Whereas this enzyme shows 77% sequence homology to PFL, and whereas it is under the same regulon as PFL and is also activated by PFL-AE by introduction of a glycyl radical, attempts to deactivate it with AdhE proved ineffective.²¹ Based on our observations, and the findings of others cited above, we propose that AdhE is co-expressed with PFL primarily for two reasons:

1. Both enzymes are needed for anaerobic metabolism, PFL being responsible for the first step consisting of non-redox conversion of pyruvate to formate and acetyl-CoA, followed by a second step comprising AdhE-mediated reduction of acetyl-CoA to ethanol, with concomitant recycling NAD^+ to feed the glycolytic cycle.
2. AdhE provides protection for the highly sensitive active PFL against destructive inactivation by traces of oxygen or any biological reductant capable of inactivating PFL.

V.5. DEACTIVATION BY THIOLS AND OTHER REDUCTANTS

The deactivation studies carried out in this project were done as an offshoot to the test for PFL deactivation by AdhE. As it turned out, however, thiols proved to be effective deactivators of PFL. This did not come as a great surprise *per se*, because one-electron oxidation to produce thiyl radical is a well-established reaction.³⁴ These radicals participate in a number of reactions including electron transfer, hydrogen abstraction and addition reactions with several biological constituents and xenobiotics, and can be detected by optical spectroscopy or by electron spin resonance (ESR) spectroscopy.³⁴ Bithiols are known to be particularly good antioxidants, providing cells with protection against oxidative damage by free radicals.³⁵ In the process, thiols undergo one-electron oxidation and form thiyl radicals (RS^\bullet). The efficacy of thiols as antioxidants stems from the fact that under physiological conditions, thiyl radicals can react with thiolate anion, yielding disulfide radical anion ($RSSR^\bullet$)⁻ as an intermediate.³⁵ The disulfide radical is then passed on to oxygen, yielding disulfide and superoxide radical anion (O_2^\bullet), which is then inactivated in a reaction catalyzed by superoxide dismutase (SOD).³⁵ Thiyl radicals are also known to undergo reaction with reductants such as ascorbate, with concomitant formation of low-activity ascorbyl radical, which subsequently undergoes a disproportionation reaction.³⁵ Thus biological systems have devised an efficacious means of using thiols to neutralize potentially harmful radicals by converting them into forms that can be disposed of enzymatically or species that are inherently self-destructive.

The deactivations that were observed in our work therefore demonstrated that when carrying out investigations on active PFL, it should be taken into account that any thiols present in the solution will have the potential to deactivate PFL. It is therefore

important to take this into consideration, so that control experiments can be designed to filter out any background deactivation that may be taking place as a result of the participation of the thiol(s). In their work on PFL, Kessler and co-workers used DTT in the assay mix at concentrations that were several-fold higher than that of active PFL.¹¹ Given the well-established reactivity of thiols towards protein-based radicals, we submit that the presence of such high concentrations of thiol relative to the radical compromised the rigor with which any radical quenching study by other components were pursued. Our study demonstrates that the deactivation observed by Knappe and Kessler¹¹ cannot be unequivocally attributed to AdhE. Indeed, we have demonstrated that AdhE, rather than deactivate PFL, actually stabilizes the radical form of PFL. This result is in direct opposition to those reported by Knappe and Kessler^{10,11}. Based on the strength of these findings and consistently with those of other workers, it is hereby proposed that AdhE is not a PFL deactivase but rather, protects PFL against deactivation.³⁰⁻³³

Clearly, more work needs to be done in order to fully understand the role(s) played by AdhE during anaerobic catabolism of pyruvate. If indeed AdhE does protect active PFL, it is expected to specifically interact with it. Such interaction, if present, should be demonstrable. One of the first studies to be done in this regard would be to carry out binding studies to show that indeed there is a specific interaction between these two enzymes. It would also be interesting to investigate the interaction between AdhE and both activated and inactive PFL to determine whether there is a discernible difference. The role of Fe(II) in this process is also intriguing. The antioxidant role of AdhE reported by Echave et al. was found to be dependant on the presence of Fe(II)¹², thus suggesting a direct role by this metal. It is curious what the role of this metal might

play, both in the putative interaction between AdhE and PFL, as well as in the apparent PFL protection that AdhE affords. The next question to answer would be whether the interaction between AdhE and PFL (active or inactive) has any dependence on the presence or absence of Fe (II). This can be done by using site-directed mutagenesis to replace the iron-binding histidine residues with phenylalanine, in order to overexpress iron-free AdhE. Based on the findings of these studies, the investigation can be carried further towards elucidation of the mechanism by which the putative PFL protection is accomplished by AdhE. The questions regarding the cooperation between PFL and AdhE are very interesting, particularly since it has become evident that this area may not be as well understood as first thought. The route towards answering them promises to be an exciting one.

V.6. SUGGESTED EXPERIMENTS FOR FURTHER STUDIES

V.6.1. Mechanistic Studies

Part of the initial motivation of this project was the desire to elucidate the mechanism by which the glycyl radical is quenched during PFL deactivation by AdhE. Although AdhE was found to be inactive with regard to PFL deactivation, several reductants, some of which are biologically relevant, were found to be effective deactivators of PFL. That deactivation rather than inactivation occurred was demonstrated in the case of 2-mercaptoethanol and ethanethiol. This was accomplished through reactivation experiments and SDS-PAGE. However, based on the data obtained by these techniques, it is not possible to gain insight into the molecular events leading to the quenching of the PFL radical. Time course deactivation studies using EPR may provide useful information about both the progress of deactivation and the nature of the radical species formed in the process. More insight would also be gained by using rapid freeze-quench to trap any transient species that may not be amenable to regular EPR.

V.6.2. In vivo studies

All studies done in this work were done outside the cell. Attempts were made to reproduce conditions that are as reasonably close to physiological as possible. However close the experimental conditions may be to physiological, they are always an approximation. The difference between the experimental and physiological conditions is particularly important when we work in the “test tube” to study changes that take place within a physiological cell. The *pflB* gene encoding PFL is FNR-regulated. Any

conclusions that we draw from such *in vitro* studies are subject to inaccuracies imposed by the difference between the realities of the situation *in vivo* and *in vitro*. Whenever possible, therefore, it is better to use a real cell to study changes that take place in the cell. It is fair to acknowledge, however, that for practical reasons, sometimes it is not possible to do *in vivo* studies. Considering the foresaid, we believe that useful information would be gained by carrying out both whole cell and *in vitro* in the study of the PFL activation and deactivation studies.

REFERENCES

1. Becker, A.; Fritz-Wolf, K.; Kabsch, W.; Knappe, J.; Schultz, S.; Wagner, A.F.V. **1999**, *Nature: Struct. Biol.* 6 (10), 969-975.
2. Ulissi-Demario, L.; Brush, E. J.; Kozarich, J.W. **1991**, *J. Am. Chem. Soc.* 113, 4341-4342.
3. Mulliez, E.; Fontecave, M.; Gaillaid, J.; Riechard, P. **1993**, *J. Biol.Chem.*, 268, 2296-2299.
4. Gault, J.W.; Eriksson, L. A. **2000**, *J. Am. Chem. Soc.*, 122, 2035
Wong, K. K.; Kozarich, J. W. In *Metal Ions in Biological Systems, Metalloenzymes Involving Amino Acid-Residue and Related Radicals*, Eds. Sigel, H.; Sigel A.; Marcel Dekker: New York, 1994; Vol. 30, p 279.
6. Becker, A.; Fritz-Wolf, K.; Kabsch, W.; Knappe, J.; Schultz, S.; Wagner, A.F.V. **1999**, *Nature: Struct. Biol.* 6 (10), 969-975.

Wagner, A.F.V.; Frey, M.; Neugebauer, F.A.; Schafer, W.; and Knappe, J. **1992**, *Proc. Natl. Acad. Sci.U.S.A* 89, 996-1000.
8. Himo, F.; Eriksson, L.A. *J. Am. Chem. Soc.* **1998**, 120, 11449.

Sofia, H.J.; Chen, G.; Hetzler, B.G.; Reyes-Spindola, J. F.; Miller, N. **2001**, *Nucleic Acids Research*, 29,5, 1097-1106.
9. Kessler, D.; Leibrecht, I.; Knappe, J. **1991**, *FEBS Lett.* 281, 1-2, 59-63.
10. Kessler, D.; Herth, W.; Knappe, J. **1992**, *J. Biol. Chem.* 267, 25, 18073-18079.
11. Echave, P.; Tamarit, J.; Cabisco, E.; Ros, J. **2003**. *J. Biol. Chem.* 278, 32, 30193-30198.
12. Asanuma, N.; Yoshii, T.; Hino, T. **2004**, *Arch. Biochem.* 181, 2, 122-128.
13. Melchiorson, C.R.; Jokumsen, K.V.; Villadsen, J.; Johnsen, M.G.; Israelsen, H.; Arnau, J. **2000**, *J. Bacteriol.* 182, 17, 4783-4788.
14. Holland-Staley, C.A.; Lee, K.; Clark, D.P.; Cunningham, P.R. **2000**, *J. Bacteriol.* 182, 21, 6049-6054.
15. Mikulskis, A.; Aristarkhov, A.; Lin, E.C.C. **1997**, *J. Bacteriol.* 179, 22, 7129-7134.

16. Kiley, P. J.; Beinert, H. **1999.** *FEMS Microbiol. Rev.* 22, 341-352.
17. Lazzazera, B. A.; Beinert, H.; Khoroshilova, N.; Kennedy, M. C.; Kiley, P. J. **1996.** *J. Biol. Chem.* 271, 2762-2768.
18. Jordan, P. A.; Thomson, A. J.; Ralph, E. T.; Guest, J. R.; Green, J. **1997.** *FEBS Lett.* 416, 349-352.
19. Popescu, C. V.; Bates, D. M.; Beinert, H.; Munck, E.; Kiley, P. J. **1998.** *Proc. Natl. Acad. Sci. USA*, 95, 13431-13435.
20. Wyborn, N.R.; Messenger, S.L.; Henderson, R.A.; Sawers, G.; Roberts R.E., Attwood, M.M.; Green, J. **2002.** *Microbiol.* 148,1015-26.
21. Iuchi, S.; Chepuri, V.; Fu, H.; Gennis, R.B.; Lin, E.C.C. **1990.** *J. Bacteriol.* 172, 6020-6025.
22. Iuchi, S.; Lin, E.C.C. **1988.** *Proc. Natl.Acad. Sci. USA*, 85, 1888-1892.
23. Rice, C.W.; Hempfling, W.P. **1978.** *J. Bacteriol.* 134, 115-124.
24. Tseng, C.P.; Albrecht, J.; Gunsalus, R.P. **1996.** *J. Bacteriol.* 178, 1094-1098.
25. Govantes, F.; Orjalo, A.V.; Gunsalus, R.P. **2000,** *Mol. Microbiol.* 38, 5, 1061-1073.
26. Michel-Angelo Sciotti, M-A.; Chanfon, A.; Hennecke, H.; Fischer, H-M. **2003,** *J. Bacteriol.* 185, 18, 5639-5642.
27. Govantes, F.; Albrecht, J. A.; Gunsalus, R.P. **2000.** *Mol. Microbiol.* 37, 6, 1456-69.
28. Becker, S.; Holighaus, G.; Gabrielczyk, T.; Uden, G. **1996.** *J. Bacteriol.* 178, 4515-4521.
29. Becker, S.; Vlad, D.; Schuster, S.; Pfeiffer, P.; Uden, G. **1997.** *Arch. Microbiol.* 168, 290-296.
30. Hansen, R.G.; Henning, U. **1966.** *Biochim. Biophys. Acta* 122, 355-358.
31. Alexeeva, S.; de Kort, B.; Sawers, G.; Hellingwerf, K.J.; Teixeira de Mattos, M. J. **2000.** *J. Bacteriol.* 182, 17, 4934-4940.

32. Poole, R. K.; Hill, S. **1997**. Biosci. Rep. 17, 303-317.
33. Kalyanaraman, B. Biochem. Soc. Symp., Portland Press, Volume 61.
34. Wodek, L. **2002**, *Pol. J. Pharmacol*, 54, 215-223.

MICHIGAN STATE UNIVERSITY LIBRARIES



3 1293 02732 5053